UNIVERSITY OF OKLAHOMA

GRADUATE COLLEGE

UPGRADING OF BIOMASS-DERIVED MOLECULES FOR FUELS VIA HYDRODEOXYGENATION ON SUPPORTED METALS

A DISSERTATION

SUBMITTED TO THE GRADUATE FACULTY

in partial fulfillment of the requirements for the

Degree of

DOCTOR OF PHILOSOPHY

By

TRUNG PHAM
Norman, Oklahoma
2010

UPGRADING OF BIOMASS-DERIVED MOLECULES FOR FUELS VIA HYDRODEOXYGENATION ON SUPPORTED METALS

A DISSERTATION APPROVED FOR THE
SCHOOL OF CHEMICAL, BIOLOGICAL AND MATERIALS ENGINEERING

BY

_____
Dr. Richard G. Mallinson, Chair

_____
Dr. Lance L. Lobban

_____
Dr. Kenneth Nicholas

_____
Dr. Dimitrios Papavasilliou

_____
Dr. Daniel E. Resasco

ACKNOWLEDGEMENTS

First and foremost, I would like to thank my parents, Du Quang Pham and Thanh Thi My Tran, for raising, loving and supporting me all my life. I am indebted to them for their love and would not be able to become who I am today without them. They teach me to be a good kid, a good student and a good citizen. They always support and encourage me for all the moments in life. And above all, they give me such great and fortunate opportunities to be an educated man, from kinder garden to high school and college. I also appreciate Mr and Mrs. Flanagan for their kind help and support to me and other Vietnamese students. They always consider us as their own children and always help us with all they could.

I also thank my younger brother and my friend Hieu Tran Quang Pham, for growing up with me, and supporting me in everyday's life. He has been my friend since my childhood and now that he grows up, we got to attend the same great University of Oklahoma. He is the only family member I have in the U.S. He took care of me when I was sick as well as other problems I have had.

I am grateful and fortunate to have the opportunity to work with Dr. Mallinson since my days when I was an undergrad. He has taught me essential things and skills on how to do research and how to think critically and independently and how to write

technically for all my time doing research at OU. I also would like to thank my Professors, Dr. Lobban and Dr. Resasco for their teaching and professionalism that nurture my knowledge over the years, particularly on how to do professional research, writing and presentations. They gave valuable discussions on my research results that helped me gain insights and knowledge on the topics. I would like to thank my committee members, Dr. Dimitrios Papavasilliou and Dr. Kenneth Nicholas for their valuable time and discussions at my General Exam and my Thesis Defense.

And I would also like to thank all my colleagues and friends for their help and support during my time studying at OU: Trung Hoang, Oat, Nguyen, Prae, Sarah, Phuong, Tanate, Xinli Zhu, Anirudh, Amalia, Steven, Air, Kyu, Quincy, Martina, Christina, Shaolong and Veronica. I would also like to thank Prof. Galiasso and both Prof. Jentofts for their ideas and valuable discussions in our group meetings.

I also am grateful and thankful for tremendous helps from OU Chemical Engineering Department Staffs: Ms. Donna King, Ms. Terry Colliver, Ms. Vernita Farrow, Ms. Sherry Childress and Alan Miles as they always provide unhesitant help in every way to make my work and my stay easier.

TABLE OF CONTENTS

LIST OF TABLES

LIST OF FIGURES

ABSTRACT

Biomass-derived molecules such as aldehydes and alcohols have been upgraded to more valuable products via hydrogenation and hydrodeoxygenation on supported metals. For unsaturated aldehydes, the competitive hydrogenation of C=C and C=O may result in an unsaturated alcohol, a saturated aldehyde, or a saturated alcohol. Hydrogenation of 2-methyl-2-pentenal has been studied for supported Pt, Pd and Cu catalysts. The activity follows the order Pt>Pd>Cu. While Pt and Pd primarily catalyzed hydrogenation of the C=C bond to 2-methyl-pentanal, Cu catalyzed hydrogenation of both C=C and C=O but more selective for C=O at low space times, and at high space times forming 2-methyl-pentanol which has good fuel property, compared to ethanol or n-butanol.

For coupling reaction to higher carbon chain length, di-methyl-pentyl ethers have been selectively produced from etherification of aldehydes and alcohols on supported Pd catalysts. A yield of 79 % ether with a selectivity of 90% was observed when feeding 2-methyl-pentanal with 2-methyl-pentanol at a molar ratio 1:1 at 125^{o}C. The side product is n-pentane from decarbonylation of the aldehyde. Cross etherification of n-butanol with 2-methyl-pentanal shows a much higher rate than that observed when the alcohol or aldehyde is fed alone. This enhanced activity is consistent with the catalyst requirement for large ensembles that allow surface alkoxide species next to an η^2 adsorbed aldehyde. The ether yield increases with increased metal loadings and

increased reduction temperatures, suggesting etherification is sensitive to metal particle sizes.

Bimetallic Pd-Cu catalysts have been studied for the hydrogenation and deoxygenation of 2-methyl-pentanal. Compared to Pd catalysts, Pd-Cu shows a decrease in conversion of 2-methyl-pentanal. At low space time, 5% Pd-2.5% Cu/SiO_2 exhibits high selectivity for hydrogenation to 2-methyl-pentanol and substantially reduces decarbonylation activity compared with pure 5% Pd/SiO_2. The bimetallic shows that selectivity for etherification is much greater than Pd alone, since the parallel decarbonylation is reduced. The bimetallic maintains good ether selectivity due to its ability to readily hydrogenate the aldehyde to the intermediate alcohol and continue to form the required surface alkoxide in proximity to the remaining η^2 sites.

CHAPTER 1: INTRODUCTION

1.1. Overview

1.1.1 U.S. Energy demand and projection for renewable energy production

In the next thirty years, the projection for the U.S. transportation consumption will be more than 30 quadrillion Btu (Quads) according to the latest report from EIA Annual Energy Outlook 2010 [1]. Historical data show that the consumption for transportation fluctuates from 20 to 30 Quads from 1980 to 2008. However, if the rate of consumption is the same for the 1980-2008 period, the transportation consumption may reach 40 Quads by 2035. The total energy consumption in 2008 was 100 Quads and projected to reach 115 Quads by 2035. The total domestic production in 2008 was 75 Quads and net import was 25 Quads that is projected to be the same for the next 30 years [1].

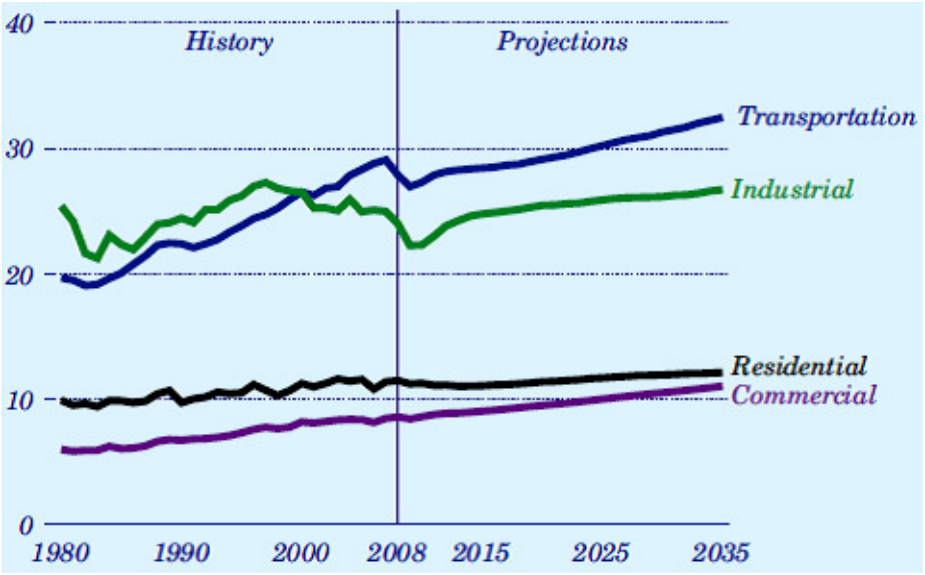

Fig. 1. 1. Delivered energy consumption by sector 1980-2035 (Quadrillion Btu) [1]

From the contributions of individual fuels in Fig. 1.2, it can be noted that the domestic liquids production is a major concern for the continued decrease from 1985 and is projected to slightly increase within 2-3 Quads for the next 30 years. The non-hydro renewables, which include biomass, are expected to increase in the future to compensate for others while keeping up with overall demand, particularly for liquid transportation fuels. In the "*Billion Ton Study*" put out in 2005 [2], the Biomass R&D Technical Advisory Committee envisioned a feasible goal of 30% replacement of petroleum consumption by 2030 and to achieve this, this would need 1 billion dry tons of biomass feedstock per year. Also, in 2005, biomass already surpassed hydropower, which is the largest domestic source of renewable energy, and provided over 3% of total energy consumption in the U.S. (>3 Quads).

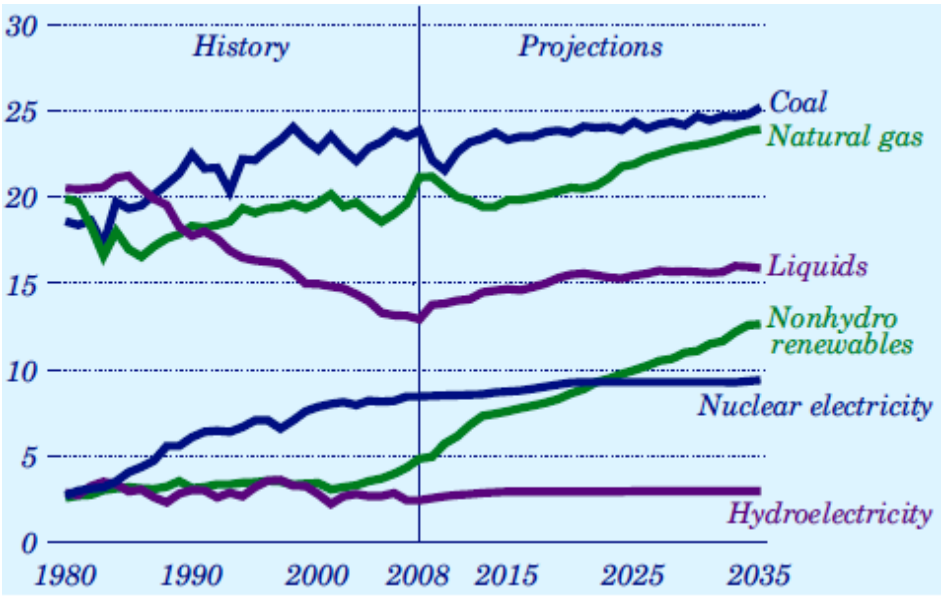

Fig. 1. 2. Energy production by fuel 1980-2035 (Quadrillion Btu) [1].

Biomass conversion has been considered as a way to provide alternatives to supply fuels and energy that reduces the consumption of conventional resources such as oil and natural gas. Furthermore, with increased environmental awareness around the world, biomass conversion has motivated efforts from researchers to the general public because the bioenergy obtained from biomass can neutralize or reduce CO_2 emissions and could potentially improve domestic production to meet the overall demand. However, the conversion processes need to take into account efficiency and other costs.

1.1.2. Biomass conversion pathways and strategies

There are various ways to convert biomass into fuels and chemicals, but the major non-biological routes have been thermochemical and catalytic conversion. Thermochemical conversion of biomass refers to non-catalytic processes that involve high temperature treatment of biomass such as pyrolysis and gasification. Gasification process has been widely known to produce gases including H_2, CO, CO_2 and CH_4 with the main objective to get high conversion to syngas (H_2 +CO) which is the platform to produce fuels and chemicals such as methanol, ethanol, dimethyl ether, FT-diesel, as shown in Fig. 1.3. Pyrolysis refers to fast pyrolysis of biomass at high temperature of 400-500^{o}C with short residence time of 1-2 seconds and high heating rate (~500^{o}C/s). The product of pyrolysis is bio-oil that is composed of thousands of compounds including aldehydes, ketones, acids, furans, phenols and other oxygenates as well as water. The crude bio-oil ($C_xH_yO_z$) that comes from fast pyrolysis has very high oxygen content that makes it unsuitable to be used directly as a fuel component, much

of these molecules are of low molecular weight from 2 to 6 carbon atoms, rather small for liquid fuels. Bio-oils are typically viscous, acidic and have low heating value [3].

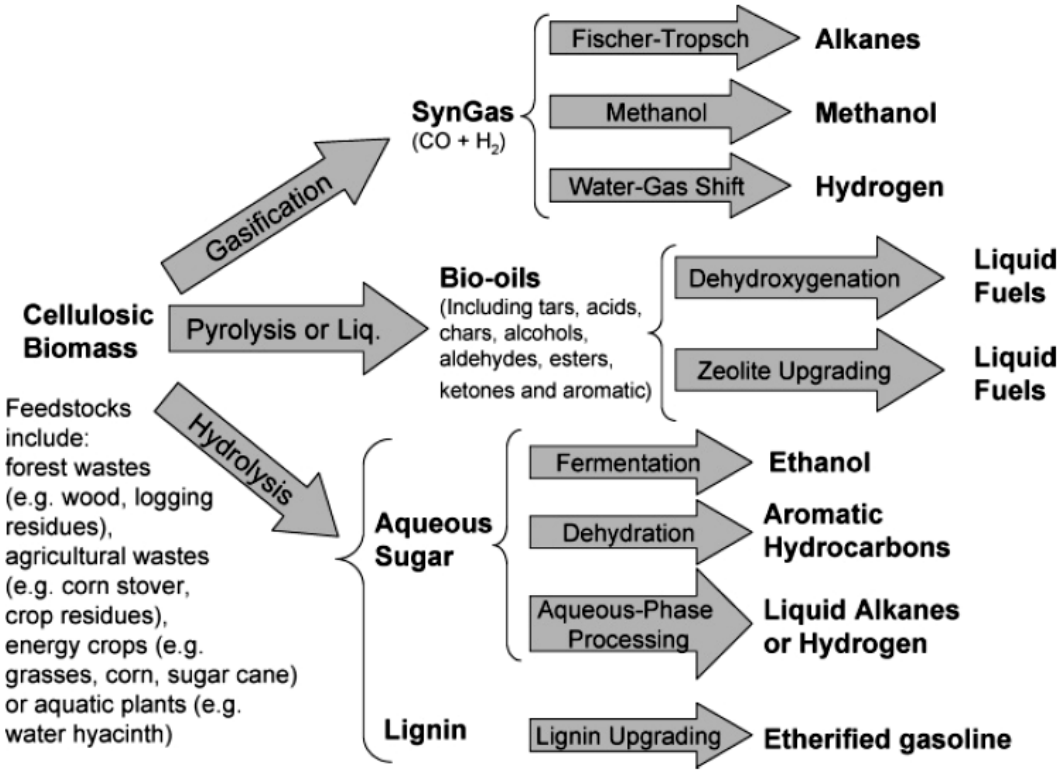

Fig. 1. 3. Strategies for production of fuels from cellulosic biomass adapted from ref. [4-5].

Upgrading bio-oil is thus necessary to stabilize and enhance the quality of the bio-oil with the removal of oxygen. The upgrading step can be carried out via deoxygenation reactions such as decarbonylation, hydrogenolysis, dehydration and condensation. However, these reactions cannot proceed thermally and require catalysts for them to take place. Heterogeneous catalysts are desirable and play an important role in

upgrading bio-oil to more valuable products. The catalyst choice is thus essential for upgrading the bio-oil and must be selective toward products that are suitable for fuel components or chemicals. Since there are thousands of oxygenates available in the bio-crude, though major groups are ketones, phenolics, furans and acids [3], it is challenging to have a "one-pot" treatment because different compounds have different chemistry toward a particular catalyst. The main strategy to upgrade bio-oil is to build up the carbon chain-length while removing oxygen via condensation reactions or alkylation followed by deoxygenation. This strategy is advantageous and efficient in that small oxygenates (C_2 –C_3 chain length) are converted to higher molecular compounds that are more desirable as fuels. One of the catalyst choices in this case is a zeolite that is capable of catalyzing condensation reactions or alkylation. A bifunctional catalyst such as metal zeolite would also be advantageous since hydrogenation or hydrodeoxygenation can take place via the metal component. Other condensation reactions suitable for the purpose of building up chain length include aldol condensation, ketonization and etherification that can be catalyzed by acid/base, oxide and metal catalysts.

For non-aromatic oxygenates, particularly light oxygenates with multifunctional groups (or conjugated C=C or C=O present), upgrading these compounds with hydrotreating or hydrodeoxygenation to more stable products such as alcohol or hydrocarbons is possible. However, light hydrocarbons resulting from hydrodeoxygenation including decarbonylation, hydrogenolysis and cracking are less

valuable due to their short chain length and low octane number that makes them unsuitable for fuels.

For ring-type structures, the aromatic oxygenates are very tough to deoxygenate with metal catalysts because it is impossible for the substituted C of the ring (bonded to the OH group) to interact with the metal due to its full valency. For example, phenols are very hard to deoxygenate. However, once the ring is partially hydrogenated in an environment of H_2, this C can bond with the metal resulting in hydrodeoxygenation that yields aromatics such as benzene, toluene, cyclohexene, cyclohexane, methyl cyclohexane, and methyl cyclopentane [6]. However, the hydrogenolysis process requires consumption of H_2 (5MPa) and the products such as methylcyclohexane or cyclohexane with saturated ring are not desirable. Note that on supports containing acidic sites, dehydration reaction is also important for deoxygenation of cyclohexanol to aromatics. Different from saturated aromatics, toluene and other alkyl benzenes (but not benzene) are more valuable and more suitable for fuel components (higher octane value and taking up less hydrogen).

A strategy of molecular engineering applied for catalytic upgrading of fuels is shown in Fig. 1.4. from ref. [7] , courtesy of Dr. Crossley et al. The methodology is to develop a database of properties of possible molecular components, which can either be obtained experimentally or predicted with reliable methods based on molecular structure (pathway 1). One also needs to obtain fundamental understanding on how

different catalysts would result in a particular product (pathway 2). This understanding is necessary to help decide which direction to achieve a desired product. Both pathways 1 and 2 are identified as molecular engineering approach that helps for a development of an empirical approach shown as path 3. By having a robust database developed with existing literature and continued experiments, one can rationally design the catalyst and reaction conditions to optimize specific structures, resulting in the optimum properties.

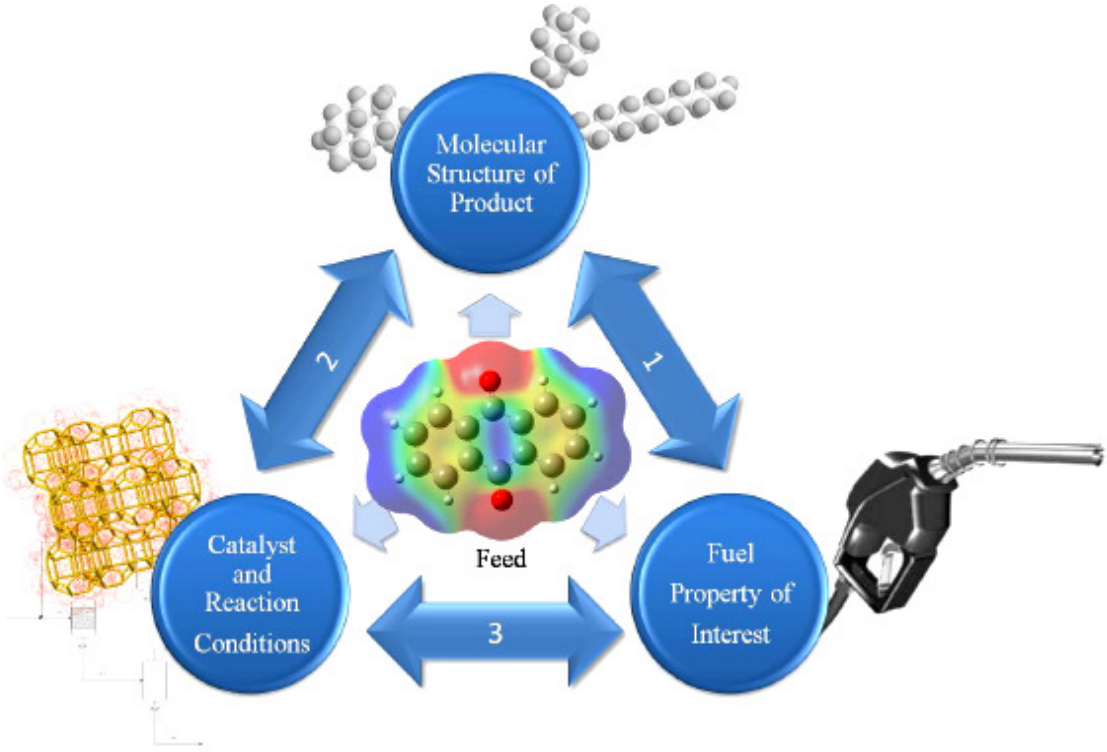

.

Fig. 1. 4. Schematic overview of molecular engineering strategy adapted from ref. [7].

With the purpose of upgrading the oxygenates to more valuable products, an example will be shown later in Chapter 3 with upgrading of a model compound aldehyde, to an alcohol that can be used as a gasoline component. To decide whether the upgrading step is worthwhile, we applied the molecular strategy approach to predict the value of the end products. Special thanks and appreciation to Dr. Steven Crossley for his evaluation of the alcohol and other oxygenate properties, using a QSAR model to predict the fuel property of different products, particularly the octane value. His approach is very fundamental and applicable for both hydrocarbons and biomass conversion. Not only does the methodology help predicting the properties of the desired products using a robust database collected from experiments and literature, the model also predicts the relationship between catalyst choice and potential selectivity for the products [7].

1.1.3. Biomass feedstock selection

Cellulosic feedstocks are abundant and available around the U.S. Particularly in Oklahoma area, switch grass is considered a cheap viable feedstock that can be grown in vast lands economically without competing with the interest for other crops, for example, corn for food. For Oklahoma, The Oklahoma Bioenergy Center (OBC) already has planted a 1,100 acre test field for cellulosic energy crops, such as switchgrass and sorghum to help meet the U.S. demand for bioenergy. The switchgrass plant will be of 1,000 acres located near Guymon, Oklahoma, and is the

first of its size in the world dedicating to biomass production. Additional acreage will be set for sorghum and switchgrass at another location[1].

Algae are another bioenergy source, of triglycerides for biodiesel production. They have high growth rates, consume solar energy and can grow in conditions that are not favorable for other biomass crops [5]. Commercial production of triglycerides from microalgae has been estimated to yield 72,000 L/ha-year (390 boe/ha-year) and it could increase as high as 130,000 L/ha-year (700 boe/ha-year) with further research [8]. Thus, triglyceride yield from algae is 45-220 times higher than that from terrestrial biomasses such as corn or switch grass, that ranges from 650 to 1590 L/ha-year [9] .

From "*BP Statistical Review of World Energy 2009*", the R/P ratio (Proved Reserves/Production ratio) of total Asia is 14.5 years, suggesting that in the next decade, Asia needs alternative energy to supply the energy demand beside crude oil and natural gas. For renewable energy, Asian countries are developing programs, particularly for biodiesel production from agricultural crops such as jatropha, palm, and rice straw.

Glycerol is a by-product from conventional biodiesel production that also can be used as a feedstock for production of fuels and chemicals. The crude glycerol can be

[1] http://okbioenergycenter.org/noble-foundation-to-plant-1000-acres-of-switchgrass-in-the-oklahoma-panhandle/

converted to aromatics and other chemicals (such as acrolein or propanal) in the presence of zeolites such as HZSM-5, HY and HZSM-22 [10]. Light oxygenates, such as acrolein and propanal, already have less oxygen than the original glycerol molecule. They are also great feedstock to build up carbon chain length via condensation reaction in acid or base catalysts. From previous work by Amen et al. [11], 2-methyl-2-pentenal can be selectively produced from the aldol condensation of propanal in basic catalysts such as MgO, NaCsX or Hydrotalcite. The unsaturated C_6 aldehyde can be upgraded to molecules that are more stable and suitable for fuels and is one of the subjects of this study.

1.2. Literature review

The concept of bio-refinery is efficient and feasible when there is available hydrogen nearby or the plant is integrated with an existing refinery. For a 100% biomass feedstock bio-refinery, H_2 can be produced from reforming of bio-mass or gasification, as shown in Fig. 1.5. Gasification is a non-catalytic process that requires high temperature and long residence time (750-900^{o}C, > 10s) relative to "fast pyrolysis" that is typically at 400^o-500^{o}C and 1-2s residence time. The products from gasification contain mostly H_2 and CO, that needs further conversion to more H_2 via catalytic water-gas-shift reaction, if H_2 production is the main target.

Hydrogen production via catalytic aqueous phase reforming of biomass sugars has been carried out extensively by the Dumesic group [12-16]. They first started trying aqueous phase reforming (APR) of various feedstocks to hydrogen back in 2002. The biomass sources include glucose, sorbitol, glycerol, ethylene glycol and methanol that are typical of polyols going from more to less in order. The original catalyst is 3 wt% Pt/Al_2O_3 and operating conditions are 498K and 538K with pressures of 29 to 56 bars, respectively. They presented reaction pathways of oxygenates conversion to H_2 and alkanes over metal catalysts, as shown in Fig. 1.5. The chemistry of C-O and C-C bond cleavage has been discussed. The O-H and C-H bond activation has also been studied [17]. On Pt catalyst, Pt-C are more stable than Pt-O, so the metal surface preferentially bonds with the adsorbate via Pt-C bonds that further facilitates C-C bond cleavage producing CO and H_2. They also found that the H_2 selectivity improves in the order of glucose < sorbitol < glycerol < ethylene glycol < methanol while the production of alkanes follow the opposite trend of H_2 for these feeds. However, one of the pitfalls of going all the way to alkanes is that it will need substantial amount of H_2 to deoxygenate although this H_2 may be produced *in situ*. Moreover, the end product n-hexane with complete oxygen removal from C_6 glucose, does not possess any desirable properties as a fuel component since it has no branching and thus low octane value [18]. An alcohol, on the other hand, may be more suitable as compared to alcohol fuels such as ethanol or n-butanol.

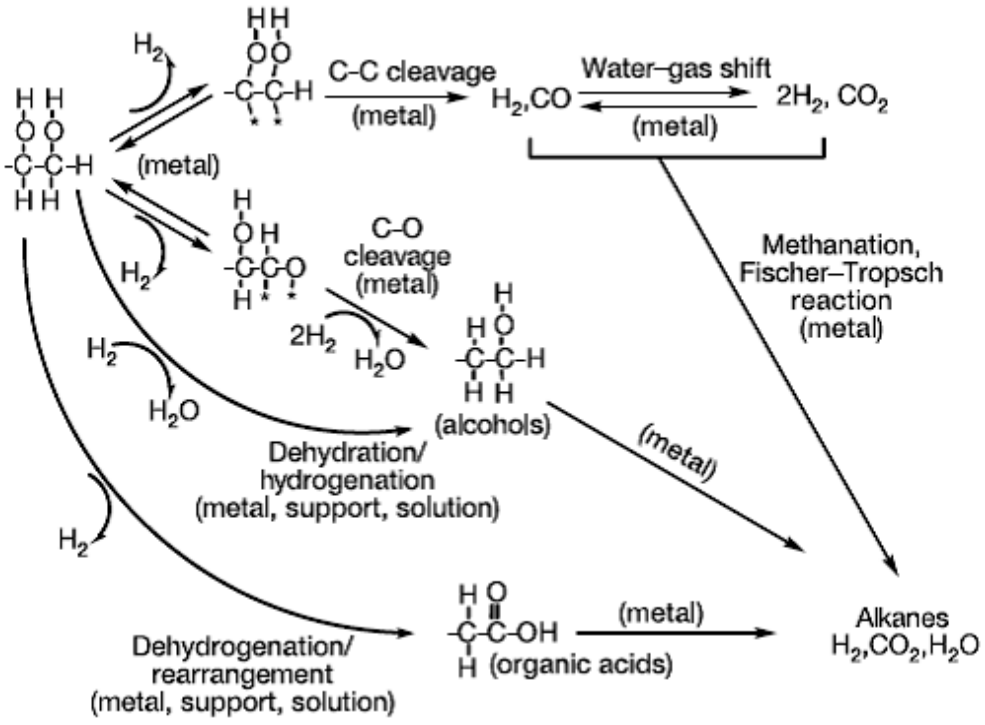

Fig. 1. 5. Reaction pathways of H_2 production oxygenates on metal catalysts adapted from ref. [12]

The traditional biodiesel production has been transesterification that produces 3 moles of fatty acid esters and 1 mole of glycerol from a triglyceride molecule, which is representative for a vegetable oil feedstock. The fatty esters still have oxygen molecules in them with the presence of carboxylic groups that make them not fungible with standard diesel. Murzin et al. have extensively studied the deoxygenation of fatty acids for production of green diesel [19-21], that is long chain neat hydrocarbons, in this case, $C_{17}H_{34}$ or $C_{18}H_{38}$ from stearic acid feed. The proposed reaction pathways are shown in Fig. 1.6. The reactions were carried in a semi-batch system at 300^{o}C and 6 bar. It has been found that Pd/C is highly active and selective in deoxygenation of

stearic acid to C_{17} hydrocarbons. The main deoxygenation reactions include decarboxylation, decarbonylation and hydrogenolysis (the author simply termed hydrogenolysis as hydrogenation, however, the C-O bond is activated and broken over metal catalysts)

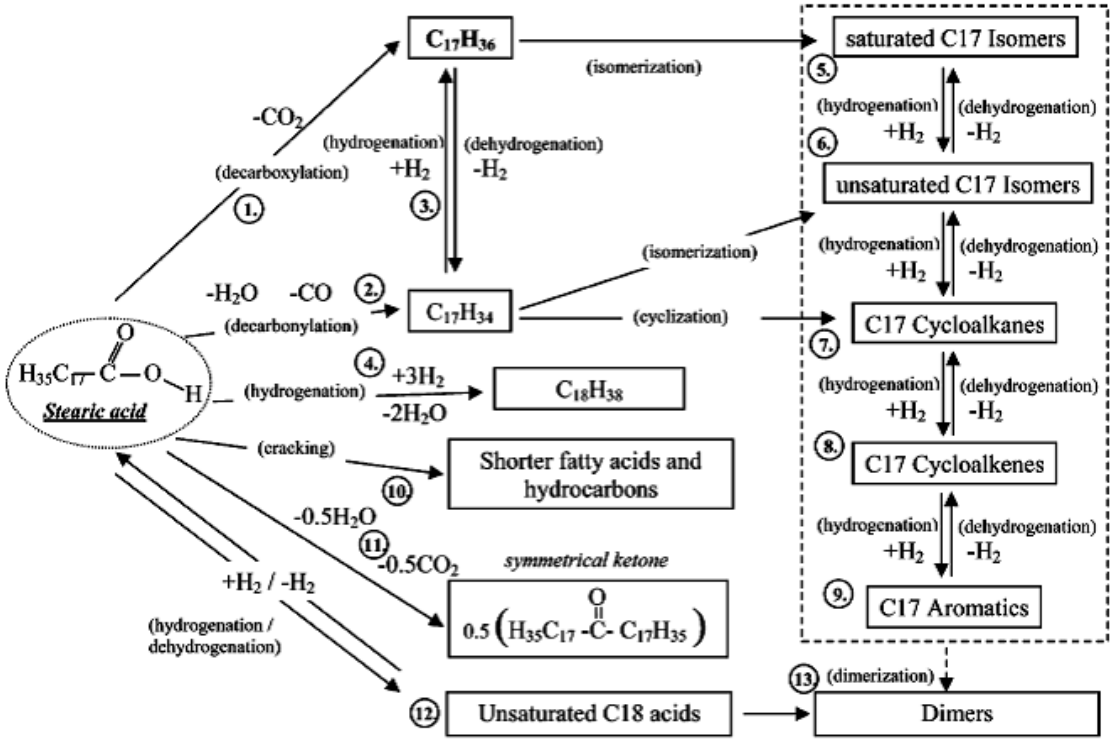

Fig. 1. 6. Reaction routs of stearic acid conversion over heterogenous catalyst at 300°C in inert atmosphere adapted from ref. [12]

According to Murzin et al. [19], from the gas phase product analysis, it was found that the decarboxylation occurs extensively on Pd/C while decarbonylation is predominant on Pt/C. The side reactions include hydrogenation, dehydrogenation,

cyclization, dimerization, ketonization, and cracking with various extents depending on the catalysts.

		ΔG_{573} (kJ/mol)	ΔH_{573} (kJ/mol)
Decarboxylation	R-COOH → R-H + CO_2	-83.5	9.2
Decarbonylation	R-COOH → R'-H + CO (g) + H_2O (g)	-17.0	179.1
	R-COOH + H_2 (g) → R-H + CO (g) + H_2O (g)	-67.6	48.1
Hydrogenolysis	R-COOH + 3H_2 (g) → R-CH_3 + 2H_2O (g)	-86.1	-115.0

where *R = saturated alkyl group* *R' = unsaturated alkyl group*

(Adapted from ref. [12])

Dehydration R-OH → olefin + H_2O at acid sites in the support

The decarbonylation and decarboxylation are quite common on the fatty acids feedstock. However, the competitive extents of these two reactions are not well reported by existing literature, for examples, the quantification of CO vs. CO_2 that are distinctive tail gases from the two reactions, although the water-gas-shift reaction may complicate the matter. Thus, even if the CO_2 is more than CO, it does not mean that decarboxylation might be predominant over decarbonylation, but other species concentrations need to be taken into considerations as well.

Ozkan et al. [22] studied the hydrogenation of aldehydes over sulfided Ni-Mo/Al_2O_3 catalysts. It was found that the main reaction is the hydrogenation of the

C=O bond (the aldehydes in the study are mostly saturated aldehydes with no C=C bond). The side reactions, however, are the self-condensation of aldehydes and condensation of aldehydes and alcohols over acid-base bifunctional sites over the exposed Al_2O_3 support. They further showed that the relative reactivity of the aldehydes follow the order: propanal > hexanal > 2-ethyl-butanal > 2-methyl-pentanal. The selectivity for heavies follow the same trend, that is, propanal > hexanal > 2-ethyl-butanal > 2-methyl-pentanal while the selectivity for lights follow the opposite direction of the feeds.

For unsaturated aldehydes with both C=C and C=O present and may be conjugated to each other, Ponec et al. [23-25] extensively studied the activity and selectivity of hydrogenation on metals as well as the effect of promoters on these reactions. They found that for all Pt based catalysts, the selectivity toward unsaturated alcohol increased with increasing substitution on the terminal olefinic carbon atom (due to steric hindrance of the olefinic group) [25]. They studied the effect of feed and substitution on the functional group but did not discuss much about the effect of the metals or their interaction with the molecules. As seen in fig. 1.7, Pt alone does not selectively hydrogenate any feed to unsaturated alcohol. Adding Na as a promoter on to Pt does not seem to improve but in fact decrease the selectivity. Promoters such as Fe, Ga and Sn seem to give highest selectivity, particularly for the 3-methyl-crotonaldehyde where the C=C group has a methyl substituent.

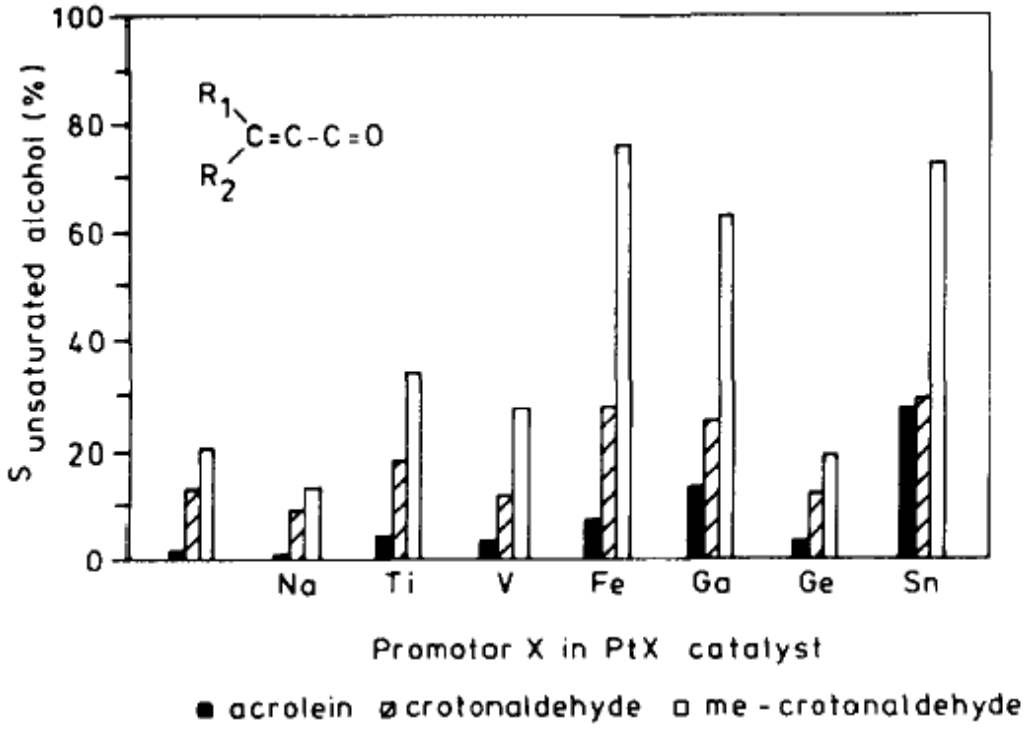

Fig. 1. 7. Selectivity to unsaturated alcohol for hydrogenation of acrolein, crotonaldehyde, and 3-methyl-crotonaldehyde over promoted platinum catalysts adapted from ref. [25].

In a mechanistic study, Delbecq and Sautet [26] employed theoretical calculations to investigate the interaction of small aldehydes and ketones on Pt(111) , Pt(110) and Pd(111) surfaces. The probe molecules are formaldehyde, acetaldehyde and acetone. They found that all the molecules preferred η^2 di-σ adsorption geometry on all surfaces, except for acetone on Pt (111) where η^1 on top is the preferred mode. In this study, they laid important foundations for calculations of the electronic effect of the metal surfaces and the adsorbates. The binding energies of various modes of

adsorption and the electron transfer have been compared and analyzed for different metal cluster sizes.

Barteau et al. [27-28] investigated the reaction pathways of oxygenates on transition metal surfaces. They found that the alcohol adsorbs on the surface as an alkoxide while the aldehyde adsorbs as an η^1 or η^2 geometry where the latter is a more stable form that could further transform to acyl and ketene that leads to decarbonylation with formation of CO and hydrocarbon species. These findings are very relevant to our study since the probe molecules under investigation are also aldehydes and alcohols, either as individuals or as mixtures. The adsorption modes are important in that it provides insights about the interaction of the molecules with Group VIII metals, particularly chemistry at the metal surfaces. Various modes of adsorption result in different product distribution/selectivity depending on the reaction conditions and the type of catalyst. More details, discussion and experimental works are shown in Chapter 4.

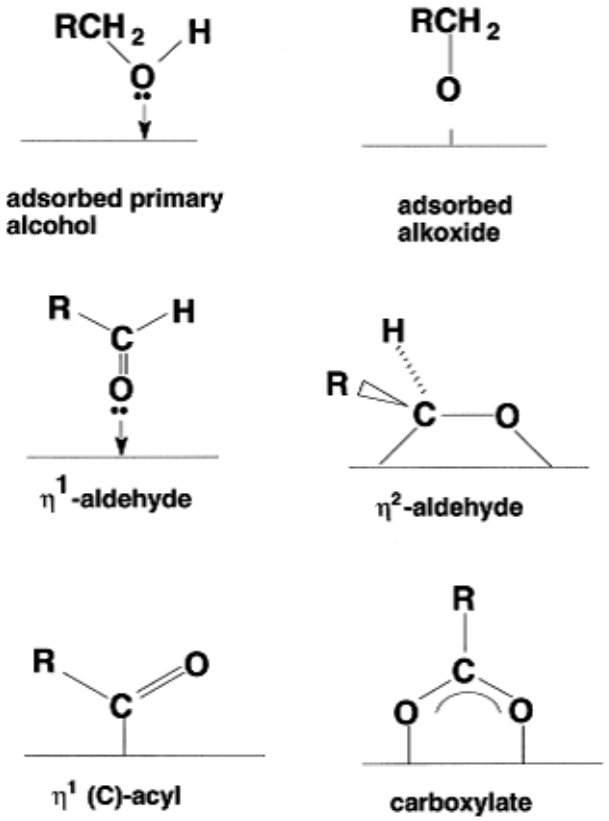

Fig. 1. 8. Oxygenate intermediates observed on transition metal surfaces adapted from ref. [27]

For deoxygenation of ring-type structures, such as phenolics, Bredenberg et al. [6] has studied the hydrotreating of phenol, o-cresol, anisol, and guaiacol on Ni-Mo/SiO_2 – Al_2O_3 in a fixed bed reactor at 250-350^oC, and 5 MP hydrogen pressure. Phenol and o-cresol were very stable under these reaction conditions. Anisole and guiacol yielded mainly phenol, o-cresol and 2,6-dimethylphenol. Guaiacol first converted to pyrocatechol at 250-275^oC, and then further converted to phenol and cresols at higher temperatures. The conversion of phenol gives C_6 hydrocarbons including benzene, cyclohexane, cyclohexane and methylcyclopentane. Yang et al. [29] also studied the hydrodeoxygenation of bio-crude using phenol as a model compound on sulfided

CoMo and CoMoP/MgO catalysts. They found that both catalysts are effective to deoxygenate phenol to benzene and cyclohexyl-aromatics, with the phosphorus promoted being superior in HDO activity. They and others [29-30] proposed that the HDO of phenol may proceed via hydrogenolysis to benzene or hydrogenation of cyclohexanol as an intermediate followed by dehydration. However, the dehydration pathway is also important for these reactions, which are catalyzed by acid sites present in the support. The pathway is summarized in Fig. 1.9. The first reaction of phenol to benzene and cyclohexane shown is not a one-step reaction but rather via sequential hydrogenation (to cyclohexane), and hydrogenolysis/dehydration followed by dehydrogenation (to benzene).

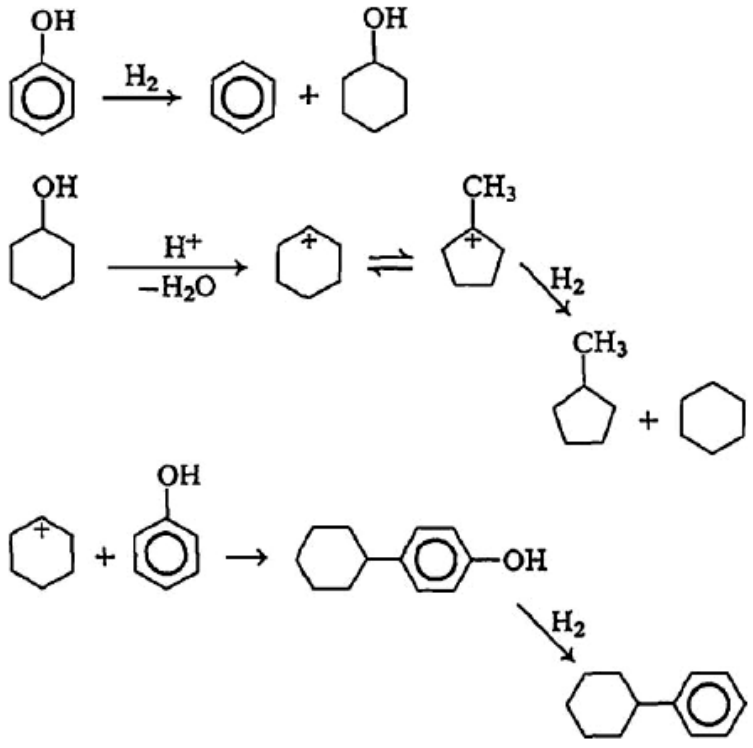

Fig. 1. 9.Possible phenol hydrotreating mechanism adapted from ref. [29-30]

Lewis et al. [31] studied the upgrading treatment of model mixed feed of bio-oil on Pt/Al_2O_3 and found that the product mixture has substantially decreased in oxygen content. (from 41.4 wt% to 2.8wt %). The model mixed feed contains methanol (5 wt%), acetaldehyde (12 wt%), acetic acid (14 wt%), glyoxal (4 wt%), acetol (8 wt%), glucose (8 wt%), guaicol (17 wt%), furfural (4 wt%), vanillin (8 wt%) and de-ionized water (20 wt%). They analyzed the composition of the products by GCMS and found high composition of aromatics, naphthalene and reduced oxygenates and phenolics. It is interesting to note that alkylation of the rings was observed and attributed to the effect of the acid support while the metal function is removing the oxygen or hydrogenation with H_2 produced in situ. The GC-MS samples of the product after treatment at 350^{o}C is shown in Fig. 1.10 a without catalyst and in Fig. 1.10 b with Pt/Al_2O_3. Without catalyst, the feed remains the same showing no thermal conversion of the model mixed feed at 350^{o}C. However, the products in Fig. 1.10 b show substantial hydrocarbon formation and deoxygenation in the presence of Pt/Al_2O_3.

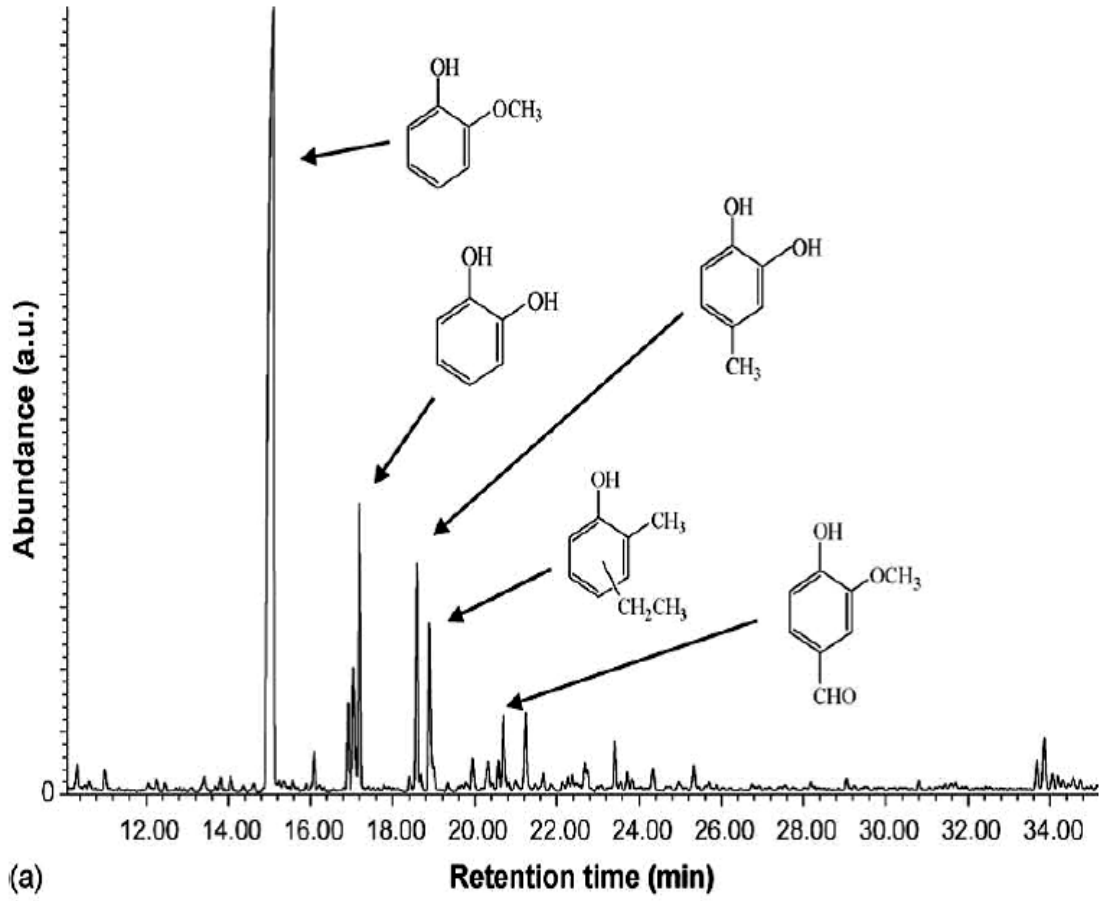
Abundance (a.u.)
0
12.00 14.00 16.00 18.00 20.00 22.00 24.00 26.00 28.00 30.00 32.00 34.00
Retention time (min)
(a)
OH
OCH3
OH
OH
OH
OH
CH3
OH
CH3
CH2CH3
OH
OCH3
CHO

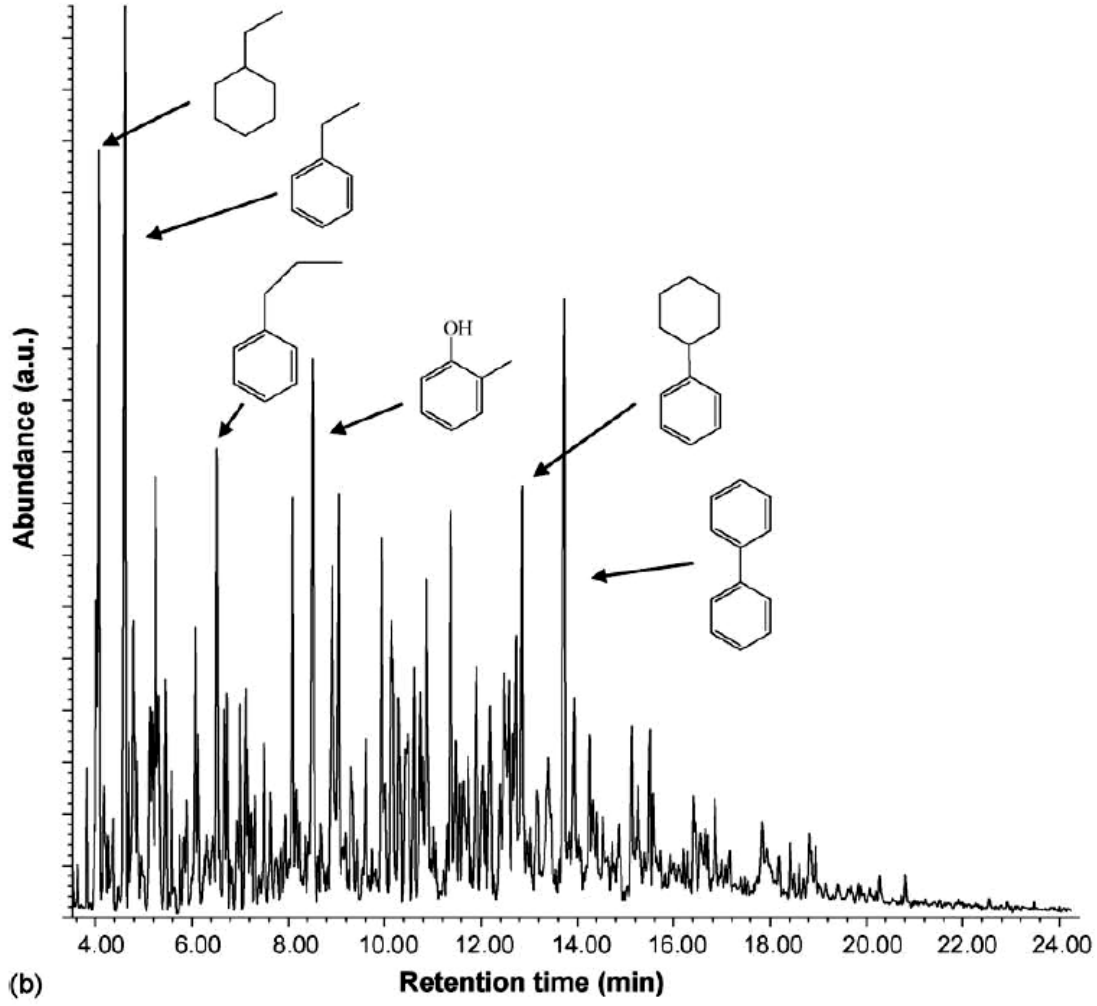

Fig. 1. 10. (a) Gas chromatogram of oil product obtained from thermal cracking of model bio-oil at 350 ^{o}C. (b) Gas chromatogram of oil product obtained from treatment of model bio-oil with Pt/Al_2O_3 (4 h reaction time) adapted from ref. [31]

For coupling reactions, the ketonization reaction is advantageous in converting carboxylic acids and ketones to longer ketones that can then be upgraded to hydrocarbons suitable for fuels [32-34]. In our catalysis group, Anirudh Gangadharan has been investigating this reaction along with the aldol condensation reaction on mixed oxides CeO_2-ZrO_2 and found good results for this approach. A recent report by Crossley et al [35] showed that hydrodeoxygenation and condensation reactions can be achieved on a phase-transfer selective catalyst containing a supported metal that stabilizes emulsions in a biphasic system. Another type of coupling reaction is etherification reacting an aldehyde and alcohol on supported metals and has been studied in Chapter 4 and 5.

1.3. Objective

The objective of this research is to study the reaction fundamentals and interactions of the bio-mass derived molecules such as aldehydes and alcohols with supported metal catalysts. These feeds are investigated individually or combined in mixtures to study their conversion and the product selectivities, whether via hydrogenation, deoxygenation or condensation reactions. With the understandings of the interaction between the feeds and the catalysts, one can control the selectivity of the products and may apply the insights for upgrading more complex feedstocks such as bio-oil with multiple components into fuels and chemicals.

The following chapters in this thesis will show examples of hydrogenation and hydrodeoxygenation of biomass-derived oxygenated compounds into more valuable products that can be used as fuel components, for either gasoline or diesel blends. The methodology will be an experimental approach to study the conversion and product selectivity. Different metal catalysts are prepared and studied for their interaction with the feed and selectivity toward desired products.

From the understanding of the metal catalysis in the conversion of oxygenates for bio-oil upgrading, the development of catalysts can evolve to more practical and novel designs such as bi-functional catalysts that are composed of metal and acid/base

functions, or metals anchored on supports such as single wall nanotubes-SiO_2 for catalyzing multiphase reactions.

References

[1] http://www.eia.doe.gov/oiaf/aeo/pdf/overview.pdf.

[2] http://feedstockreview.ornl.gov/pdf/billion_ton_vision.pdf.

[3] D. Mohan, C.U. Pittman, P.H. Steele, *Energ Fuel*, 20 (2006) 848.

[4] G.W. Huber, J.A. Dumesic, *Catal. Today.*, 111 (2006) 119.

[5] G.W. Huber, S. Iborra, A. Corma, *Chem. Rev.*, 106 (2006) 4044.

[6] J.B.S. Bredenberg, M. Huuska, J. Raty, M. Korpio, *J. Catal.*, 77 (1982) 242.

[7] S.P. Crossley, Vol. PhD, University of Oklahoma, 2009.

[8] A.M. Hill, D.A. Feinberg, Fuel Products from Microalgae, National Renewable Energy Laboratory: Golden, CO., 1984.

[9] D.L. Klass, Biomass for Renewable Energy, Fuels and Chemicals, Academic Press: San Diego, 1998.

[10] T.Q. Hoang, Vol. PhD Desertation, University of Oklahoma, 2010.

[11] Q.V. Amen, Vol. M.S. Desertation, University of Oklahoma, 2009.

[12] R.D. Cortright, R.R. Davda, J.A. Dumesic, *Nature*, 418 (2002) 964.

[13] R.R. Davda, J.A. Dumesic, *Angew. Chem. Int. Ed. Engl.*, 42 (2003) 4068.

[14] R.R. Davda, J.A. Dumesic, *Chem Commun (Camb)*, (2004) 36.

[15] G.W. Huber, R.D. Cortright, J.A. Dumesic, *Angew Chem Int Ed Engl*, 43 (2004) 1549.

[16] G.W. Huber, J.W. Shabaker, J.A. Dumesic, *Science*, 300 (2003) 2075.

[17] J. Greeley, M. Mavrikakis, *JACS*, 124 (2002) 7193.

[18] R.H. Heck, N.Y. Chen, *Ind Eng Chem Res*, 32 (1993) 1003.

[19] M. Snare, I. Kubickova, P. Maki-Arvela, K. Eranen, D.Y. Murzin, *Ind Eng Chem Res*, 45 (2006) 5708.

[20] P. Maki-Arvela, M. Snare, K. Eranen, J. Myllyoja, D.Y. Murzin, *Fuel*, 87 (2008) 3543.

[21] P. Maki-Arvela, I. Kubickova, M. Snare, K. Eranen, D.Y. Murzin, *Energ Fuel*, 21 (2007) 30.

[22] X.Q. Wang, R.Y. Saleh, U.S. Ozkan, *J. Catal.*, 231 (2005) 20.

[23] T.B.L.W. Marinelli, J.H. Vleeming, V. Ponec, D. Wang, D.G. Blackmond, D. Arntz, G. Jannes, K. Kunimori, C.H. Rochester, *Stud. Surf. Sci. Catal.*, 75 (1993) 1211.

[24] V. Ponec, *Appl. Catal. A-Gen*, 149 (1997) 27.

[25] T.B.L.W. Marinelli, S. Nabuurs, V. Ponec, *J. Catal.*, 151 (1995) 431.

[26] F. Delbecq, P. Sautet, *Surf. Sci.*, 295 (1993) 353.

[27] M. Mavrikakis, M.A. Barteau, *J Mol Catal a-Chem*, 131 (1998) 135.

[28] J.L. Davis, M.A. Barteau, *Surf. Sci.*, 235 (1990) 235.

[29] Y. Yang, A. Gilbert, C.B. Xu, *Appl. Catal. A-Gen*, 360 (2009) 242.

[30] R.K.M.R. Kallury, T.T. Tidwell, D.G.B. Boocock, D.H.L. Chow, *Can J Chem*, 62 (1984) 2540.

[31] C.A. Fisk, T. Morgan, Y.Y. Ji, M. Crocker, C. Crofcheck, S.A. Lewis, *Appl. Catal. A-Gen*, 358 (2009) 150.

[32] R. Pestman, A. van Duijne, J.A.Z. Pieterse, V. Ponec, *J. Mol. Catal. A: Chem.*, 103 (1995) 175.

[33] E.L. Kunkes, E.I. Gurbuz, J.A. Dumesic, *J. Catal.*, 266 (2009) 236.

[34] E.I. Gürbüz, E.L. Kunkes, J.A. Dumesic, *Applied Catalysis B: Environmental*, In Press, Corrected Proof.

[35] S. Crossley, J. Faria, M. Shen, D.E. Resasco, *Science*, 327 (2010) 68.

CHAPTER 2: EXPERIMENTAL SETUP

2.1. Feeds

The biomass-derived compounds in this study are organic chemicals including different aldehydes and alcohols. They are namely 2-methyl-2-pentenal (97% grade), 2-methyl-pentanal (98% grade), 2-methyl-pentanol, propanal (99% grade), propanal (97%), propanol (99.7%) and n-butanol (>99% grade). These chemicals were purchased from Sigma-Aldrich.

2.2. Reactor set-up

A schematic flow diagram of the reactor is shown in Fig. 2.1. A feed pump, single syringe, infusion pump KD Scientific KDS100**,** obtained from Fischer Scientific, was used to deliver organic feeds. A typical flow rate for the experiments ranged from 0.05 to 0.2 ml/hr. The carrier gas H_2 used in study was kept constant with a molar ratio of 12:1 relative to the molar flow rate of the organic feed. The weight-to-flow ratio (W/F - g of catalyst/g of organic feed per hour) represents the time necessary for the organic feed spent on a certain amount of the catalyst to achieve conversion. However, the true residence time is determined by the carrier gas flow rate and the volume of the catalyst bed. For example, for a gas flow rate of H_2 of 36 cc/min, given the inner diameter of the reactor to be 0.295 in or 0.75 cm and the catalyst bed depth of 1 cm, the true residence time through the bed is 0.012 min, or 0.74 sec. The residence time was maintained by keeping the same molar ratio at 12:1 of the carrier gas and the organic flow rate for a certain amount of catalyst.

The reactor is an 3/8 in-OD stainless steel tube (ID = 0.295 in) with an overall length of 20 inches inside a one heating zone hinged split tube furnace purchased from Thermcraft Inc. The heating element is located in the center of the furnace (10 in from the top). To measure the temperature of the catalyst bed, an Omega quick connect thermocouple SMP-NP K-type was connected inside the reactor tube with the tip touching the bottom of the catalyst bed, that is supported by a thin layer of quartz wool. The temperature of the bed was calibrated to vary within $5^{o}\pm1^{o}$C per cm height by varying the tip position of the thermocouple. The thermocouple was fitted with the reactor tube using Swagelok fitting and connected to a temperature controller to measure and control the temperature in the reactor. Heating tapes, which were connected to a Variac portable transformer, were wrapped around reactor lines exposed outside the furnace to keep the feed and products vaporized. A secondary thermocouple with removable miniature connectors, SCASS-125G-6 K-type purchased from Omega was used to monitor the temperature of the heating lines which were normally kept at 180-200^{o}C. This secondary thermocouple was connected to a handheld thermometer CL3512A that were also obtained from Omega. The actual apparatus picture is shown in Fig. 2.2.

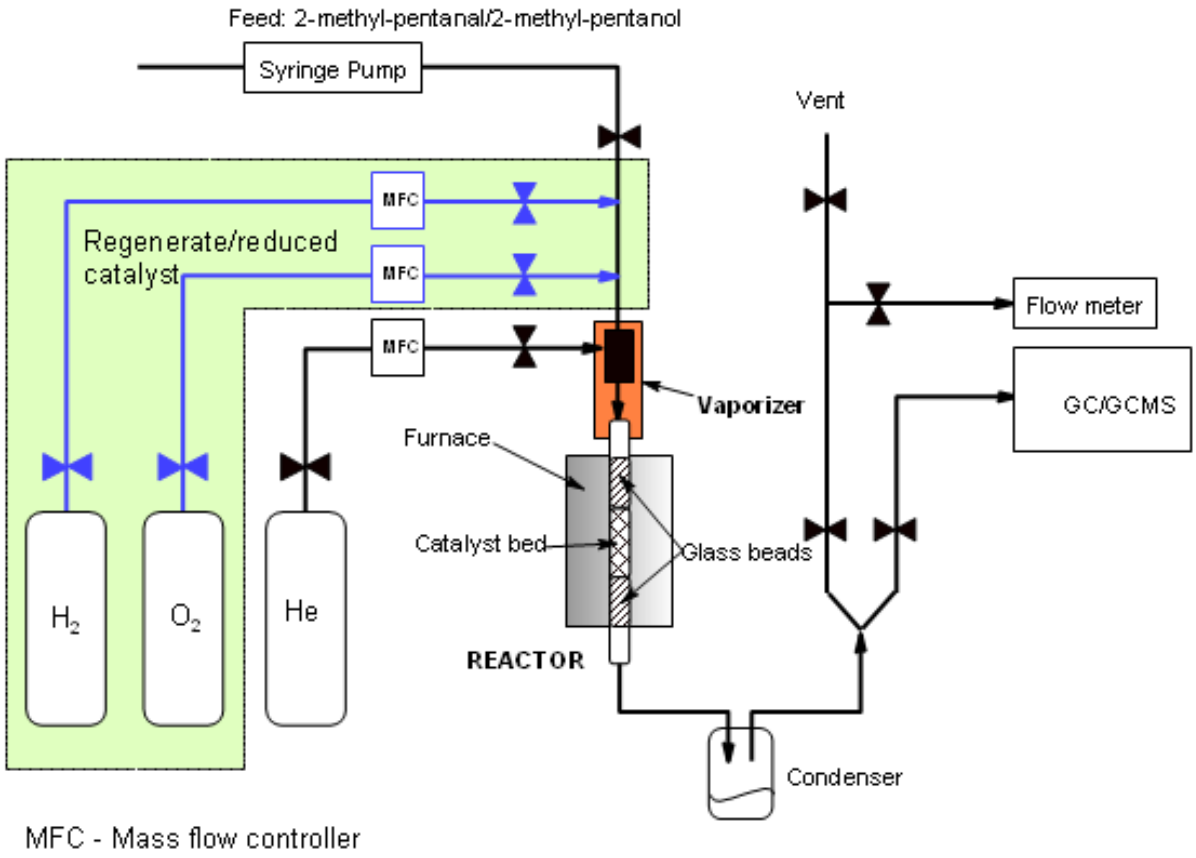

Fig. 2. 1. Schematic chart flow equipments used for hydrogenation and hydrodeoxygenation of biomass-derived molecules.

Fig. 2. 2. Actual equipment setup for hydrogenation and hydrodeoxygenation of biomass-derived molecules

2.3. Catalyst preparation

The catalysts were prepared by incipient wetness impregnation of the metal precursors on precipitated silica (HiSil 210 obtained from Pittsburg Plate Glass Co.) having a surface area of 135 m^2/g. The metal loading in each catalyst was calculated based on the amount of metal precursor incorporated in the catalyst by impregnation.

The liquid/solid ratio used to achieve incipient wetness was 1.26 ml/g. The precursors of Pt, Pd and Cu metals were H_2PtCl_6, $Pd(NO_3)_2$ and $Cu(NO_3)_2.2.5H_2O$, respectively, purchased from Sigma Aldrich. After impregnation, the catalysts were dried overnight in an oven, and then calcined in air at 400^oC for 4 hours. The bimetallic Pd-Cu were prepared by sequential impregnation of $Cu(NO_3)_2$. $2.5H_2O$ onto the previously calcined Pd/SiO_2 catalyst.

2.4. Catalyst characterization

2.4.1. CO chemisorption

CO chemisorption was used to determine dispersion of the metal catalysts. It was conducted in a dynamic chemisorption unit, including a pulse system with an SRI Model 310C Gas Chromatograph equipped with a Thermal Conductivity Detector (TCD). All the catalysts were reduced in H_2 with a ramp rate of 10^oC/min, held for 1 hour, then flushed in He for 30 min and cooled down to room temperature before injecting CO. A pre-mixed gas of 5% CO in He was used for pulse injection with a 0.1 ml loop size. CO adsorption on the blank SiO_2 was carried out at room temperature to subtract any adsorption on the support. However, no CO adsorption was detected.

2.4.2. Transmission Electron Microscopy (TEM)

The average particle size for all pre-reduced catalysts was obtained by TEM. The TEM images were obtained on a JEOL JEM-2000FX TEM. For this analysis, a suspension in ethanol was made by stirring the solid sample in an ultrasonic bath for 10 min. A few drops of the resulting suspension were deposited on a TEM grid and subsequently dried and evacuated before the analysis.

2.4.3. Temperature Programmed Reduction (TPR)

100 to 200 mg of catalyst was loaded into a fixed bed 1/8-in ID quartz tube reactor. 5% H_2 in Argon obtained from AirGas Co. was used as the carrier in order to measure the H_2 uptake. The outlet was connected to a tube filled with Drierite (to absorb moisture produced during the reduction) and then to a TCD detector. A temperature ramp rate of 10 ^{o}C/min was used.

2.4.4 In situ CO FTIR.

DRIFTS experiments were carried out in a Perkin Elmer Spectrum 100 FTIR Spectrometer equipped with an MCT detector and a Reaction Chamber (HVC-DRP) fitted with KBr windows (Harrick Scientific Products, Inc). 50-100 mg of catalyst was loaded to the reaction cell and reduced in H_2 flowing at 30 sccm by heating at a 10^{o}C/min ramp rate to 200^{o}C, then holding for 1 hour followed by flushing with He

for 30 minutes before cooling to room temperature. CO (5% in He) then flowed through the chamber for 30 minutes at room temperature and that was then flushed with He for 20 min before sample spectra were taken. Spectra were acquired at a resolution of 4 cm^{-1} averaging 64 scans.

2.5. Catalyst testing

Catalytic activity measurements were carried out in a continuous flow system that includes a syringe pump delivering the organic feed to a heated line into a stream of H_2 that feeds to a 20-in long 3/8 in-OD (ID =0.295 in) stainless steel tube within an electric furnace. Loads of 50 to 400 mg catalysts were used, with the appropriate flow rate to achieve the desired space time (W/F). Operating conditions were from 125°-400°C and atmospheric pressure. Experiments were continued for 2-3 h. All the lines were heated with heating tapes to keep the feed and products in gas phase. The carrier gas, H_2, was used to reduce the catalyst and also flown during reaction with the organic feed at a relative molar ratio 12:1. Quantitative product analysis was done by online gas chromatography using a HP 6890A with a flame ionization detector. A Shimadzu GCMS-QP2010S was used for product identification. The light gas products were monitored by online gas chromatography using a Carle series 400 AGC with TCD.

2.6. Model fitting

Pseudo first-order models were fitted to the data for the tested catalysts over the low W/F range (0-0.35 h). These simple models therefore assume that at low W/F (low conversion), competitive adsorption of products on the surface is not significant. For a particular catalyst, the product yields and conversion data were simultaneously fitted for a plug flow reactor using the integral reactor method.

CHAPTER 3: HYDROGENATION AND HYDRODEOXYGENATION OF 2-METHYL-2-PENTENAL ON SUPPORTED METAL CATALYSTS

Abstract

Platinum, palladium, and copper catalysts supported on precipitated silica have been studied for the hydrodeoxygenation and hydrogenation of 2-methyl-2-pentenal in the 200-400 ^{o}C temperature range. The activity follows the order Pt>Pd>Cu. It has been found that at low temperatures Pt and Pd are primarily active for hydrogenation of the C=C bond to make 2-methyl-pentanal, with some decarbonylation, yielding n-pentane and CO as products. Decarbonylation increases at higher temperatures. Cu catalyzes hydrogenation of both C=C and C=O bonds. In both cases, the initial products are further hydrogenated to form 2-methyl-pentanol at higher space times. At higher temperatures on Cu, hydrogenolysis of 2-methyl-pentanol takes place, giving 2-methyl-pentane (and H_2O) as the dominant product while no decarbonylation is observed.

3.1. Introduction

This study investigates the performance of Pt, Pd, and Cu supported on precipitated silica catalysts for the hydrodeoxygenation of 2-methyl-2-pentenal. This aldehyde represents a molecule with reactive functional groups (C=C double bond and C=O) that are typical in the oxygenate fractions of bio-oils produced from pyrolysis. Such molecules are potential feedstocks for fuels and chemicals, but are too reactive to include as fuel components themselves and must be refined to remove the active oxygen and the unsaturation [1-3]. This molecule is also produced from the aldol condensation of glycerol, a low value by-product of biodiesel production. Pt and Pd are well known for their ability to hydrogenate C=C double bonds in preference to carbonyls [4-10]. Hydrogenolysis of fatty acid methyl esters to form alcohols is also an important reaction in the production of detergents that can be catalyzed by copper-based catalysts [11-14]. While most metals show higher activity for C=C in preference to C=O bonds [7-10], Cu has been shown to be an exception [15-16]. The potential for hydrogenation of the C=O bond, leaving the unsaturated C=C bond, is also of interest in the production of fine chemicals [17].

The objective of this study is to gain an understanding of the catalytic pathways for selective hydrodeoxygenation reactions over different catalysts and operating conditions. Fig. 3.1 shows various products that can be obtained from hydrogenation and hydrodeoxygenation of 2-methyl-2-pentenal on metals. In general, for fuel utilization, removal of oxygen from biomass-derived fuels is necessary to improve the

stability of the fuel and to reduce water solubility. As an initial screening tool, research octane number (RON) of individual molecules is one of the important indicators to determine whether a molecule has potential as a gasoline component. However, for many oxygenated biomass derived molecules, no such property measurements have been made. Substantial previous work [18] has been done to show that a database of octane number (and other relevant fuel properties) may be used to develop a predictive capability for molecules of similar type with useful reliability. The octane number values of product molecules found in this study were predicted for the alcohol products using QSAR models [19-20] that correlate molecular descriptors, i.e., numerical values calculated from the molecular structure, to specific properties of the corresponding compounds (in this case, octane number). Molecular descriptors involve geometric, steric, and electronic aspects of the molecule. In Fig. 3.1, it may be seen that the octane numbers predicted for the alcohols obtained from hydrogenation of 2-methyl-2-pentenal are quite high. At the same time, they have vapor pressures within the range of gasoline. Within the hydrocarbon products n-pentane has the lowest octane number. While 2-pentene has a good octane number, the concentration of this product is very low since, in excess of H_2, equilibrium favors pentane. Note that the octane numbers for the aldehyde compounds are not shown since these are highly reactive and are undesirable molecules for fuels.

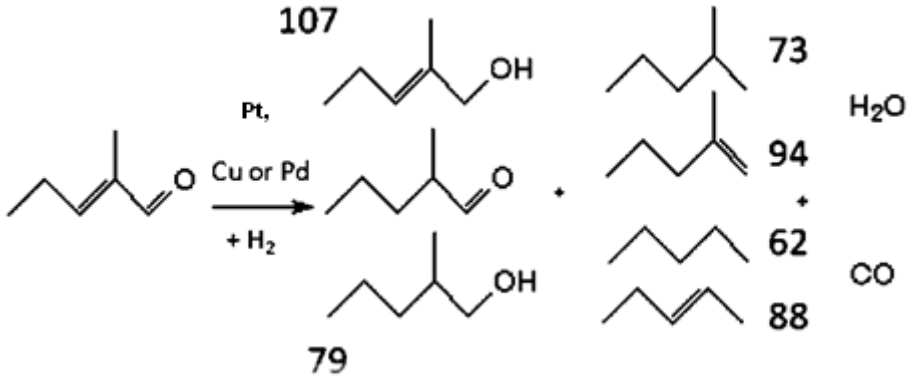

Fig. 3. 1. Research octane numbers (RON) for products of 2-methyl-2-pentenal conversion. Alcohols predicted by QSAR, hydrocarbons from literature [18].

3.2. Experimental

3.1.1. Catalyst preparation

The catalysts were prepared by incipient wetness impregnation of the metal precursor on precipitated silica (HiSil 210 obtained from Pittsburg Plate Glass Co.) having a BET surface area of 135 m^2/g. The metal loading in each catalyst was calculated based on the amount of metal precursor incorporated in the catalyst by impregnation. The liquid/solid ratio used to achieve incipient wetness was 1.26 ml/g. The precursors of Pt, Pd and Cu metals were H_2PtCl_6, $Pd(NO_3)_2$ and $Cu(NO_3)_2.2.5H_2O$, respectively, purchased from Sigma Aldrich. After impregnation, the catalysts were dried overnight in an oven, and then calcined in air at 400^oC for 4 hours. For the catalytic measurements, catalysts (0.05-0.15 g) were loaded in a tubular reactor and reduced in-situ in flowing H_2 at 400^oC for 2 h, then cooled down to the

reaction temperature at 200°C. In this study, each catalyst sample is identified by the type of metal and weight percent loading.

3.2.2 Catalyst characterization

CO chemisorption was used to determine dispersion of the Pd and Pt catalysts. It was conducted in a dynamic chemisorption unit, including a pulse system with an SRI Model 310C Gas Chromatograph equipped with a Thermal Conductivity Detector (TCD). All the catalysts were reduced in H_2 heating to 350°C with a ramp rate of 10°C/min, held for 1 hour, then flushed in He for 30 min and cooled down to room temperature before injecting CO. A pre-mixed gas of 5% CO in He was used for pulse injection with a 0.1 ml loop size. CO adsorption on the blank SiO_2 was carried out at room temperature to subtract any adsorption on the support. However, no CO adsorption was detected . Likewise, no CO adsorption was observed on the Cu catalyst at this temperature. The results of CO chemisorption on Pt and Pd are reported in Table 3.1.

The average particle size for all pre-reduced catalysts was obtained by TEM. The TEM images were obtained on a JEOL JEM-2000FX TEM. For this analysis, a suspension in ethanol was made by stirring the solid sample in an ultrasonic bath for 10 min. A few drops of the resulting suspension were deposited on a TEM grid and subsequently dried and evacuated before the analysis. To estimate average particle

size, the particles were considered spherical, and the average diameter (d_{TEM}) was obtained using the expression [21].

$$d_{TEM} = \frac{\sum n_i . d_i^3}{\sum n_i . d_i^2}$$

where n_i is the number of particles with diameter d_i

Table 3. 1. Dispersion of Pt, Pd and Cu from chemisorption and average d_{TEM} measurements.

Metal	Pt 0.5%	Pd 0.5%	Cu 5%
Dispersion			
CO / M	0.038	0.15	0
d_{TEM} (nm)	12 ± 3	3.6 ± 0.3	2.7 ± 0.5

3.2.3. Catalyst testing

Catalytic activity measurements were carried out in a continuous flow system that includes a syringe pump delivering the 2-methyl-2-pentenal to a heated line into a stream of H_2 that feeds to a 20-in long 3/8 in-OD stainless steel tube within an electric furnace. Loads of 50 to 150 mg catalyst were used, with the appropriate flow rate to achieve the desired space time (W/F). Operating conditions were 200°C and atmospheric pressure. Experiments were continued for 2-3 h. No significant changes

in activity or selectivity were observed over these reaction times, indicating a very low extent of catalyst deactivation. All the lines were heated with heating tapes to keep the feed and products in gas phase. The carrier gas, H_2, was used to reduce the catalyst and also flown during reaction with the 2-methyl-2-pentenal at a relative molar ratio 12:1. Quantitative product analysis was done by online gas chromatography using a HP 6890A with a flame ionization detector. A Shimadzu GCMS-QP2010S was used for product identification. The light gas products were monitored by online gas chromatography using a Carle series 400 AGC with TCD.

3.2.4. Model fitting

Pseudo first-order models were fitted to the data for the tested catalysts over the low W/F range (0-0.35 h). These simple models therefore assume that at low W/F (low conversion), competitive adsorption of products on the surface is not significant. For each catalyst, all product yield and conversion data were simultaneously fitted for a plug flow reactor model and the results are shown as the solid lines on the figures, together with the experimental data points.

3. 3. Results and Discussion

The overall conversion of 2-methyl-2-pentenal on the metals is compared over the same range of space time W/F (0-0.33 h). The observed catalytic activity order under the conditions investigated is Pt > Pd > Cu. To quantify the intrinsic activity of the different metals, turnover frequencies (TOF) were calculated from the initial linear conversion region per surface metal atom and shown in Table 3.2. For Pt and Pd the percent metal exposed was estimated from the CO chemisorption values; for Cu, it was estimated from the metal particle sizes observed in TEM.

Table 3. 2. Turnover frequencies over different catalysts at 200^{o}C, H_2: feed ratio = 12:1

Catalyst	Pt	Pd	Cu
wt. (%) loading	0.5%	0.5%	5%
TOF (s^{-1})	341	39	1.3

Interesting differences among the three catalysts were observed in the product distribution. From analyzing the slope at W/F=0, one can differentiate the primary from the secondary products. For example, on the 0.5 wt.% Pt/SiO_2 catalyst, three primary products were observed, as shown in Fig. 3.2.a: 2-methyl-pentanal, with smaller amounts of n-pentane (any 2-pentene formed would be rapidly hydrogenated under these conditions) and 2-methyl-2-pentenol. 2-Methyl-pentanal is the dominant

product arising from the hydrogenation of the C=C bond, 2-methyl-2-pentenol is formed by hydrogenation of the C=O bond, and n-pentane is the primary product of the decarbonylation of 2-methyl-2-pentenal. The by-product CO was also observed. In this figure, the lines represent the fits obtained with the first order models for the reaction pathways discussed below.

Fig. 3.2 (a)

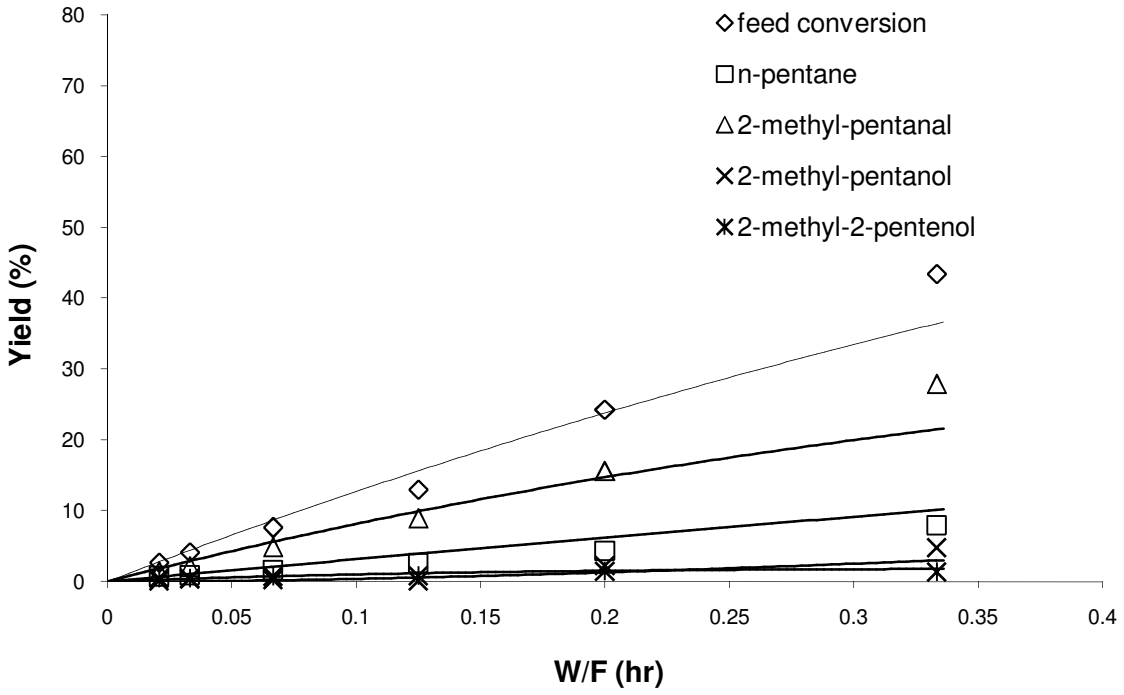

Fig. 3.2 (b)

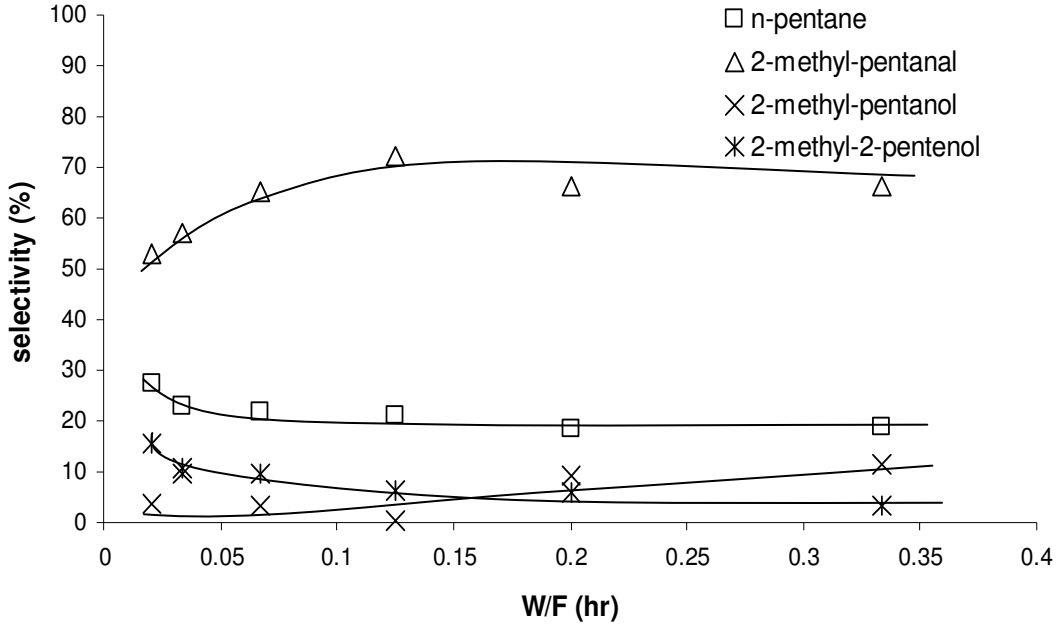

Fig. 3. 2. (a). Conversion and product yield of 2-methyl-2-pentenal on 0.5 wt.% Pt/SiO_2 at 200°C at different W/F. H_2: feed ratio = 12:1. (b). Selectivity of 2-methyl-2-pentenal conversion on 0.5 wt.% Pt/SiO_2 . Solid lines in Fig. 3.2(a) represent fits for first order models for each reaction pathway shown in Figure 3.4. Solid lines in Fig. 3.2(b) are added to show the trends.

2-Methyl-pentanol is observed as a secondary product, resulting from the hydrogenation of either 2-methyl-pentanal or 2-methyl-2-pentenol. In Fig. 3.2.b, it may be observed that the selectivity of 2-methyl-2-pentenol decreases and that of 2-methyl-pentanol increases as W/F increases which indicates that 2-methyl-pentanol mainly comes from hydrogenation of 2-methyl-2-pentenol in this range of W/F. In Fig. 3.2.b, the lines are not results of the fitting, but simply show the trends.

In Figs. 3.3.a. and 3.3.b., the results for 0.5 wt.% Pd/SiO_2 are shown. The solid lines in Fig. 3.3.a represent the first order model fits. It is clear that conversion is significantly lower over Pd than over Pt, over the same range of W/F. The data show that in comparison to Pt, the yield of 2-methyl-pentanal on Pd is particularly reduced relative to the yields of other products.

Fig. 3.3 (a)

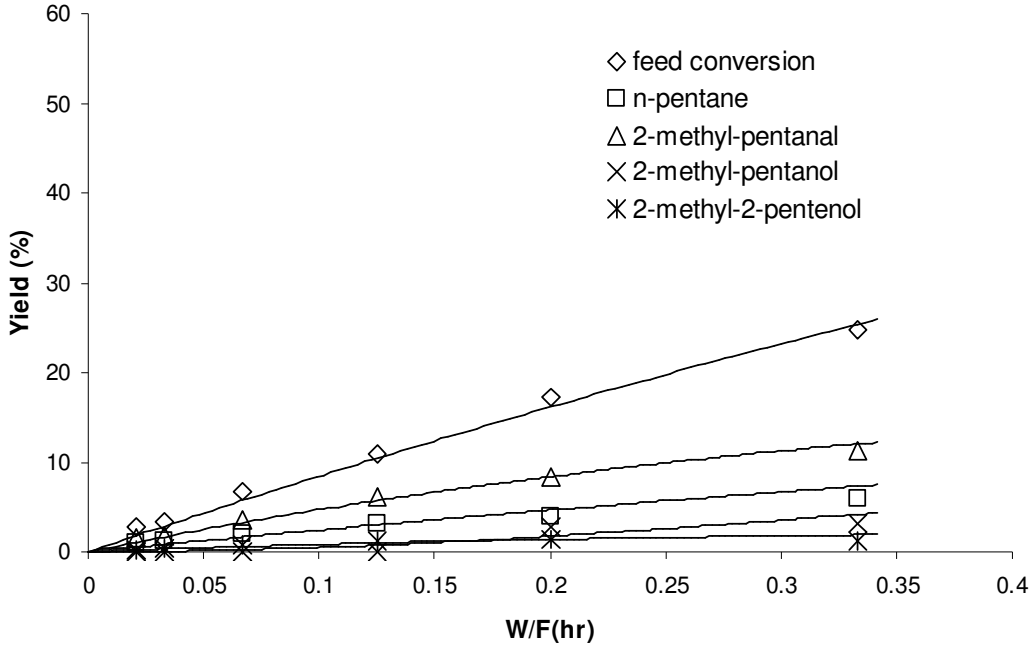

Fig. 3.3 (b)

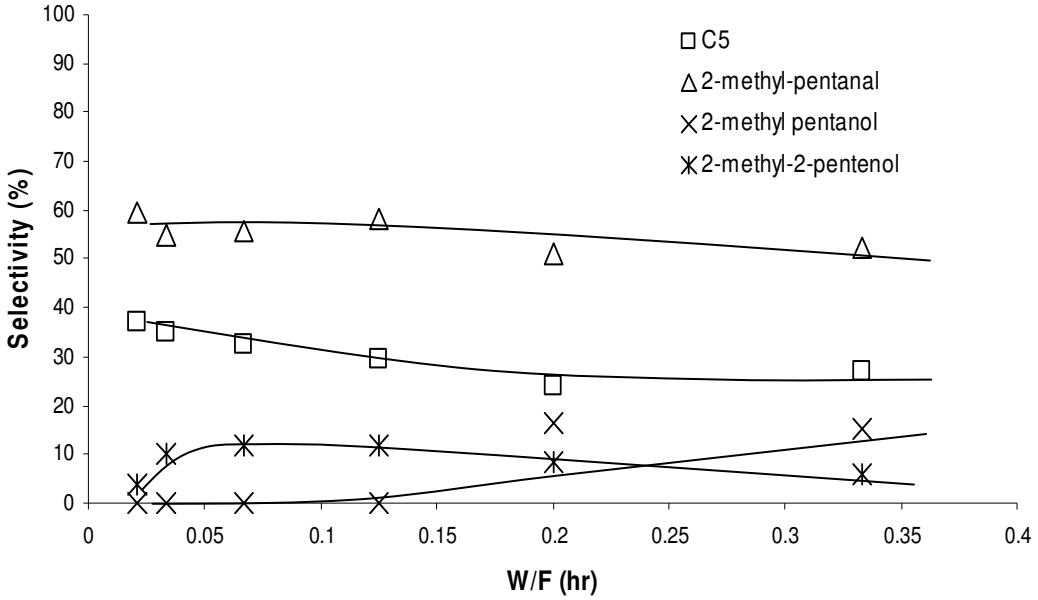

Fig. 3. 3. (a). Conversion and product yield of 2-methyl-2-pentenal on 0.5 wt.% Pd/SiO_2 at 200°C at different W/F. H_2:feed ratio=12:1. (b). Selectivity of 2-methyl-2-pentenal conversion on 0.5 wt. % Pd/SiO_2.

To better visualize the relative trends for the different reaction pathways over the two catalysts, a plot of yield of n-pentane vs. yield of 2-methyl-pentanal is shown in Fig. 3.4. This graph allows a direct comparison of each catalyst's relative activity for decarbonylation compared to hydrogenation of the C=C bond. The higher slope of the curve for Pd indicates that the decarbonylation activity of Pd is higher than that of Pt

for the same yield of hydrogenated aldehyde, indicating that Pd has a stronger preference for decarbonylation than Pt.

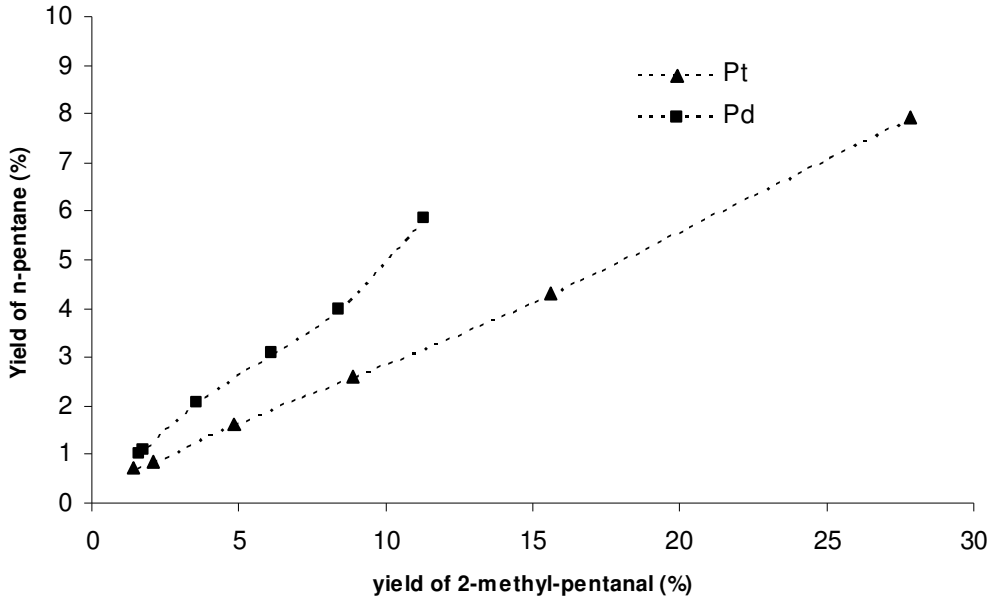

Fig. 3. 4. Yield of n-pentane vs. Yield of 2-methyl-pentanal to compare activity of decarbonylation with hydrogenation of C=C bond on Pt and Pd catalysts

Compared to Pt and Pd, the 0.5 wt.% Cu/SiO_2 catalyst shows a much lower activity at the same weight loading. Therefore, to get a comparable range of conversions, Cu/SiO_2 was tested at a higher metal loading (5 wt. %). Fig. 3.5.a shows the different product yields at conversions up to 33% with the lines representing the first order model fits. 2-Methyl-pentanal is again the most abundant product at higher conversion, but essentially no n-pentane is observed. In Fig 3.5.b, the scale is expanded to show the low W/F region. It may be seen that initially the yield of 2-

methyl-2-pentenol is the highest, but it goes through a maximum at about W/F =0.2 and decreases at higher W/F, while the secondary product 2-methyl-pentanol increases.

Fig. 3.5 (a)

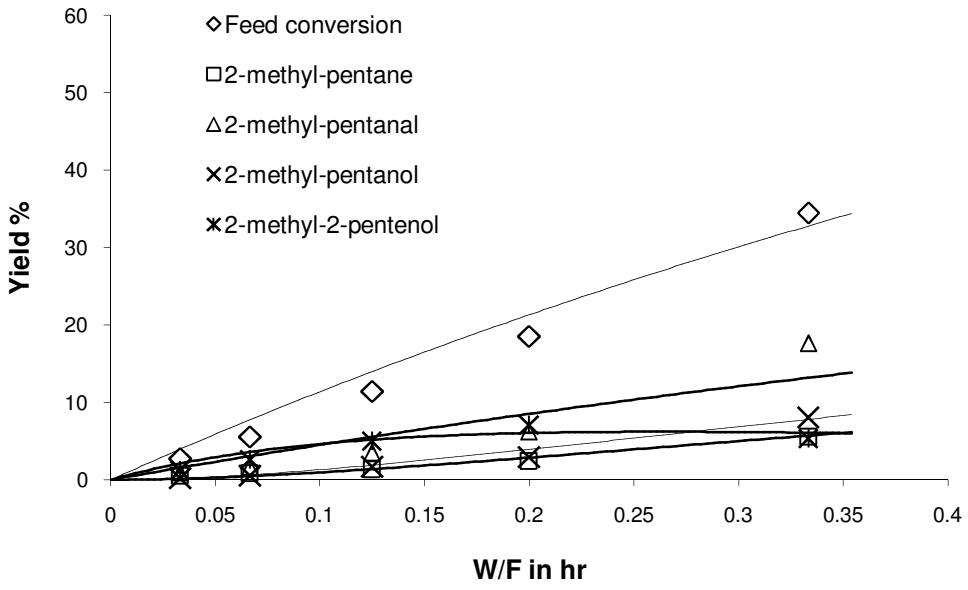

Fig. 3.5 (b)

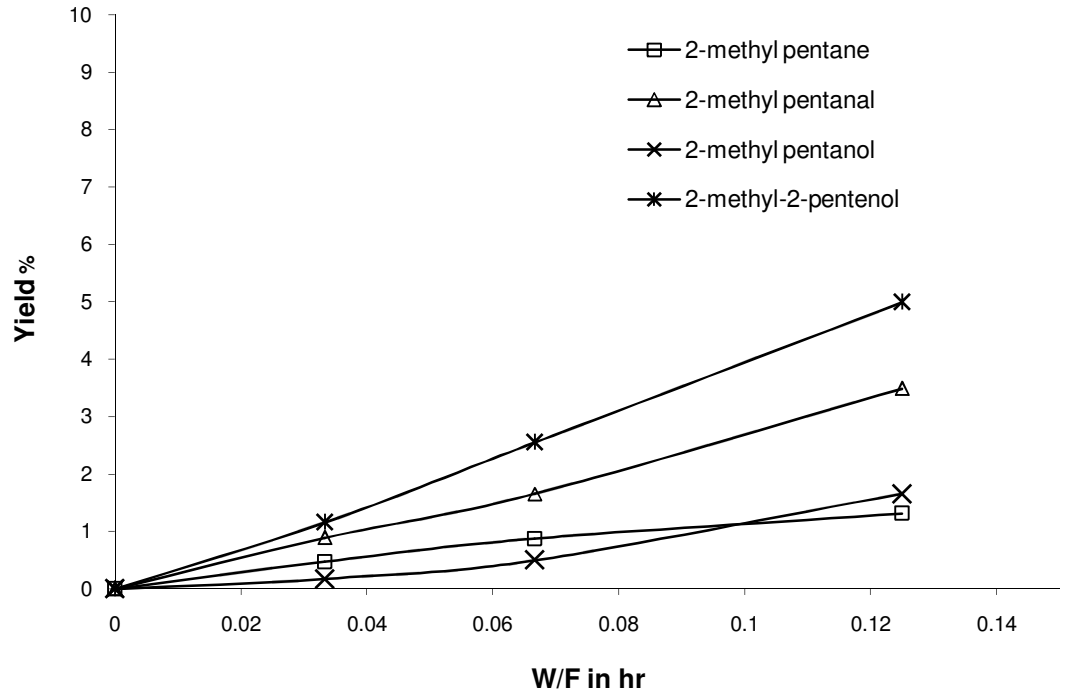

Fig. 3. 5. (a). Conversion of 2-methyl-2-pentenal and product yield on 5 wt.% Cu/SiO_2 at 200°C at low W/F. H_2: feed ratio = 12:1. (b). product yields in the low W/F region.

Thus, it is clear that on the Cu catalyst, the hydrogenation of the C=O bond is faster than that of the C=C bond, which is the opposite trend to that observed on Pt and Pd. The only hydrocarbon observed is 2-methyl-pentane with no n-pentane (or CO) as observed over the Pt and Pd catalysts. C_6 is primarily formed by hydrogenolysis of 2-methyl-2-pentenol that yields 2-methyl-2-pentene, which is then rapidly hydrogenated to 2-methyl-pentane (initially, a small amount of 2-methyl-2-pentene is also observed). Thus, the methyl-pentane is not a primary product, but is formed by the pathway shown in Fig. 3.6.

The schematic conversion of 2-methyl-2-pentenal on Pt, Pd and Cu in H_2 is summarized in Fig. 3.6. Each reaction is labeled with the corresponding k values from the fits of the pseudo first-order models. The fitting results are shown as solid lines in Figs. 3.2.a, 3.3.a, and 3.5.a. In all cases, the fittings are very good. For Pd and Pd, the dominant product in the W/F range 0 - 0.33 h is 2-methyl-pentanal. n-Pentane comes from both 2-methyl-2-pentenal and 2-methyl-pentanal but mainly from the latter. At longer contact times, the dominant product is expected to be n-pentane as 2-methyl-pentanal is consumed by the decarbonylation reaction. Under the conditions of the study, the yields of 2-methyl-pentanol and 2-methyl-pentanal shift toward the aldehyde because of the favorable equilibrium. Although 2-methyl-pentanol is favored as W/F becomes higher, ultimately (W/F = 2.4, 100 % feed conversion) the decarbonylation of the 2-methyl-pentanal to make n-pentane becomes the dominant product even at 200 ^{o}C.

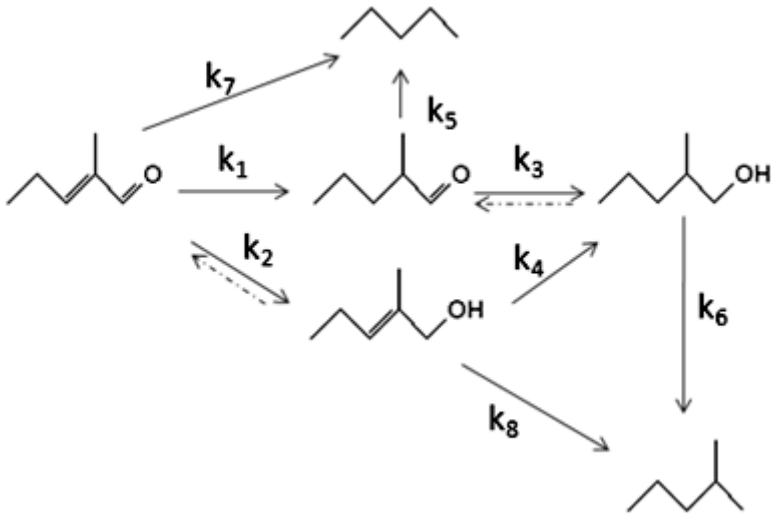

Fig. 3. 6. Schematic conversion of 2-methyl-2-pentenal on Pt, Pd and Cu

Table 3. 3. First order model rate constants (s^{-1} on a per surface atom basis)

Metal	Pt	Pd	Cu
loading (wt.%)	0.5%	0.5%	5%
k_1	2.65	0.20	0.01
k_2	0.41	0.04	0.01
k_3	0.29	0.44	0.00
k_4	19.64	1.12	0.09
k_5	0.29	0.02	0
k_6	0	0	0.01
k_7	0.93	0.10	0
k_8	0	0	0.02
k_1/k_2 ratio	6.50	5.67	0.65
k_7/k_1 ratio	0.35	0.47	0
Total least square error	35.7	10.4	75.3

The k values summarized in Table 3.3 are reported on the basis of the estimated surface atom density. Note that for Pt and Pd catalysts, no C_6 hydrocarbon product was formed, and therefore, both k_6 and k_8 are listed as zero. Conversely, on Cu, there was no C_5 hydrocarbon product, so k_7 is zero. The relative rate of hydrogenation of C=C bond vs. C=O bond is best reflected by the ratio of k_1/k_2 for all three catalysts. For Pt and Pd, the k_1/k_2 ratio is about 6, that is, these metals are much more selective for C=C hydrogenation. On Cu, it is about 10 times lower, 0.65, indicating that on this metal, hydrogenation is much less selective. This behavior is clearly illustrated in Fig. 3.7 showing the yield of 2-methyl-2-pentenol (C=O hydrogenation) vs. yield of 2-methyl-pentanal (C=C hydrogenation). Fig. 3.7 shows that while Pt and Pd are highly selective for C=C hydrogenation to form the saturated pentanal, Cu is much less selective, but hydrogenates C=O with a preference over C=C. At higher conversions, secondary reactions may mask this effect.

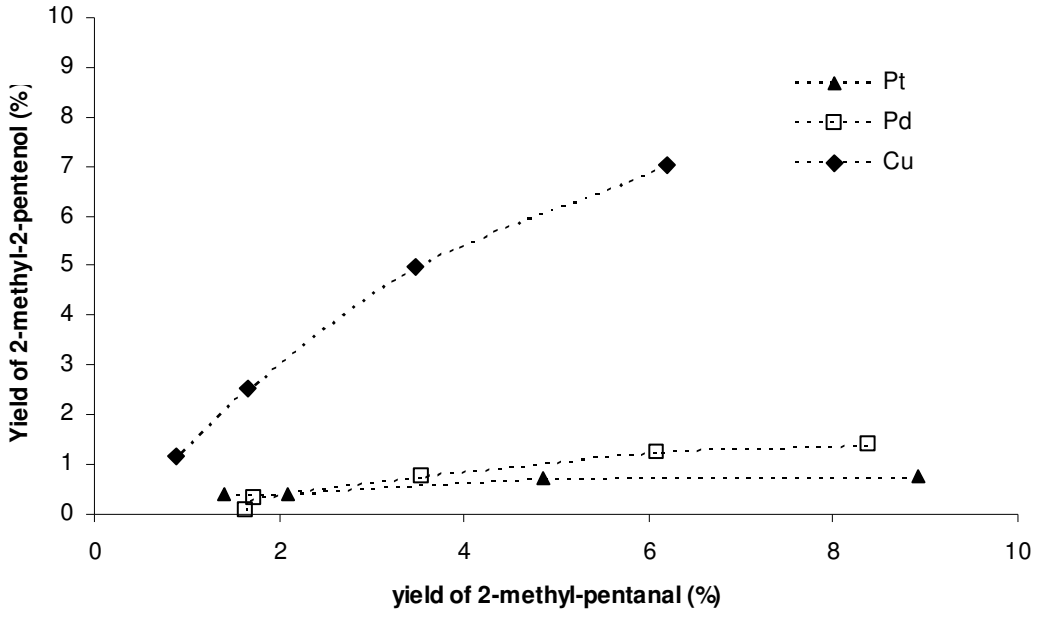

Fig. 3. 7. Yield of 2-methyl-2-pentenol vs. Yield of 2-methyl-pentanal on Pt, Pd and Cu catalysts, comparing C=O vs. C=C hydrogenation activity.

The k_7/k_1 ratios give an indication of the relative rates of decarbonylation and C=C bond hydrogenation. As shown above, these values illustrate the slightly stronger tendency of Pd towards decarbonylation compared to Pt and quantify the trend shown in Fig. 3.4. By contrast, Cu shows no decarbonylation activity.

Results from experiments at higher W/F on 5 wt.% Cu/SiO_2 are shown in Fig. 3.8. These experiments were conducted to see the predominant products at high conversion at 200°C. At W/F ≥1 h, conversion of 2-methyl-2-pentenal was 100%. The highest selectivity was for 2-methyl-pentanol followed by 2-methyl-pentanal. No 2-methyl-2-pentenal was observed, showing complete hydrogenation of 2-methyl-2-pentenal to 2-

methyl-pentanol. However, hydrogenation of 2-methyl-pentanal to 2-methyl-pentanol is not complete, due to equilibrium limitations. Equilibrium experiments were carried out by feeding 2-methyl-pentanol in H_2 with molar ratio 1:12 at 200°C at high W/F (1 to 3 h). At W/F = 2 - 3 h, there is no change in product selectivity so equilibrium is presumably reached. The equilibrium constant K is defined as a ratio of partial pressures [alcohol] / [aldehyde] x [H_2]. From the data, the equilibrium constant was calculated to be K= 2.71. As shown in Fig. 3.8, at 200ºC and this range of W/F, only small amounts of the hydrocarbon 2-methyl-pentane are observed.

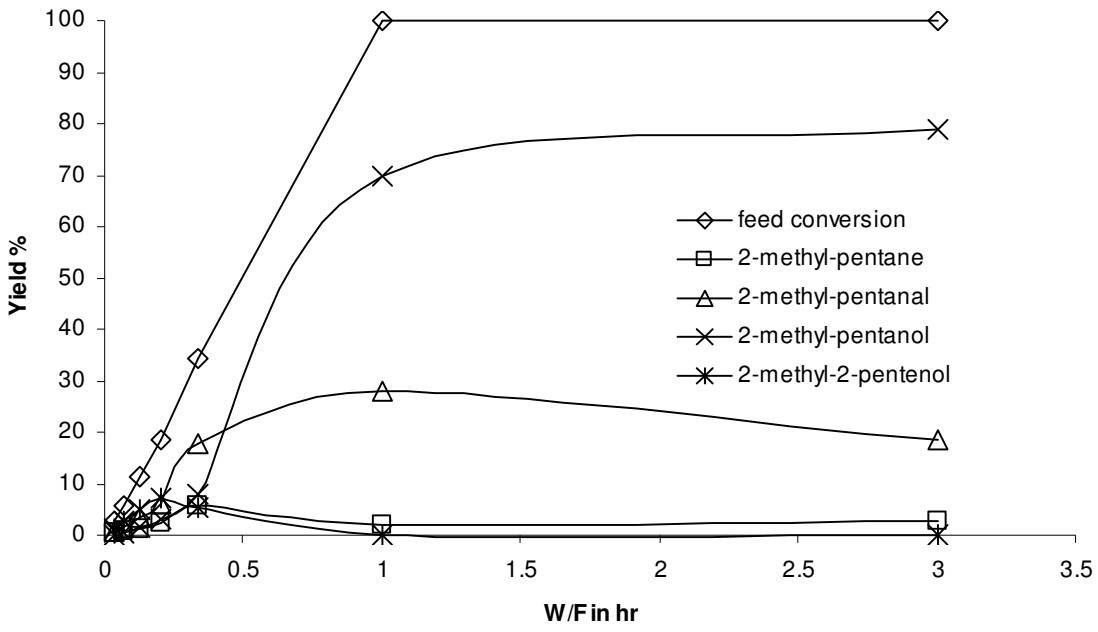

Fig. 3. 8. Conversion and product yield of 2-methyl-2-pentenal on 5 wt.% Cu/SiO_2 at 200°C at different W/F. H_2: feed ratio=12:1

On 5 wt.% Cu/SiO_2, it is interesting that at higher W/F, 2-methyl-pentanol and 2-methyl-pentanal are the main products. Further increasing W/F does not change the product ratios since equilibrium is approached. Thus, varying temperature one can change the product selectivity. Fig. 3.9 shows the effect of temperature on selectivity over the Cu catalyst at W/F of 1 h. Under these conditions, the conversion of 2-methyl-2-pentenal is 100% in the entire temperature range. At the lowest temperature (200ºC), selectivity is determined predominantly by the equilibrium between 2-methyl-pentanol and 2-methyl-pentanal. At 300ºC, this equilibrium is shifted towards the aldehyde 2-methyl-pentanal since the hydrogenation reaction (aldehyde + H_2 → alcohol) is exothermic. Also at 300ºC, selectivity to the hydrocarbon product 2-methyl-pentane has increased as the rate of hydrogenolysis becomes significant. As the temperature increases, the equilibrium ratio of alcohol/aldehyde decreases further. At the highest temperature, the hydrogenolysis reaction is fast, with selectivity to 2-methyl-pentane approaching 90%. High temperature experiments were also conducted on Pd catalyst, and the results showed high selectivity to n-pentane as a function of temperature. Decarbonylation is thus predominant at elevated temperatures.

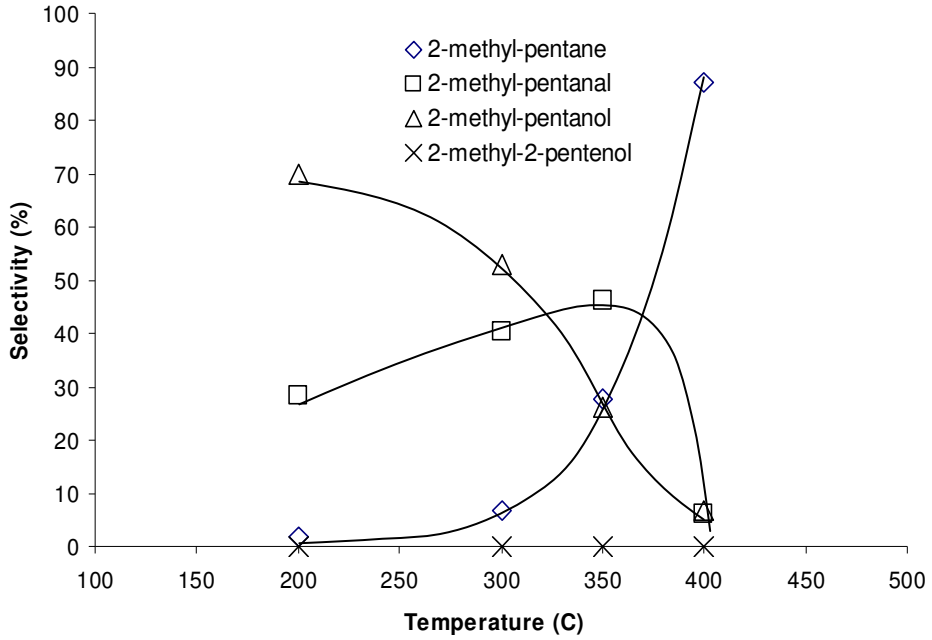

Fig. 3. 9. Selectivity of 2-methyl-2-pentanal conversion on 5 wt.% Cu/SiO_2 at W/F=1, X=100%. H_2: feed ratio = 12:1

Based on the results at 200ºC, the equilibrium constant for the reaction 2-methyl pentanal + H_2 ↔ 2-methyl-pentanol was determined. Values at higher temperatures were calculated using heat of reaction data [22] and the Van't Hoff's equation for the range of 200^o to 400^{o}C. Fig. 3.10 shows the equilibrium OH/AL ratio together with experimental OH/AL values. The experimental ratio of alcohol and aldehyde (Exp OH/AL) tracks the equilibrium ratio from 200^{o}C to 250^{o}C, then deviates above 250^{o}C as secondary hydrogenolysis becomes dominant. The advantage of C-OH hydrogenolysis that occurs on Cu is the retention of the original carbon chain length whereas the C-C hydrogenolysis that occurs on Pd and Pt shortens the chain length, losing carbon as CO.

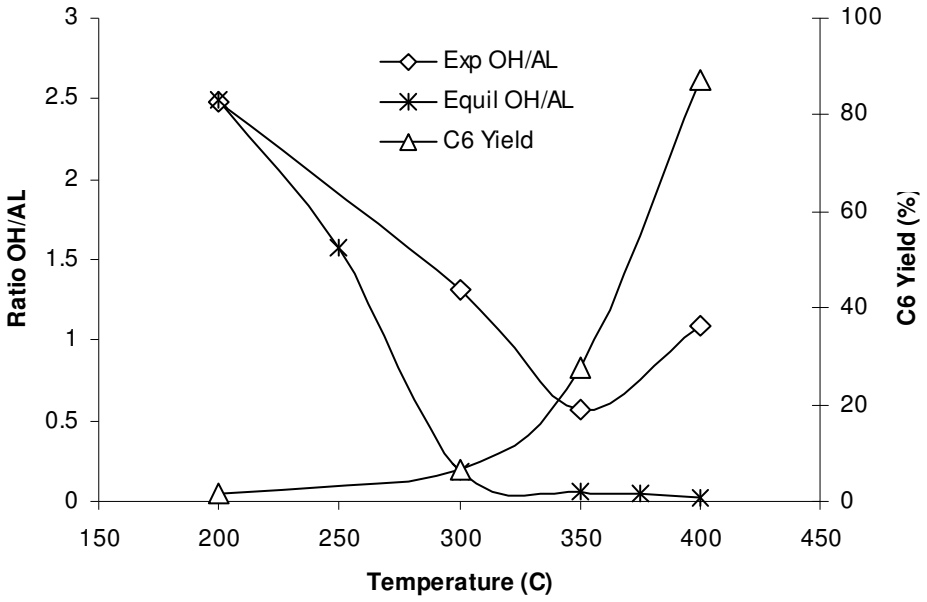

Fig. 3. 3. Ratios of alcohol: aldehyde from experiments and equilibrium, and yield of C6 with temperature.

In agreement with the results shown here, previous studies have reported that on Pd catalysts, hydrogenation of the C=C bond is generally more favored than C=O [23]. It is believed that when a molecule containing both functional groups adsorbs on a metal surface, activation of the π-bond of C=C is preferred, and once on the surface, this interaction may hinder activation of the C=O group. The C=C activation occurs via two possible modes: (1) π -complex or (2) di-σ bond with the metal. Ponec [23] and Delbecq and Sautet [24] have shown that for a conjugated system, the adsorption on Pd and Pt usually occurs involving both π-bonds. In this adsorption mode, the molecule then transforms into an enol that isomerizes to a saturated aldehyde, which is the same result as a direct C=C hydrogenation. This preference for C=C

hydrogenation when both groups are present has also been reported by other authors [25-27]. This trend is consistent with the results observed in this study, that on Pd (and also Pt), the major primary product is 2-methyl-pentanal, which comes directly from C=C hydrogenation of 2-methyl-2-pentenal. The 2-methyl-pentanol is initially low, but slowly increases with W/F due to further hydrogenation of 2-methyl-pentanal and 2-methyl-2-pentenol.

Crotonaldehyde has been a popular probe molecule to study competitive hydrogenation on metals [28-31]. As 2-methyl-2-pentenal, crotonaldehyde is an α, β unsaturated aldehyde, however it does not have a methyl substituent group. The results reported for this molecule also indicate differences in Cu compared to Pt catalysts. It has been reported that the selectivity towards the unsaturated alcohol is lower than the selectivity towards the saturated aldehyde. On Pt the selectivity for C=C hydrogenation is 88% while on Cu it is only 59 %. Comparison among different metals, Ag, Au, Co, Cu, Ir, Ni, Pt and Ru, shows that the selectivity for C=O hydrogenation on crotonaldehyde is lowest on Ni, Ir, and Pt. By contrast, the highest selectivities are seen on Ag, Au and Co catalysts.

As discussed above, Mertens [29] shows that without the methyl group, crotonaldehyde has only moderate selectivity for hydrogenation of C=O on Cu (S = 41% [29]). The presence of the methyl substituent group at the α-carbon may affect

the selectivity for hydrogenation of C=O. In our study, the unsaturated aldehyde feed is 2-methyl-2-pentenal, with a methyl substitution at the α-position. The methyl group may hinder C=C hydrogenation, resulting in the observed S = 61% (from the k_1/k_2 ratio in Table 3.3), a higher C=O hydrogenation selectivity compared to that for crotonaldehyde in [29]. Mertens [29] also found, for Au and Ag catalysts, a small increase in selectivity for C=O hydrogenation when an α-methyl is added to crotonaldehyde (tiglic aldehyde) with about half of the reactivity. Their results suggest that the improvement in C=O bond hydrogenation selectivity on Cu observed in this study may be due in part to the presence of the α-methyl group.

3.4. Conclusions

The conversion of 2-methyl-2-pentenal was studied over Pt, Pd and Cu supported on precipitated silica at 200 ^{o}C. On all catalysts, hydrogenation activity was observed for both C=C and C=O bonds. 0.5 wt.% Pd, and Pt showed strong hydrogenation of the C=C bond to form primarily 2-methyl-pentanal. At very low conversion, 5 wt.% Cu/SiO_2 showed strong initial hydrogenation activity of C=O to form primarily 2-methyl-2-pentenol that is converted to 2-methyl-pentanol in equilibrium with 2-

methyl-pentanal at higher conversion. On Pt and Pd catalysts, decarbonylation leads to n-pentane via C-C cleavage, becoming significant at higher W/F or at higher temperature. On Cu, 2-methyl-pentane via C-O hydrogenolysis was observed on Cu as a minor product at 200 ^{o}C, but became the dominant product on Cu as the temperature was increased to 400 ^{o}C.

From the practical point of view, it may be desirable to produce the 2-methyl-pentanol using the Cu catalyst at lower temperatures, since these alcohols are stable and have fairly good octane numbers. At higher temperatures, Cu is a good catalyst for total removal of oxygen without loss of carbon. The high selectivity for C=C hydrogenation on Pt and Pd offers no advantage in producing the more desirable alcohol and despite much higher activity, the loss of carbon (and molecular size) via decarbonylation is a distinct disadvantage when building small molecules to useful fuel range molecules is the objective.

Acknowledgements

Support from the Oklahoma Secretary of Energy and the Oklahoma Bioenergy Center are gratefully acknowledged. The assistance of Steven Crossley in performing the QSAR octane estimates is greatly appreciated.

References

[1] X.Q. Wang, R.Y. Saleh, U.S. Ozkan, *J. Catal.*, 231 (2005) 20.

[2] M. Snare, I. Kubickova, P. Maki-Arvela, D. Chichova, K. Eranen, D.Y. Murzin, *Fuel*, 87 (2008) 933.

[3] T. Sooknoi, T. Danuthai, L.L. Lobban, R.G. Mallinson, D.E. Resasco, *J. Catal.*, 258 (2008) 199.

[4] N. Gyorffy, Z. Paal, *J Mol Catal a-Chem*, 295 (2008) 24.

[5] P.N. Rylander, Hydrogenation Methods, Academic Press, San Diego, CA, 1985.

[6] G.C. Bond, Catalysis by Metals, Academic Press, New York, 1962.

[7] P. Sautet, J.F. Paul, *Catal. Lett.*, 9 (1991) 245.

[8] F. Delbecq, P. Sautet, *Catal. Lett.*, 28 (1994) 89.

[9] F. Delbecq, P. Sautet, *Langmuir*, 9 (1993) 197.

[10] F. Delbecq, P. Sautet, *Surf. Sci.*, 295 (1993) 353.

[11] D.S. Brands, E.K. Poels, A. Bliek, *Appl. Catal. A-Gen*, 184 (1999) 279.

[12] J.v. Beijnum, Ph.D. Thesis, University of Ultrech, 1991.

[13] C.J.G. Vandergrift, A.F.H. Wielers, B.P.J. Joghi, J. Vanbeijnum, M. Deboer, M. Versluijshelder, J.W. Geus, *J. Catal.*, 131 (1991) 178.

[14] F.T. Vandescheur, B. Vanderlinden, M.C. Mittelmeijerhazeleger, J.G. Nazloomian, L.H. Staal, *Appl. Catal. A-Gen*, 111 (1994) 63.

[15] J. Jenck, J.E. Germain, *J. Catal.*, 65 (1980) 141.

[16] N.M. Bertero, C.R. Apesteguia, A.J. Marchi, *Appl. Catal. A-Gen*, 349 (2008) 100.

[17] G.V. Smith, F. Notheisz, Heterogeneous Catalysis in Organic Chemistry, Academic Press, 1999.

[18] P. Do, S. Crossley, M. Santikunaporn, D.E. Resasco, Catalysis 2007.

[19] J.M. Luco, E. Marchevsky, *Curr. Comput.-Aided Drug Des.*, 2 (2000) 31.

[20] R.P. Verma, *Mini Rev. Med. Chem.* , 6 (2006) 467.

[21] F. Pompeo, N.N. Nichio, O.A. Ferretti, D. Resasco, *Int. J. Hydrogen Energy*, 30 (2005) 1399.

[22] CRC, Handbook of Chemistry and Physics, 2007-2008.

[23] V. Ponec, *Appl. Catal. A-Gen*, 149 (1997) 27.

[24] F. Delbecq, P. Sautet, *J. Catal.*, 152 (1995) 217.

[25] P. Beccat, J.C. Bertolini, Y. Gauthier, J. Massardier, P. Ruiz, *J. Catal.*, 126 (1990) 451.

[26] T. Birchem, C.M. Pradier, Y. Berthier, G. Cordier, *J. Catal.*, 146 (1994) 503.

[27] R.L. Augustine, *Catal Rev*, 13 (1976) 285.

[28] E.L. Rodrigues, A. Marchi, C.R. Apesteguia, J.M.C. Bueno, *Appl. Catal. A-Gen*, 294 (2005) 197.

[29] P.G.N. Mertens, P. Vandezande, X.P. Ye, H. Poelman, I.F.J. Vankelecom, D.E. De Vos, *Appl. Catal. A-Gen*, 355 (2009) 176.

[30] M. Boronat, M. May, F. Illas, *Surf. Sci.*, 602 (2008) 3284.

[31] M. Consonni, D. Jokic, D.Y. Murzin, R. Touroude, *J. Catal.*, 188 (1999) 165.

CHAPTER 4: ETHERIFICATION OF 2-METHYL-PENTANAL ON SUPPORTED PALLADIUM CATALYSTS

Abstract

Dialkyl ethers have been selectively produced from etherification of aldehydes and alcohols on supported Pd catalysts. A yield of 79 % ether with a selectivity of 90% was observed when feeding 2-methyl-pentanal with 2-methyl-pentanol at a molar ratio 1:1 at 125^{o}C. Cross etherification of n-butanol with 2-methyl-pentanal shows a much higher rate than that observed when the alcohol or aldehyde is fed alone. This enhanced activity is in line with the catalyst requirement for large ensembles that allow surface alkoxide species next to an η^2 adsorbed aldehyde. Etherification when only aldehyde or alcohol is fed arises predominantly due to aldehyde-alcohol interconversion to produce the necessary co-reactant. The ether yield at the same reaction conditions increases with metal loading in the order 16 > 10 > 3 wt % Pd. Increasing reduction temperature also increases ether yield. It is apparent that etherification reaction is highly sensitive to metal particle morphology, consistent with needing ensembles that accommodate the two adjacent adsorption sites.

4.1. Introduction

Biofuel production has attracted substantial attention in recent years [1-4]. There is strong motivation to produce fuels from oxygenated molecules generated from biomass conversion. Much research has been focused toward production of fungible molecules that may be readily incorporated into the existing transportation fuel infrastructure. Ethers are one of the potential fuel components made from oxygenates that might be used either in gasoline or diesel blends. Ethers were first commercially introduced in Italy in 1973 as a blending component in gasoline [5]. More recently, Olah [6] patented the use of C_2-C_{24} alkyl ethers as blending components for diesel fuels, demonstrating cetane number improvement from 2 to 20 points. Use of short alkyl ethers such as methyl-tert-butylether (MTBE), methyl-tert-amylether (TAME) and ethyl-tert-butylether (ETBE) as fuel additives have had negative environmental impact due to their high solubility in water, which enhances their dispersion in the environment. These problems are much less severe with larger alkyl ethers, which exhibit much lower solubility. However, despite their excellent combustion and physical properties [7,8], overcoming perceived environmental issues will be required before ethers can be added to the fuel pool.

Alcohol etherification on acid catalysts is a well established reaction [5,9-12]. Much less attention has received the study of ether formation on metal catalysts [13-18]. While studies focusing on etherification of alcohol and aldehyde have identified the need for ensembles of sites to accomplish the condensation [14-16], the influence of

metal surface structure on ether selectivity has not been demonstrated in a systematic way.

In recent work [19], we have shown that 2-methyl-pentanal may be selectively produced from hydrogenation of 2-methyl-2-pentenal, itself produced from aldol condensation of glycerol or from propanal. These compounds are representative of types of bio-derived aldehydes and analogous alcohols from processes such as biomass pyrolysis. The present contribution investigates the etherification of 2-methyl-pentanal to form di-2-methyl-pentyl ether (DMPE) on Pd catalysts of varying particle size and morphology to help understanding the pathways of etherification of smaller bio-derived oxygenates by metal catalysts.

4.2. Experimental

4.2.1. Catalyst synthesis.

Different loadings (3, 10 and 16 wt.%) of Pd catalysts were prepared by incipient wetness impregnation of the metal precursor on precipitated silica (HiSil 210 obtained from Pittsburg Plate Glass Co.) having a BET surface area of 135 m^2/g. The metal loading on each catalyst was calculated based on the amount of metal precursor incorporated into the support. The liquid/solid ratio used to achieve incipient wetness was 1.26 ml/g. The precursor was $Pd(NO_3)_2$, purchased from Sigma Aldrich. After impregnation, the catalysts were dried overnight in an oven and then calcined in air at

400°C for 4 hours. To study the effect of alkali addition, two catalysts were synthesized by adding controlled amounts of K onto the 10% Pd/SiO_2 catalyst using KOH (>90% grade, flakes) precursor.

4.2.2. Catalyst characterization

Dynamic pulse chemisorption was used to determine the Pd percent exposed. CO adsorption was conducted in a dynamic chemisorption unit, consisting of a pulse system with detection by an SRI Model 310C Gas Chromatograph equipped with a Thermal Conductivity Detector (TCD). All of the catalysts were reduced in H_2 by heating from ambient to 150°C with a ramp rate of 10°C/min, held for 1 hour, then flushed with He for 30 min and cooled down to room temperature. A pre-mixed gas of 5% CO in He was used for pulse injection with a 0.1 ml loop size. Pulses of CO were sent over the catalyst at 25 °C until breakthrough occurred and the size of the pulse peak no longer increased. The SiO_2 support was tested and no CO adsorption was detected.

Temperature Programmed Reduction (TPR) of 3% Pd/SiO_2 shows one peak centered at 50°C. Therefore, the changes observed after different reduction temperatures do not reflect different degrees of reduction, but rather morphological changes.

DRIFTS experiments were carried out in a Perkin Elmer Spectrum 100 FTIR Spectrometer equipped with an MCT detector and a High Temperature, Low Pressure Reaction Chamber (HVC-DRP) fitted with KBr windows (Harrick Scientific Products, Inc). 50-100 mg of catalyst was loaded to the reaction cell and reduced in H_2 flowing at 30 sccm by heating at a 10°C/min ramp rate to 150° or 250° or 350°C, then holding for 1 hour followed by flushing with He for 30 minutes before cooling to room temperature. CO (5% in He) then flowed through the chamber for 30 minutes at room temperature and then flushed with He for 20 min before sample spectra were taken. Spectra were acquired at a resolution of 4 cm^{-1} averaging 64 scans.

4.2.3. Catalyst tests

Catalytic activity measurements were carried out in a continuous flow 3/8-in OD (0.295-in I.D) stainless steel tubular reactor within an electric furnace. Runs were conducted for 2-3 h at 125°C and atmospheric pressure, using 0.05-0.15 g of catalyst and the appropriate flow rate to achieve the desired W/F (g cat/g feed/h). Hydrogen was used to reduce the catalyst and as a carrier gas for the organic feed that was delivered by a syringe pump into the gas stream, keeping a relative molar ratio 12:1 during the entire reaction period. The reactants used were: 2-methyl-pentanal (MPAL) and/or 2-methyl-pentanol (MPOL) or n-butanol (BOL) as the alcohol. Experiments substituting n-propanal for either MPOL or MPAL were also conducted. Heating tapes were used in all the lines to keep the feed and products in the vapor phase. Quantitative product analysis was made online in an HP 6890A gas

chromatograph, equipped with flame ionization detector. Composition of organic compound is reported as mole fractions. A Shimadzu GCMS-QP2010S was used for product identification. The light gas products (mostly CO) were detected online via gas chromatography using a Carle series 400 AGC with TCD.

4.3. Results

4.3.1. Effect of varying feed composition

*Pure aldehyde feed***.** 2-methyl-pentanal was fed on the 16% Pd catalyst reduced at 150^{o}C to study the conversion of the aldehyde. The W/F was varied from 0.25 to 2 h to obtain conversions from 8.4% to 28.9%. The yields of products are plotted against conversions in Fig. 4.1. At low conversion, the major products are n-pentane and MPOL that result from decarbonylation and hydrogenation, respectively. As the conversion increases, the yield of the ether (DMPE) becomes predominant, much higher than the yields of n-pentane and MPOL. The yield of MPOL decreases suggesting that it is consumed to form the secondary product, DMPE. No other products were observed.

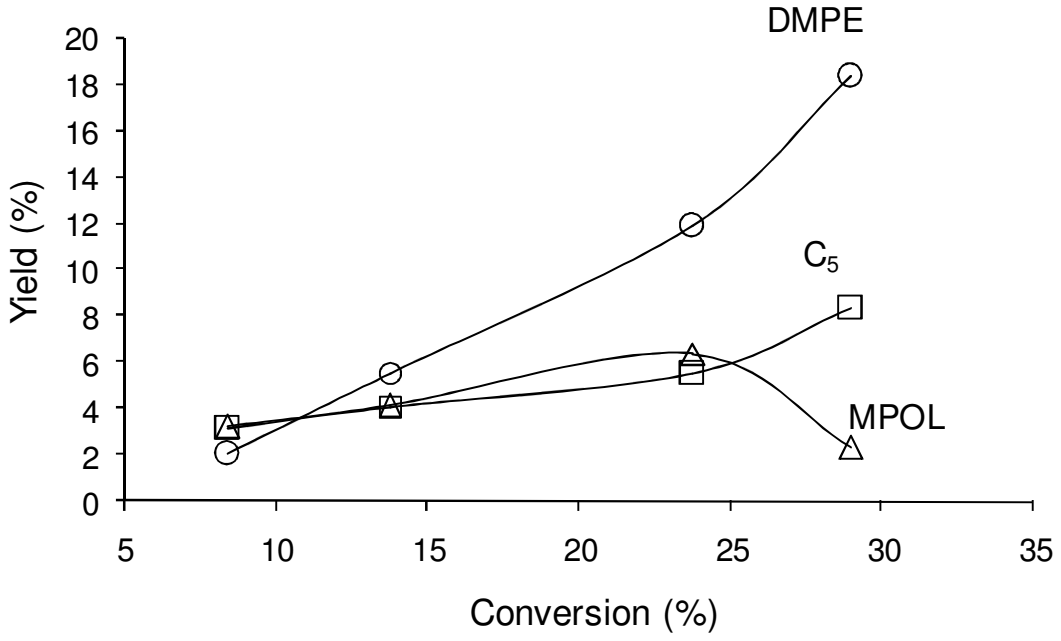

Fig. 4. 1. Yields of products from MPAL on 16% Pd/SiO_2 reduced at 150°C and run at 125°C, 1 atm, H_2: MPAL =12:1

Pure alcohol feed. In order to compare the behavior of the aldehyde and alcohol, 2-methyl-pentanol was fed over the 16% Pd catalyst reduced at 150 °C. The reactivity of MPOL was found to be considerably lower than that of MPAL and its conversion increases from 3.6 to 11.9% over longer W/F, from 1 to 4 h. The product yields are shown in Fig. 4.2. The products were DMPE, MPAL, n-pentane, and a small amount of 2-methyl-pentane (2MP). The yield of ether shows a slight induction period that could suggest that as the aldehyde increases, this enhances the rate of etherification. MPAL is formed from dehydrogenation while 2MP comes from hydrogenolysis of the MPOL. n-Pentane is produced from decarbonylation of the MPAL.

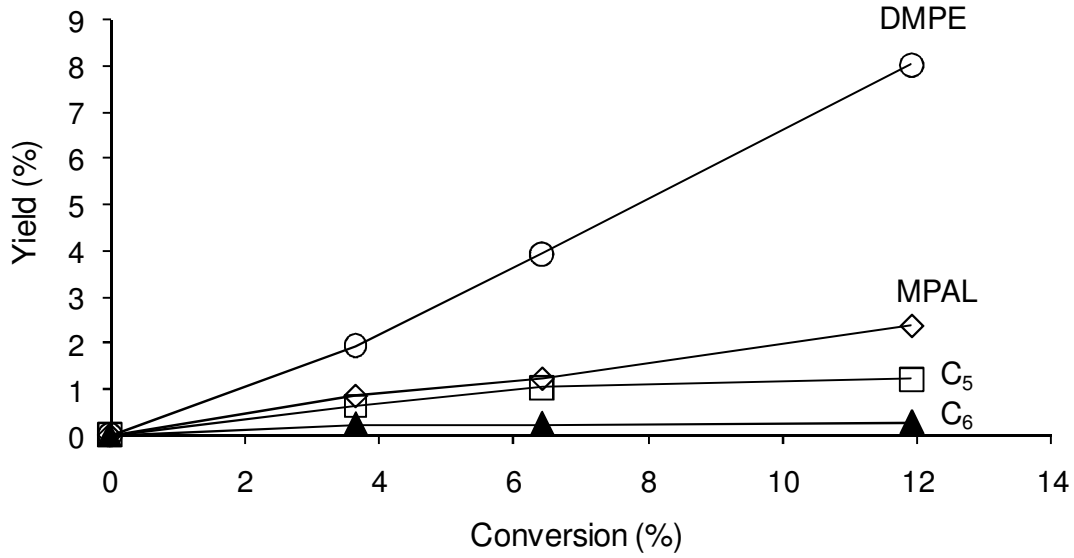

Fig. 4. 2. Yields of products from MPOL on 16% Pd/SiO_2 reduced at 150°C and run at 125°C, 1 atm, H_2: MPOL =12:1

Mixtures of 2-methyl-pentanal with 2-methyl-pentanol at different feed ratios. When either the aldehyde or the alcohol is fed alone, the ether is the predominant product. Because under the reaction conditions a significant extent of interconversion of the two molecules may occur both species may be present in every run. Therefore, it is unclear to what extent the etherification reaction depends upon the concentration of both species. To quantify the contribution of each one, experiments with mixed feeds at different ratios of MPAL and MPOL were carried out. The results are shown in Fig. 4.3. Much higher ether yield was observed when using the mixtures than when using the pure feeds of either compound. The highest ether selectivity (90%) was achieved at a 1:1 feed molar ratio (y_{MPAL} =0.5) with a yield, based upon conversion of

both reactants, of 79 %. These results show that etherification is enhanced when significant amounts of both MPAL and MPOL are present.

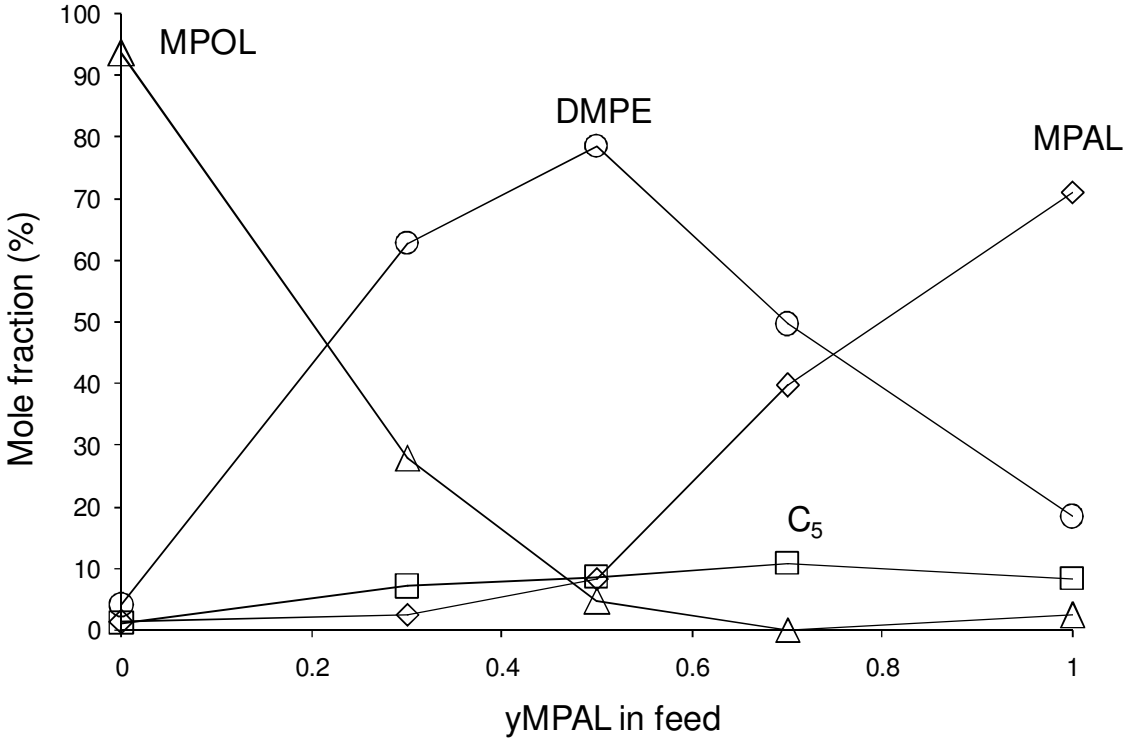

Fig. 4. 3. Co-feed mixtures of MPAL and MPOL on 16% Pd/SiO_2 reduced at 150°C and run at 125°C, W/F = 2h, H_2: feed = 12:1

Mixtures of n-butanol and 2-methyl-pentanal. Because MPAL and MPOL both have the same alkyl chain, they produce a symmetric ether and the degree to which either aldehyde or alcohol may be incorporated is not made clear from the above results. Therefore, n-butanol and 2-methyl-pentanal were co-fed at a 1:1 volume ratio (or 1.3 to 1 molar ratio, respectively). The composition of feeds and products are

shown in Fig. 4.4 with increasing W/F. The results show that both C_{10} and C_{12} (DMPE) ethers are the major products, but only a trace of C_8 ether, suggesting low etherification from alcohol-alcohol etherification along with a low reactivity of the alcohol. MPAL is also consumed to a minor extent by decarbonylation and hydrogenation. The comparative rates for C_{10} and C_{12} ether formation are best shown by the ratio of the two at very low W/F, in this case 0.25 and 0.5 h are used. This ratio is 5.0 for C_{10}/C_{12}. MPAL reacts readily with BOL to form the C_{10} ether. The alcohol is highly reactive for ether formation with an aldehyde, but has low reactivity for other reactions, whereas the aldehyde decarbonylates and hydrogenates to some extent, giving it a higher rate of conversion.

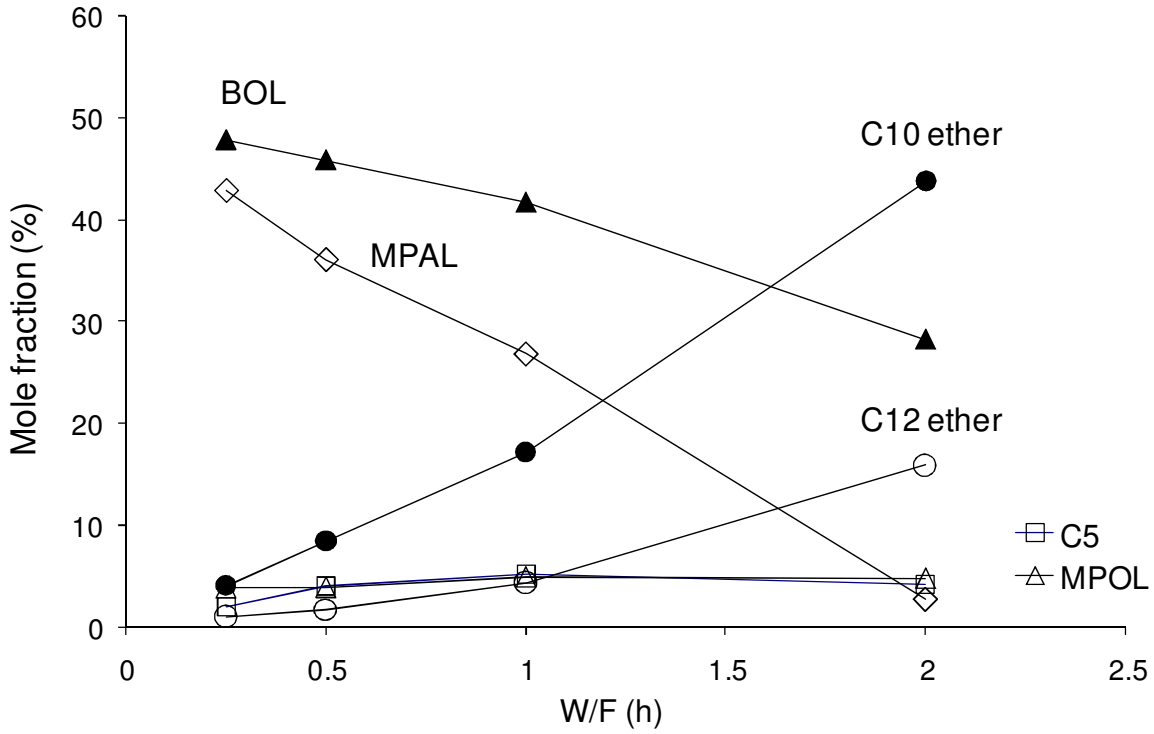

Fig. 4. 4. Cross etherification of n-butanol and 2-methyl-pentanal on Pd reduced at 150^{o}C and run at 125^{o}C, W/F = 2h. H_2: feed ratio = 12:1

Mixtures of n-propanal and 2-methyl-pentanol. A similar experiment to study cross etherification was carried out for a mixed feed of C_3AL (n-propanal) with MPOL, molar ratio 1:1 on 16% Pd/SiO_2 reduced at 150^{o}C and run at 125^{o}C, W/F= 2h. The cross C_9 ether yield was 47.5%, much higher than the C_6 and C_{12} ethers whose yield are 0.05% and 2.28%, respectively. This result also confirms the high yield of the mixed ether, similar to the previous experiment when feeding both BOL + MPAL. The results of ether formation from the mixed feed experiments are summarized in Table 4.1.

Table 4. 1. Etherification of mixed feeds of aldehydes + alcohols on 16% Pd/SiO_2, molar H_2: feed = 12:1

Feed	MPAL + MPOL[a]		MPAL + n-butanol[b]
		C8 ether	0.02
C12 ether	78.5	C10 ether	43.8
		C12 ether	15.9
Feed	**Propanal + MPOL[c]**		**Propanal + MPAL**
C6 ether	0.05	C6 ether	0.09
C9 ether	47.5	C9 ether	11.3
C12 ether	2.28	C12 ether	2.11

All mixed feed experiments are on 16% Pd/SiO_2 reduced at 150°C and run at 125°C at W/F = 2 h

[a] molar ratio of MPAL: MPOL = 1:1

[b] volume ratio of MPAL: n-butanol =1:1, molar ratio of MPAL: n-butanol = 1:1.3

[c] molar ratio of MPOL: propanal = 1:1

Mixtures of n-propanal and 2-methyl-pentanal. From previous mixed feed experiments, it is clear that high yields of the cross ether are achieved when reacting an aldehyde and an alcohol. This confirms the hypothesis that etherification requires both adsorbed aldehyde and alcohol with abundant amounts on the surface. However, it remains unclear if etherification can proceed to a significant extent without an alcohol in the system. Therefore an experiment with a mixed feed of only aldehydes in the absence of hydrogenation will help demonstrate whether this occurs.

Experiments were conducted with n-propanal and 2-methyl-pentanal and with either He or H_2 as the carrier gas. In a He carrier, no hydrogenation or ether formation was observed and the only reaction observed was decarbonylation of the aldehydes to hydrocarbons. In a H_2 carrier, the observed products are hydrogenated alcohols from the corresponding aldehydes, as well as hydrocarbons and ethers. The yields of ethers are much smaller than feeding mixed alcohol and aldehyde. Yields of C_9 and C_{12} ethers are 11.3 % and 2.11%, respectively. The C_6 ether yield is much smaller than the others, and very little propanol is observed compared to MPOL. This could indicate either that the propanal is not effectively hydrogenated and the C_9 ether is produced from propanal and MPOL or that the propanal is readily hydrogenated and reacts with the MPAL to form the C_9 ether.

An experiment using only propanal as a feed was conducted under the same conditions as the other experiments. As shown in Table 4.2, when compared at the same conversion level (24 %), much less etherification was observed with propanal than with methyl pentanal, while the hydrogenation to propanol was substantially higher than for the larger aldehyde.

Table 4. 2. Etherification of propanal or methyl pentanal at 125°C on 16% Pd/SiO_2 reduced at 150°C, molar H_2: feed = 12:1

Feed		Propanal		Methyl pentanal
W/F (h)		2		1
Conversion (%)		23.8		23.8
Yield (%)				
	Ethane	2.5	n-pentane	5.5
	Propanol	14.6	MPOL	6.4
	Dipropyl ether	6.7	DMPE	11.9
Ether/hydrocarbon ratio		2.7		2.2

4.3.2. Effect of metal loading

Reaction of 2-methyl-pentanal on 3, 10 and 16 wt.% Pd/SiO_2. Catalysts with different metal loadings, reduced at 150°C, were compared for etherification at similar levels of conversions. As shown in Table 4.3, CO chemisorption measurements indicate that increasing the loading from 3 to 16 wt % resulted in increased particle size. The estimated aldehyde reaction rate per surface atom is similar for the three catalysts. The ether yield and selectivity are highest for the 16 wt % Pd catalyst, also shown in Tables 4.3. The other major products are n-pentane, which is produced by decarbonylation and 2-methyl-pentanol from hydrogenation.

Table 4. 3. Activity of 3, 10 and 16 wt% Pd/SiO_2 reduced at 150°C with product yields from MPAL conversion at 125°C, molar H_2 :MPAL = 12:1

Catalyst		3% Pd	10% Pd	16% Pd
Dispersion		7.10%	5.30%	3.90%
W/F (h)		2	1	1
Conversion (%)		20.9	20.4	23.8
TOF (molecule/site.s)		1.44E-02	1.13E-02	1.14E-02
Yield (%)				
	n-pentane	7.0	5.3	5.5
	MPOL	6.7	7.4	6.4
	C12 ether	7.2	7.7	11.9
Selectivity (%)				
	n-pentane	33.4	26.0	23.1
	MPOL	32.0	36.4	26.8
	C12 ether	32.6	37.6	50.1

4.3.3. Effect of reduction temperature

When the 3 wt.% Pd was reduced at 150°C, the yield of ether was 7.2 % at W/F = 2h, lower compared to the ether yields for the 10% Pd and 16%Pd, as shown in Table 4.4. However, when the reduction temperature on the 3% Pd was increased from 150°C to 200° and 250°C for experiments at a conversion of about 20 %, the ether yield was found to increase from 7.2 % to 9.2% and 10.2%, respectively, as shown in Table 4.4. When the reduction temperature was increased to 250 °C for the 16% Pd, an increased ether yield from 11.9% to 13.1% was observed, even while the conversion was reduced from 23.8 % to 20%.

Table 4. 4. Effect of reduction temperature of 3% Pd and 16% Pd catalysts on MPAL conversion at 125°C, molar H_2 :MPAL = 12:1

Catalyst		3%Pd			16% Pd	
	$T_{reduction}$ (°C)	150	200	250	150	200
W/F (h)		2	2	2	1	1
Conversion (%)		20.9	24.2	22.7	23.8	20.0
Yield (%)						
	n-pentane	7.0	5.1	5.3	5.5	6.4
	MPOL	6.7	10.1	7.2	6.4	0.6
	C12 ether	7.2	9.1	10.2	11.9	13.1
Selectivity (%)						
	n-pentane	33.4	21.0	23.2	23.1	31.7
	MPOL	32.0	41.6	31.7	26.8	3.0
	C12 ether	34.6	37.4	45.1	50.1	65.3

4.3.4. Effect of the alkali addition

The results obtained on the K-containing catalysts are summarized in Table 4.5. It is observed that even at half the space velocity, the conversion on the K-doped catalysts is significantly lower than that obtained on the K-free Pd catalyst. The etherification selectivity decreases with the addition of K, while that of decarbonylation greatly increases. Note that the K added comes from KOH (>90% grade, flakes) precursor.

Table 4. 5. Effect of K addition to 10% Pd/SiO_2 catalysts in the 2-methyl-pentanal conversion at 125°C, molar H_2 : MPAL = 12:1, after reduction at 150°C

Catalyst		10% Pd	0.2%K-10%Pd	2%K-10%Pd
W/F (h)		1	2	2
Conversion (%)		20.4	14.9	9.8
Selectvity (%)				
	n-pentane	26.0	55.7	95.0
	MPOL	36.4	25.5	4.2
	C12 ether	37.6	18.8	0.8

4.3.5. In situ DRIFTS

The spectra from CO chemisorption on 3% Pd at different reduction temperatures are shown in Fig. 4.5. The peaks at 1980 and 1940 cm^{-1} are assigned to bridge and multi-bonded CO species, respectively, typical of relatively large particles, in agreement with the rather low metal dispersions estimated from chemisorption measurements [20,21]. The much weaker band ascribed to linear CO appearing at around 2070 cm^{-1} [22,23] overlaps with the two branches resulting from residual gas phase CO remaining in the optical path after flushing with He for 20 min. As the reduction temperature increases, not only do both the bridge and multibonded CO peaks become relatively larger, but the multibonded-to-bridge ratio also increases. The bridge form is mostly associated with the presence of Pd (100) faces in the metal particle [24,25] while the multibonded species is more typical of Pd (111) faces [24,25]. This tendency is not only consistent with an increase in metal particle size,

but also with a smoothing of the surface caused by the crystal annealing occurring as the reduction temperature increases.

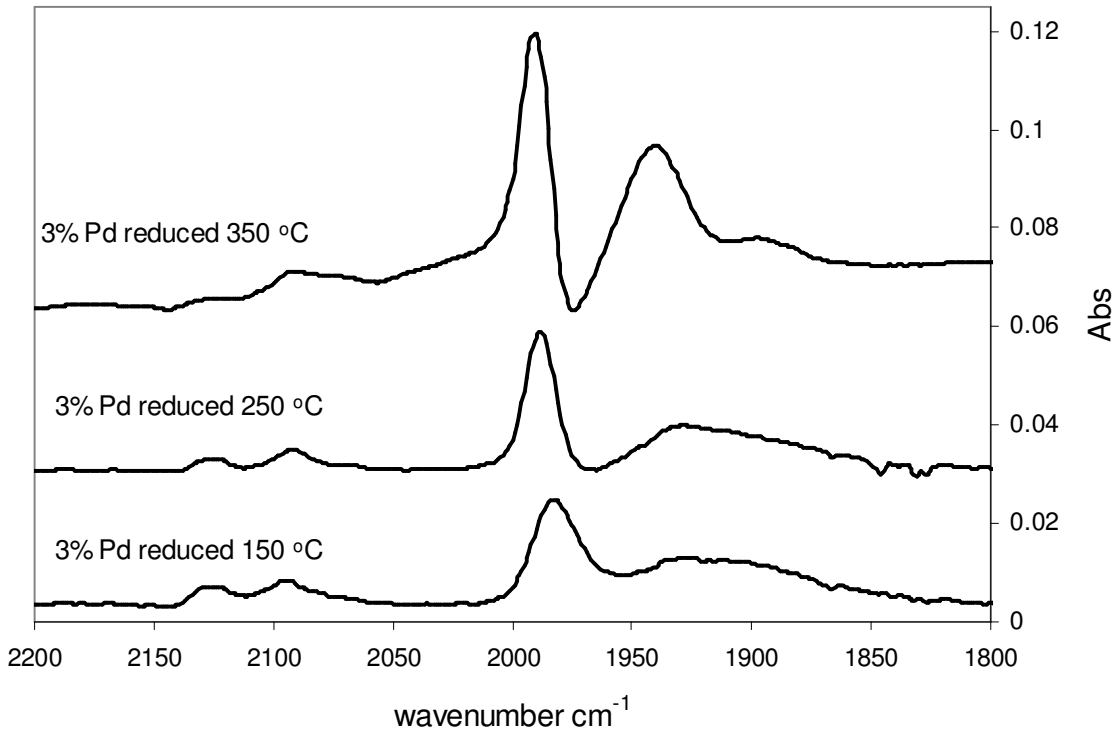

Fig. 4. 5. FTIR of CO on 3% Pd reduced at 150°C, 250°C and 350°C

4.4. Discussion

In an early work that is very relevant to the current study, Ponec et al. [16] observed the production of ether when pulsing different mixtures of alcohol and aldehyde over metal catalysts. In agreement with this early work we show here that when fed individually, both aldehydes and alcohols form ethers. However, etherification is

significantly enhanced when both are fed simultaneously. When only one is present in the feed, etherification apparently occurs due to the inter-conversion of aldehyde to alcohol or vice versa. The proposed reaction pathways are shown in Fig. 4.6. Note that alcohol and aldehyde can also react to form a hemiacetal in equilibrium. However, this reaction takes place via acid catalysts. Product analysis did not show hemiacetal in the gas phase in a blank reactor as well as in the presence of Pd catalysts.

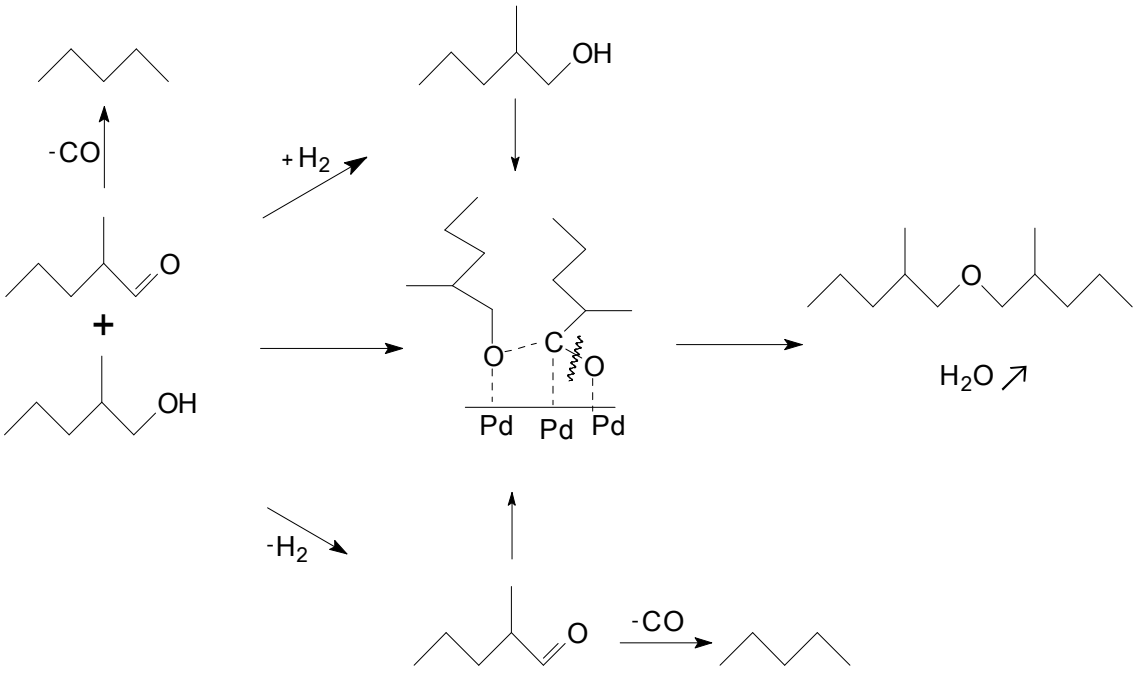

Fig. 4. 6. Schematic reaction pathway of 2-methyl-pentanal on Pd catalyst.

As mentioned above, because both the aldehyde and alcohol have the same methyl-pentyl alkyl group, the resulting ether is symmetric and the relative contribution of

each is not discernible. The results from the mixture experiment with MPAL and BOH clearly show that both are required to maximize ether, confirming the results of the MPAL-MPOL experiments. This condition suggests that each oxygenate forms a unique surface intermediate that is needed for the formation of the ether bond and is not efficiently inter-converted. An alcohol molecule is typically adsorbed on metal surfaces as an alkoxide. When an aldehyde adsorbs as an η^2 (C,O) species adjacent to the alkoxide [17,18,26], this enables the formation of a C-O-C bond generating an ether [14,16]. Accordingly, etherification should be favored on metal catalysts that promote the co-existence of both species. Under these conditions, the η^2 adsorbed C-O may cleave and the ether bond is formed with the alkoxide oxygen [14,26]. The residual oxygen from the aldehyde is removed from the surface as water in the presence of hydrogen. The formation of this surface hydroxyl should provide the driving force for the oxygen cleavage from the adsorbed aldehyde carbon, allowing formation of the ether bond.

Formation of the alkoxide species is a relatively easy process that most metal surfaces are able to promote [27-29]. On Pt-group metals (including Pt [30,31], Ni [32] and Pd [33]), adsorption of alcohols result in the formation of an alkoxide on the surface via hydroxyl-hydrogen elimination, followed by α-hydrogen abstraction that leads to an aldehyde intermediate bonded onto the surface via both carbon and oxygen atoms (as an η^2 (C,O) configuration) or an oxygen atom only (η^1 (O) configuration), as illustrated in Fig. 4.7. Kinetic experiments for CH_3OH decomposition on Ni (111)

and Ni (110) surfaces [34,35] revealed that the cleavage of the C-H bond of the methoxide is the rate-limiting step in methanol decomposition to surface H_2CO species. They also found the same results when using ethanol.

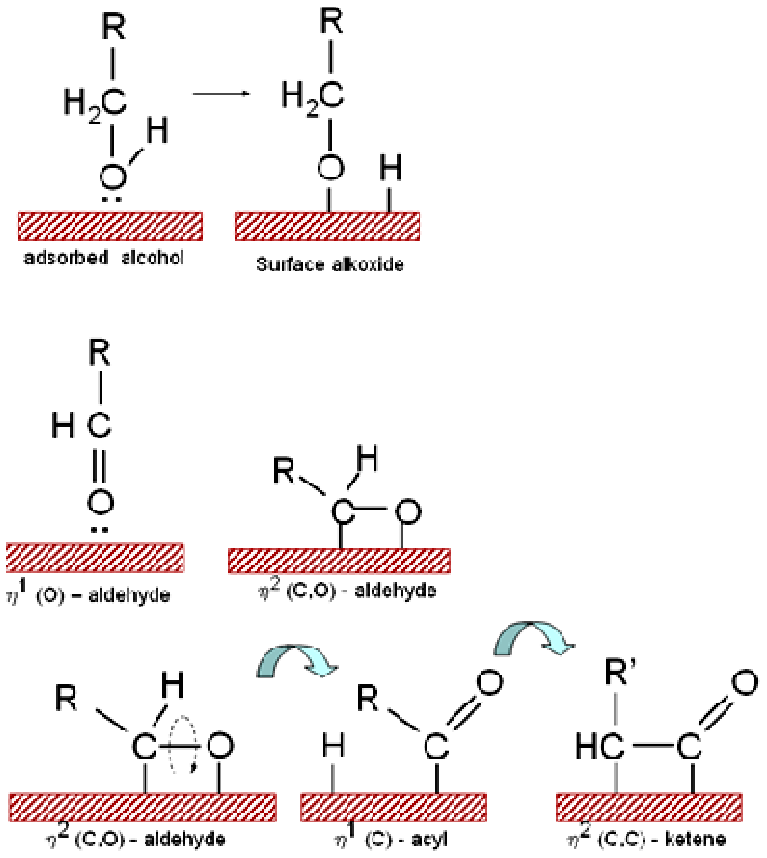

Fig. 4. 7. Adsorption modes of alcohols and aldehydes on Pd (111) and sequence from η^2 (C,O)-aldehyde to η^2 (C,C)-ketene of decarbonylation[26]

By contrast to alkoxides, the surface species that result from the adsorption of aldehydes strongly depend on the type of metals used. On Group IB metals, aldehydes adsorb exclusively in an η^1 configuration, but they adsorb in both η^1 and η^2

configurations on Group VIII metals, at a ratio that strongly depends on the specific metal.[27] In the former configuration, the aldehyde binds to the surface through the O lone pair, in the latter it binds though the π orbital of the carbonyl, overlapping the d electrons from the metal with the antibonding π^* orbital in the carbonyl. As a result, when there is significant backdonation from the metal, this configuration can be readily stabilized.[26] Therefore, the preference to form either η^1 or η^2 surface species can be ascribed to the electronic characteristics of the metals. For example, the much greater η^2 / η^1 ratio observed on Ru compared to Pt has been ascribed to a higher extent of electron back-donation from the metal to the π^* orbital of carbonyl, resulting from the higher position of the Fermi level in Ru compared to Pt. It is well known that a more efficient transfer of electron into the antibonding states of the molecule's π system enhances the strength of interaction with the metal, while it weakens the C-O bond, favoring the η^2 mode.

In the specific case of Ru, it has been observed [29] that while η^2 is the preferred adsorption species on clean Ru surfaces, only η^1 is present on oxygen-covered surfaces. These authors propose that while the hindrance of η^2 formation can be ascribed to simple geometric blockage of sites, electronic effects are much more significant in determining which configuration is preferred [27]. It is expected that co-adsorption of an electronegative atom results in an increase in the work function of the metal, lowering the Fermi level and making the back-donation less favorable. By contrast, they have observed that η^2 species are favored by co-adsorption of K, which

causes a decrease in work function. It is also expected that the specific surface plane over which the aldehyde adsorbs will affect the type of surface species formed.

In this contribution, we have demonstrated that the generation of smooth planes (e.g. Pd(111)) on the particle surface by increasing either the metal loading or the reduction temperature results in higher etherification rate. This enhancement in rate cannot be due to a higher concentration of η^2 species, since it cannot be expected that Pd(111) planes result in a higher $\eta^2/\ \eta^1$ ratio. In fact, it has been recently shown [36-38] that in high-coordination smooth surfaces the d-band center is located at a lower energy, farther from the Fermi level than rougher surfaces with lower coordination numbers. Accordingly, one may expect that a catalyst with larger and smoother Pd particles, such as those present in the high Pd loading samples studied here, particularly after high temperature reduction, should not present a higher concentration of η^2 species than a catalyst with smaller and rougher particles. Therefore, the enhanced etherification activity of these surfaces must be ascribed to their ability to co-adsorb the two required species in adjacent sites rather than an enhanced ability to adsorb either one.

The 16 wt % Pd, with the largest particle size, may have a higher density of large ensembles necessary for condensation to form the ether (DMPE), thus increasing its yield, while decreasing the yields of the other products. The increased ether yield with increasing reduction temperature, suggests that the Pd surface anneals into the

thermodynamically more stable surfaces (i.e. (111)), resulting in a surface structure having larger ensembles, selective for ether formation. The FTIR results show structural changes to the surface that are consistent with this view.

The decarbonylation reaction requires further transformation of an η^2 (C,O) species with its conversion to an η^1 (C) acyl configuration with the O angled away from the surface (by further H-abstraction by the metal) [26]. This then may form an η^2 (C,C) ketene with the adjacent C bonding to the surface [26]. C-C bond scission occurs, leaving the alkyl fragment and CO [26]. The ether yield is higher than the decarbonylated C_5 hydrocarbon because the ether is more readily formed when there are adjacent surface alkoxides.

The experiments conducted on K-promoted catalysts further support the explanations given above and add another important concept into the discussion. In the first place, as mentioned above, the presence of K on Pd surfaces should result in increased concentration of η^2 species [27]. However, this increase does not result in enhanced etherification activity, but rather a decrease that may be explained by the dilution of the ensemble sites, necessary for the bimolecular surface reaction. A final interesting point is the dramatic increase in selectivity for decarbonylation observed for the 2% K-doped catalyst. This selectivity change may be associated not only with an electronic modification of the Pd activity, but also to a direct participation of K in

the reaction interacting directly with the carbonyl oxygen of the aldehyde and enhancing its C-C bond cleavage.

4.5. Conclusions

The etherification reaction has been studied for 2-methyl-pentanal (MPAL) and 2-methyl-pentanol (MPOL) on supported Pd catalysts. While alcohols adsorb as alkoxide species on the surface, aldehydes adsorb as η^2 (C,O). For high rates of ether formation, it is necessary to have both alkoxide and η^2- adsorbed species on the surface and a stoichiometric mixture of 1:1 of aldehyde and alcohol has been found to be the optimum.

Larger metal particles, that have been sintered and annealed by high reduction temperatures, show lower conversion but higher ether selectivity due to enhancement of the ensembles required for etherification.

Acknowledgment. The support of the Oklahoma Secretary of Energy, the Oklahoma Bioenergy Center, The National Science Foundation (EPSCoR), and the US Department of Energy are gratefully acknowledged.

References

[1] J.N. Chheda, J.A. Dumesic, *Catal. Today*, 123 (2007) 59.

[2] R.M. West, Z.Y. Liu, M. Peter, C.A. Gärtner, J.A. Dumesic*, J. Mole. Catal. A*, 296 (2008) 18.

[3] T. Sooknoi, T. Danuthai, L.L. Lobban, R.G Mallinson, D.E. Resasco, *J. Catal*, 258 (2008) 199.

[4] M. Snare, I. Kubickova, P. Maki-Arvela, D. Chichova, K. Eranen, D.Y. Murzin, *Fuel* 87 (2008) 933.

[5] L. Karas, W.J. Piel, "Ethers", Kirk-Othmer Encyclopedia of Chemical Technology, John Wiley & Sons, Inc, 2004, pp. 567.

[6] G.A. Olah, US Patent 5 520 710 1996.

[7] E.W. Flick, Industrial Solvents Handbook, 5th edition, 1998.

[8] R.J.J. Nel, A. De Klerk , *Ind. Eng. Chem. Res.* 48 (2009) 5230.

[9] A. Corma, M. Renz, *Angew. Chem. Int. Ed.* 46 (2007) 298.

[10] R.H. Clark, W.E. Graham, A.G. Winter, *J. Am. Chem. Soc.* 47 (1925) 2748.

[11] R. Figueras Roca, L. De Mourgues, Y. Trambouze, *J. Catal.* 14 (1969) 107.

[12] H. Feuer, J. Hooz, The Chemistry of the Ether Linkage (Ed.: S.Patai), Interscience, London, (1967) 457.

[13] T.P. Kobylinski, H. Pines, *J. Catal*. 17 (1970) 384.

[14] A. van der Burg, J. Doornbos, N.J. Kos, W.J. Ultee, V. Ponec, *J. Catal.* 54 (1978) 243.

[15] G.M.R. van Druten, V. Ponec, *Appl. Catal. A.* 191 (2000) 153.

[16] G.M.R. van Druten, V. Ponec, *Appl. Catal. A*. 191 (2000) 163.

[17] F. Delbecq, P. Sautet, *Surf. Sci.* 295 (1993) 353.

[18] R. Shekhar, M.A. Barteau, R.V. Plank, J.M. Vohs, *J. Phys. Chem. B*, 101 (1997) 7939.

[19] T.T. Pham, L.L. Lobban, D.E. Resasco, R.G. Mallinson, *J. Catal*. 266 (2009) 9.

[20] A. Palazov, C.C. Chang, R.J. Kokes, *J. Catal*. 36 (1975) 338.

[21] A. Arteaga, F.M. Hoffmann, A.M. Bradshaw, *Surf. Sci*. 119 (1982) 79.

[22] L.L. Sheu, Z. Karpinski, W.M.H. Sachtler*, J. Phys. Chem*. 93 (1989) 4890.

[23] F. Skoda, M.P. Astier, G.M. Pajonk, M. Primet, *Catal. Lett*. 29 (1994) 159.

[24] M. Fernandez-Garcia, J.A. Anderson, G.L. Haller*, J. Phys. Chem*. 100 (1996) 16247.

[25] F.M. Hoffmann, *Surf. Sci. Rep*. 3 (1983) 107.

[26] M. Mavrikakis, M.A. Barteau, *J. Mol. Catal. A*. 131 (1998) 135.

[27] N.R. Avery, W.H. Weinberg, A.B. Anton, B.H. Toby, *Phys. Rev. Lett*. 51 (1983) 682.

[28] N.R. Avery, *Surf. Sci*. 125 (1983) 771.

[29] A.B. Anton, N.R. Avery, B.H. Toby, W.H. Weinberg, *J. Am. Chem. Soc*. 108 (1986) 684.

[30] J.L. Davis, M.A. Barteau, *Surf. Sci.* 187 (1987) 387.

[31] J.L. Davis, M.A. Barteau, *Surf. Sci*. 235 (1990) 235.

[32] S.M. Gates, J.N. Russell, Jr., J.T. Yates, Jr., *Surf. Sci*. 171 (1986) 111.

[33] B.A. Sexton, K.D. Rendulic, A.E. Hughes, *Surf. Sci*. 121 (1982) 181.

[34] S.R. Bare, J.A. Stroscio, W. Ho, *Surf. Sci.* 150 (1985) 399.

[35] S.M. Gates, J.N. Russell Jr., J.T. Yates, Jr., *Surf. Sci*. 159 (1985) 233.

[36] B. Hammer, J.K. Nørskov, *Adv. Catal*. 45 (2000) 71.

[37] M. Mavrikakis, B. Hammer, J.K. Nørskov, *Phys. Lett*. 81 (1998) 2819.

[38] C.E. Tripa, T.S. Zubkov, J.T. Yates, Jr., M. Mavrikakis, J.K. Nørskov, *J. Chem. Phys*. 111 (1999) 8651.

CHAPTER 5: REACTIONS OF 2-METHYL-PENTANAL ON BIMETALLIC Pd-Cu CATALYSTS

Abstract

Bimetallic Pd-Cu catalysts have been studied for the hydrogenation and deoxygenation of 2-methyl-pentanal. Compared to Pd catalysts, Pd-Cu shows a decrease in conversion of 2-methyl-pentanal. At low W/F, 5% Pd-2.5% Cu/SiO_2 exhibits high selectivity for hydrogenation to 2-methyl-pentanol and substantially reduced decarbonylation activity compared with pure 5% Pd/SiO_2. The bimetallic shows that the ratio of etherification of the alcohol product with the 2-methyl-pentanal is much greater than for Pd alone, since the parallel decarbonylation is reduced. Compared at the same 25 % conversion of 2-methyl-pentanal, the ratio of di-methyl-pentyl ether/pentane is 4 times higher on the 5% Pd-2.5% Cu/SiO_2 than on the 5% Pd/SiO_2. The addition of Cu decreases the number of η^2 sites that are needed for both decarbonylation and etherification. However, the bimetallic maintains good ether selectivity due to its ability to readily hydrogenate the aldehyde to the intermediate alcohol and continue to form the required surface alkoxide in proximity to the remaining η^2 sites.

5.1. Introduction

A major objective of catalytic upgrading of bio-oils [1-6] is to produce molecules that are fungible with existing fuels. Hydrogenation and hydrodeoxygenation are established processes to convert aldehydes to alcohols or hydrocarbons that are more stable and suitable for fuels. In previous work [7], etherification of 2-methyl-pentanal has been studied on supported Pd catalysts. The desired product is an ether that may be blended with regular diesel to increase cetane value [8-10]. An aldehyde that adsorbs as an η^1 (O) can be hydrogenated to an alcohol or converted to an alkoxide on the surface that can further couple with an η^2 (C,O) adsorbed aldehyde in proximity to form an ether. However, an undesirable side product is n-pentane that is produced from the decarbonylation reaction that also requires an η^2 (C,O) aldehyde on the surface.

Barteau et. al [11-12] demonstrated the stepwise adsorption modes of an aldehyde on Pd (111) beginning with η^2 (C,O) with conversion to η^1 acyl (C) and then an η^2 (C, C) ketene followed by C-C bond scission of decarbonylation. It is desirable to stabilize the η^2 (C,O) aldehyde on the surface without letting it further convert to η^1 acyl (C) and η^2 (C, C) ketene in order to increase the ether product.

This study investigates the reactions of 2-methyl-pentanal and its product selectivity by modifying the Pd catalyst by addition of Cu. Ponec et. al [13] found that by alloying Cu with Ni, the selectivity for etherification is strongly suppressed with the

dilution of ensembles (η^2 sites) that are required for ether formation. However, the hydrogenation activity was only slightly influenced.

5.2. Experimental

5.2.1 Catalyst synthesis. The 5 wt.% Pd catalyst was prepared by incipient wetness impregnation of the metal precursor on precipitated silica (HiSil 210 obtained from Pittsburg Plate Glass Co.) having a BET surface area of 135 m^2/g. The metal loading on each catalyst was calculated based on the amount of metal precursor incorporated in the catalyst by impregnation. The liquid/solid ratio used to achieve incipient wetness was 1.26 ml/g. The precursor was $Pd(NO_3)_2$, purchased from Sigma Aldrich. After impregnation, the catalyst was dried overnight in an oven and then calcined in air at 400°C for 4 hours. Pd-Cu/SiO_2 catalysts were prepared by impregnation of the $Cu(NO_3)_2 \cdot 2.5H_2O$ precursor to give the desired amount onto the previously prepared and calcined 5 wt.% Pd/SiO_2 catalyst. These were then dried overnight, and calcined in air at 400°C for 4 hours.

5.2.2 Temperature Programmed Reduction. 0.1 to 0.2g of catalyst was loaded into a fixed bed 1/8-in ID quartz tube reactor. 5% H_2 in Argon obtained from AirGas Co. was used as the carrier in order to measure the H_2 uptake. The outlet was connected to a tube filled with Drierite (to absorb moisture produced during the

reduction) and then to a TCD detector. A temperature ramp rate of 10 ^{o}C/min was used.

5.2.3 Chemisorption. CO chemisorption was used to determine the exposed Pd on the Pd and Pd-Cu catalysts. This was conducted in a dynamic chemisorption unit, including a pulse system with an SRI Model 310C Gas Chromatograph equipped with a Thermal Conductivity Detector (TCD). All the catalysts were reduced in H_2 by heating to 200^{o}C with a ramp rate of 10^{o}C/min, held for 1 hour, then flushed with He for 30 min and cooled to room temperature before injecting CO pulses. Pre-mixed 5% CO in He was used for pulse injection with a 0.1 ml loop size. CO adsorption on the blank SiO_2 was carried out at room temperature to subtract any adsorption on the support. However, no CO adsorption was detected. Likewise, no CO adsorption was observed on the Cu only catalyst at this temperature [14]. The results of CO chemisorption on Pd and Pd-Cu are reported in Table 5.1

5.2.4 In situ CO FTIR. DRIFTS experiments were carried out in a Perkin Elmer Spectrum 100 FTIR Spectrometer equipped with an MCT detector and a Reaction Chamber (HVC-DRP) fitted with KBr windows (Harrick Scientific Products, Inc). 50-100 mg of catalyst was loaded to the reaction cell and reduced in H_2 flowing at 30 sccm by heating at a 10^{o}C/min ramp rate to 200^{o}C, then holding for 1 hour followed by flushing with He for 30 minutes before cooling to room temperature. CO (5% in He) then flowed through the chamber for 30 minutes at room temperature and that was

then flushed with He for 20 min before sample spectra were taken. Spectra were acquired at a resolution of 4 cm^{-1} averaging 64 scans.

5.2.5 Catalyst testing. Catalytic activity measurements were carried out in a continuous flow system that included a syringe pump delivering the organic feed to a heated line into a stream of H_2 that flows to the reactor tube within an electric furnace. 0.05 to 0.15 g of catalyst was used with the appropriate flow rate to achieve the desired W/F (g cat/g feed/h). Operating conditions were 125°C and atmospheric pressure. Experiments were continued for 2-3 h. All the lines were heated with heating tapes to keep the feed and products in the vapor phase. The carrier gas, H_2, was used to reduce the catalyst and also flowed at a relative molar ratio 12:1 during reaction with the 2-methyl-pentanal (MPAL). Quantitative product analysis was by online gas chromatography using an HP 6890A with a flame ionization detector. A Shimadzu GCMS-QP2010S provided product identification.

5.3. Results and Discussion

5.3.1 Temperature Programmed Reduction. The TPR results of 5% Pd, 5% Cu and 5% Pd-Cu are shown in Fig. 5.1. The 5% Pd profile consists of 2 peaks at 91°C and 103°C. The negative peak at 91°C occurs due to the decomposition of the β-palladium hydride phase [15-16] since Pd can be reduced as low as 270K [17]. The peak at 103°C is due to further reduction of the palladium [15]. The pure Cu/SiO_2

TPR shows two peaks at 270° and 400°C, consistent with previously reported literature [16]. The 5% Pd-0.25% Cu and 5% Pd-2.5% Cu showed reduction peaks at higher temperatures than for pure palladium. On the 5% Pd-0.25% Cu, the peaks are at 102°, 104° C and a shoulder at 108° C. The 5% Pd-2.5% Cu exhibits peaks up to 250° C; lower than for pure Cu. Strukul et. al [16] observed that above 0.1 wt% Cu (with respect to 2.2 wt% Pd), the negative band disappeared. They also found the major peak at 190°C that is attributed to alloy formation and bands at 390-400° C to be any CuO that does not interact with Pd. The TPR results, with the disappearance of the high temperature peaks, show that the alloy is the predominant phase.

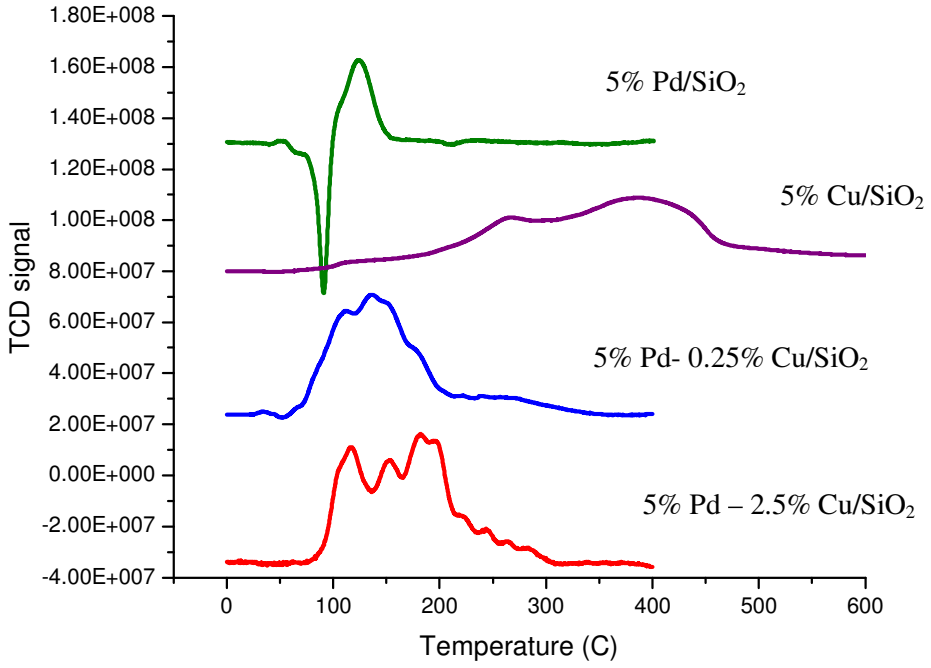

Fig. 5. 1. TPR of 5% Pd, 5% Cu, 5% Pd-0.25% Cu and 5% Pd-2.5% Cu ramping from 25°C to 400°C at 10°C/min rate.

5.3.2 CO Chemisorption. Chemisorption results on 5% Pd and 5% Pd-2.5% Cu are summarized in Table 5.1. For the 5% Pd/SiO_2, the exposed Pd on the surface is 7.94% (the catalyst is reduced at 200^o C to compare with 5% Pd-2.5% Cu). For the bimetallic 5% Pd-2.5% Cu/SiO_2, the exposed Pd is greatly reduced (4.64 times) to 1.71%, as shown in Table 5.1. Previous chemisorption work on Cu [14] showed no adsorbed CO on Cu surface. The large reduction of CO uptake by the bimetallic suggests that the Pd-Cu alloy does not adsorb CO. The remaining CO adsorption suggests that there is some exposed Pd or Pd rich regions present.

Table 5. 1. Dynamic pulsed CO chemisorption on 5% Pd/SiO_2 and 5% Pd-2.5% Cu/SiO_2.

Catalyst	5% Pd	5% Pd - 0.25% Cu	5% Pd -2.5% Cu
% Pd exposed			
CO/M	0.079	0.024	0.017

5.3.3 In situ CO FTIR. In situ DRIFTS CO spectra for the 5% Pd, and 5% Pd-Cu are shown in Fig. 5.2. The peaks at 1980 and 1940 cm^{-1} are assigned to the bridge and multi-bonded CO species, respectively. This is typical of relatively large particles, in agreement with the rather low metal dispersions estimated from chemisorption measurements [18-19]. The much weaker band ascribed to linear CO appearing at around 2070 cm^{-1} [20-21] overlaps with the two peaks resulting from residual gas

phase CO remaining in the optical path after flushing with He for 20 min. It can be seen that as little as 0.25% Cu greatly reduces the area of the bridge and multi-bonded region with the multi-bonded being more affected. At the same time, the linear CO on Pd slightly increases with the growth of a band at 2125 cm^{-1}. This in agreement with Skoda [21] and Hutchings [22] who found that Cu with Pd increases the linear CO band with a reduction of bridge and multi-bonded CO. The band at 2125 cm^{-1} is attributed to CO adsorption on Cu^{+} sites [22-23]. Since the reduction temperature in this work is at 200^{o} C, there may still be a small fraction of CuO present, and this is indicated in the TPR profile of 5% Pd- 2.5% Cu where small shoulders appear between 200^{o} and 300^{o} C.

For the 5% Pd -2.5 % Cu, the bridge and multi-bonded bands are almost gone. However, the linear CO at 2070 cm^{-1} increases, consistent with previous work [21-22] and indicating the presence of predominantly the alloy.

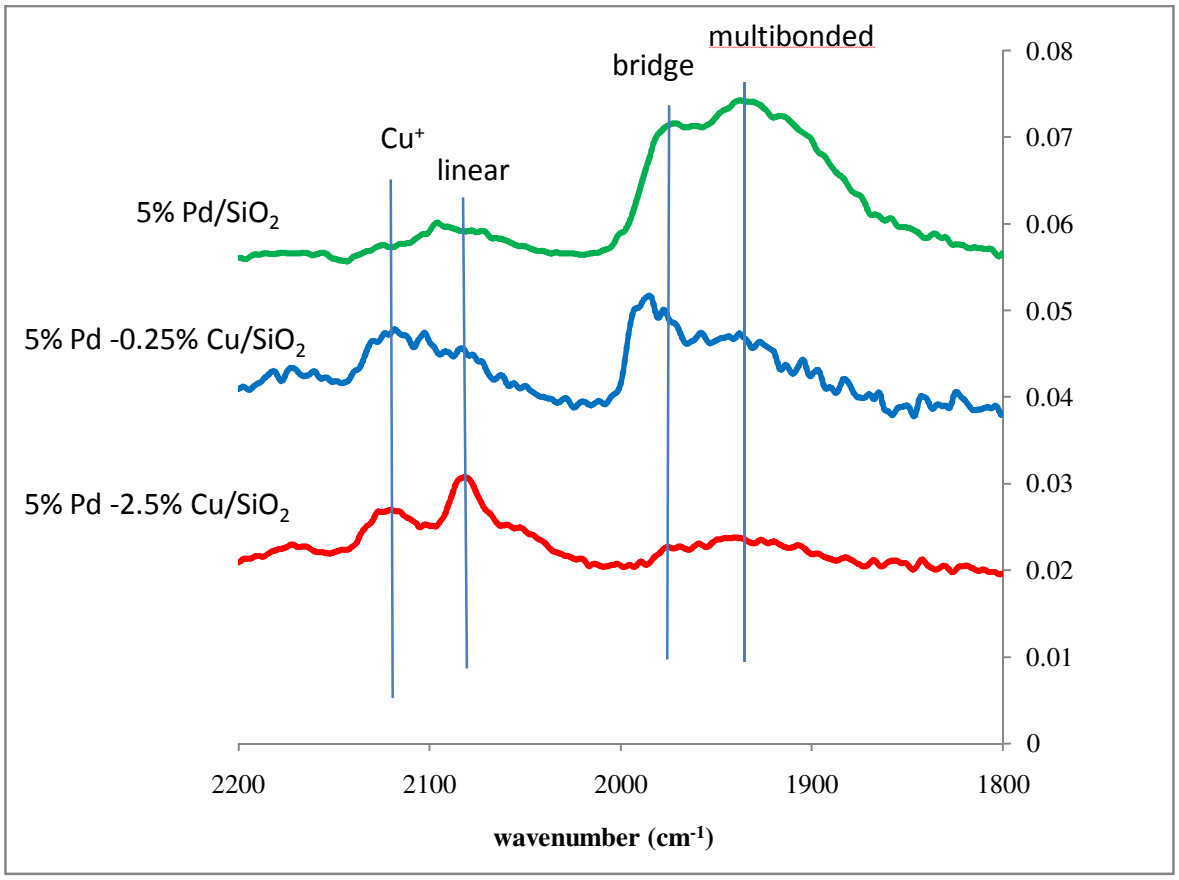

Fig. 5. 2. CO FTIR of 5% Pd, 5% Pd-0.25% Cu and 5% Pd-2.5% Cu all reduced at 200°C in H_2, flushed and cooled down in He.

5.3.4 Reactions of 2-methyl-pentanal on 5% Pd/SiO_2

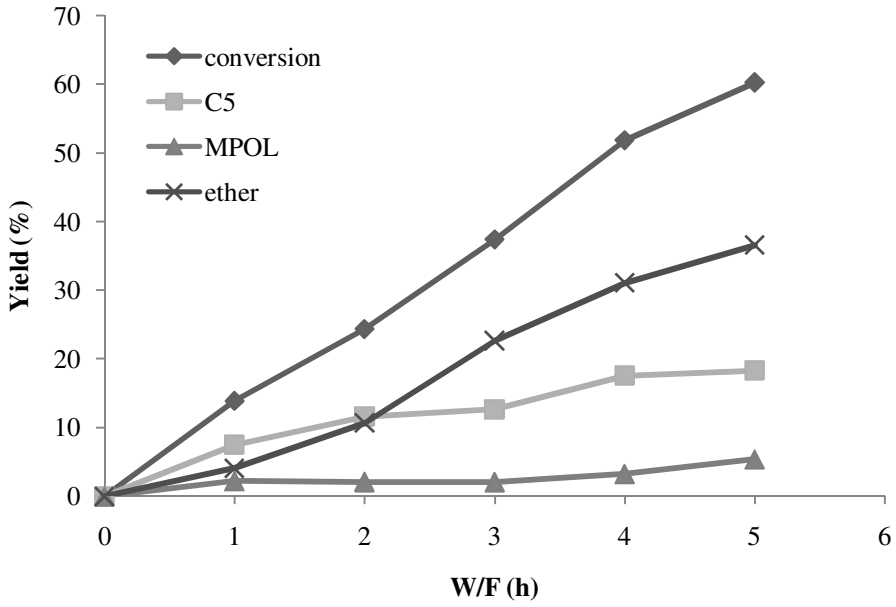

Fig. 5. 3. Conversion and yields of products from 2-methyl-pentanal on 5%Pd/SiO_2 reduced at 200°C and run at 125°C, H_2: MPAL = 12:1

To discern the effects of individual components of the bimetallic catalyst, the reaction of 2-methyl-pentanal has been tested on the 5% Pd/SiO_2 alone to study the conversion and its product distribution. Conversion of the feed and yields of products are plotted in Fig. 5.3. Upon increasing W/F from 1 to 5 h, the conversion increases from 15 to 60%. Ether and n-pentane yields both increase with increased W/F. The 2-methyl-pentanol yield stays relatively flat as it is an intermediate that is continually consumed with the MPAL feed to form the ether (DMPE) [7]. The n-pentane results from the decarbonylation of MPAL that happens parallel with the hydrogenation and subsequent etherification reactions.

5.3.5 Reactions of 2-methyl-pentanal on 5% Cu/SiO_2

The 5% Cu/SiO_2 was tested for the reaction of 2-methyl-pentanal in hydrogen as a comparison with the bimetallic and pure palladium catalysts. The only reaction of 2-methyl-pentanal on 5% Cu/SiO_2 is the hydrogenation reaction forming 2-methyl-pentanol. The conversion at W/F = 2h is 15.6% with 100% selectivity to 2-methyl-pentanol. At the reaction temperature of 125^{o}C, the equilibrium ratio of alcohol to aldehyde is 44.1 , so one can expect alcohol as a major product. However, at this level of conversion, the alcohol/aldehyde ratio is far from equilibrium. These results are consistent with previous work [14].

5.3.6 Comparison of 5% Pd/SiO_2 vs. 5% Pd-0.25% Cu/SiO_2

The results of the reaction of 2-methyl-pentanal on 5% Pd-0.25% Cu/SiO_2 are shown in Fig. 5.4. It can be observed that although the activity is lower, the overall trend of conversion and product yields are similar to the 5% Pd/SiO_2 catalyst. The major product is n-pentane. The yields of DMPE and MPOL are lower. However, as W/F increases to 3 hr, the yield of ether increases and the rate of ether formation becomes higher than that of n-pentane. Note that on the 5% Pd/SiO_2. the crossover point for ether and n-pentane occurs at similar conversion, X~ 25% (at W/F= 2h compared to W/F =3h on the 5% Pd-0.25% Cu). Thus, the product selectivities are similar on both catalysts at similar conversions. This is because the bulk atomic ratio of Pd:Cu is 12:1 with predominantly pure Pd, thus the catalyst behaves very similar to pure Pd.

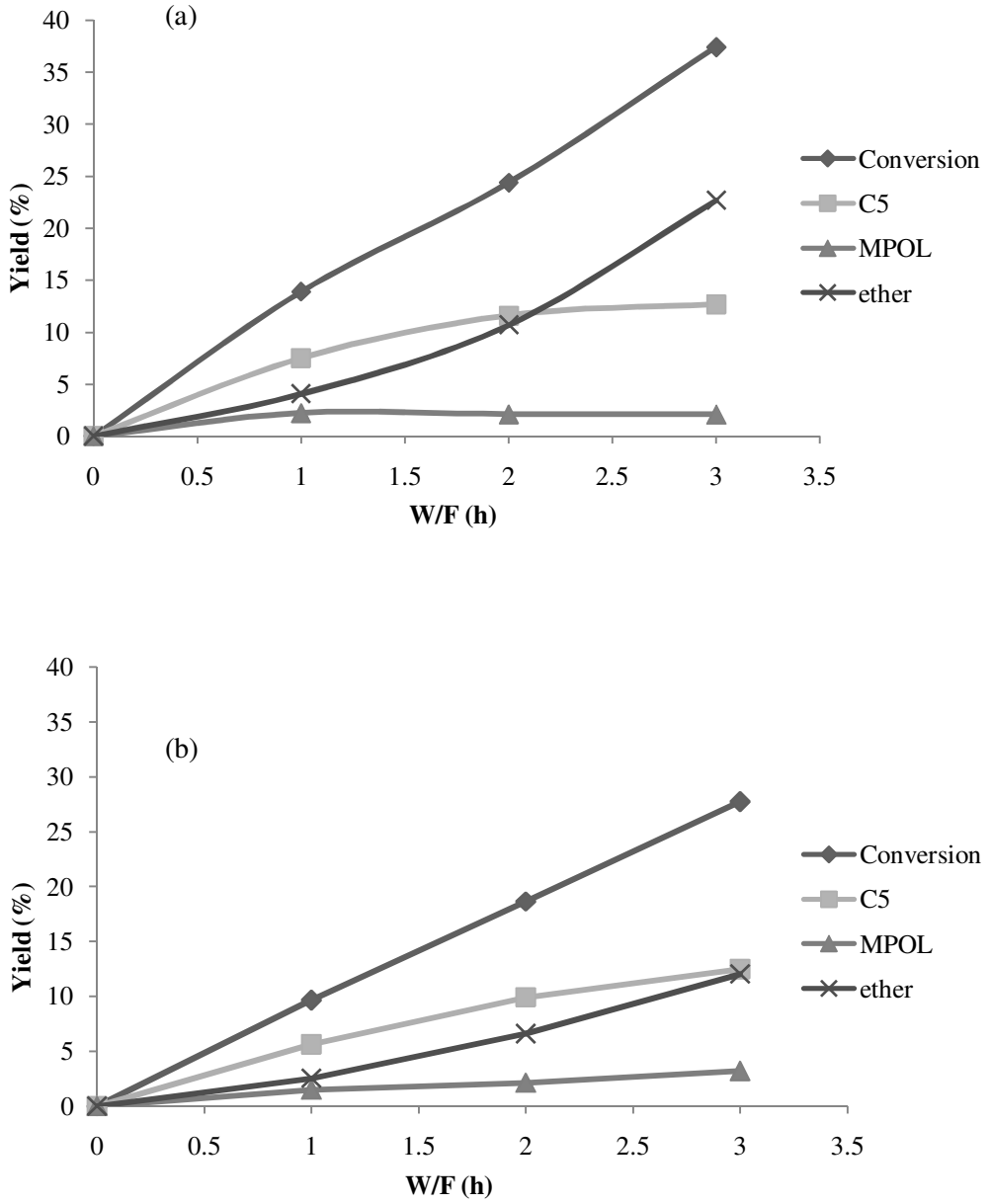

Fig. 5. 4. (a) Conversion and yields of products from 2-methyl-pentanal on 5% Pd/SiO_2 reduced at 200°C and run at 125°C, H_2: MPAL = 12:1 at lower W/F.(b) Conversion and yields of products from 2-methyl-pentanal on 5% Pd-0.25% Cu/SiO_2 reduced at 200°C and run at 125°C, H_2: MPAL = 12:1

5.3.7 Reactions of 2-methyl-pentanal on 5% Pd-2.5% Cu/SiO_2

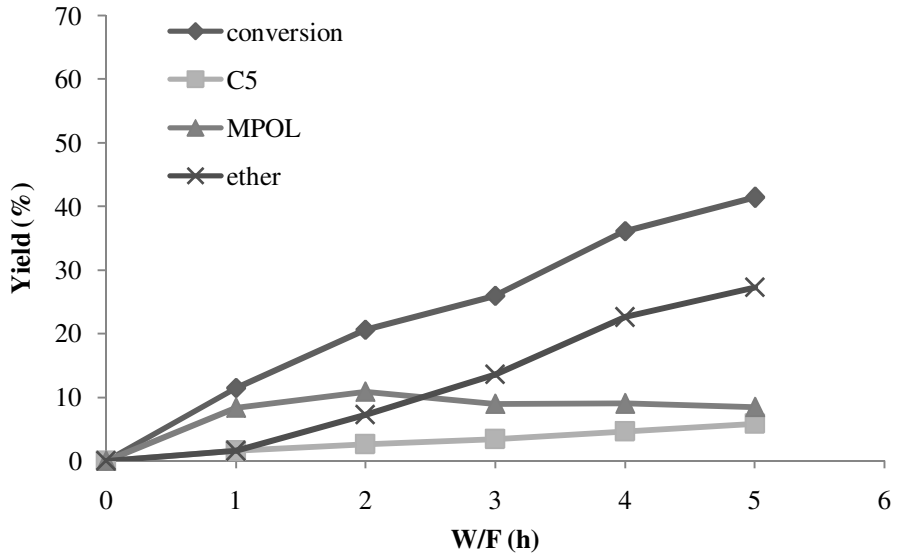

Fig. 5. 5. Conversion and yields of products from 2-methyl-pentanal on 5% Pd-2.5% Cu/SiO_2 reduced at 200°C and run at 125°C, H_2: MPAL = 12:1

The conversion and product distribution from feeding 2-methyl-pentanal on 5% Pd-2.5% Cu/SiO_2 is shown in Fig. 5.5. The conversion and ether and n-pentane yields increase with increased W/F. The yield of MPOL increased up to W/F = 2h and then slightly decreased at higher W/F. This shows that initially (up to W/F = 2h) the rate of hydrogenation is much higher compared to etherification and decarbonylation. However, once the alcohol concentration builds up, the secondary reaction rate of etherification starts to increase. Thus, MPOL is consumed to form ether. The formation rate of n-pentane is relatively low compared to the others.

Comparing the 5% Pd catalyst (Fig. 5.3) with the 5 % Pd- 2.5 % Cu (Fig. 5.5), the pure Pd shows much higher decarbonylation activity compared to the alloyed Pd. The addition of Cu clearly suppresses the decarbonylation activity while enhancing the hydrogenation activity. The alcohol yield is considerably higher on the alloy than on the Pd, indicating a shift in the relative rate of the two reactions. The ether yield is initially lower on the alloy. It has been shown in previous work [7] that the formation of the ether requires both aldehyde and alcohol, thus these results show that the formation of the ether occurs as a secondary product that is enhanced by the higher amount of alcohol with higher selectivity for ether at longer W/F. The activity for decarbonylation and etherification (after some hydrogenation) represent parallel pathways and understanding the control of these pathways is one of the objectives of this study. This relative balance is most clearly impacted by the suppression of the decarbonylation pathway, though overall activity is also lower. This balance can be shown by viewing the ratio of the two pathways in the form of the ratio of the ether to pentane, shown in Fig. 5.6.

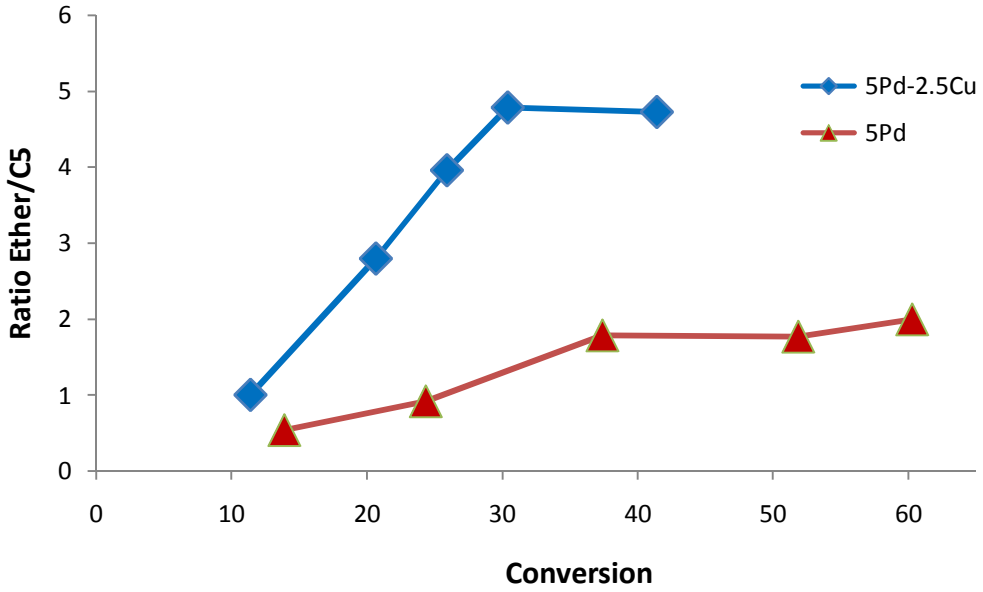

Fig. 5. 6. Comparison of Ratio of Ether/C_5 vs. Conversion for 5% Pd and 5% Pd-2.5% Cu.

It may be seen that the ratio of Ether/C_5 increased with increased conversion on both catalysts. This is primarily because the ether is a secondary product from condensation of the aldehyde with the alcohol and the alcohol takes some time to increase in concentration. However, the ratio increased with a greater slope on 5% Pd-2.5% Cu than on the 5% Pd up to about 30 % conversion due to the higher amount of alcohol produced at lower conversion on the alloy. Also, at the same conversion, the ratio of Ether/C_5 is always higher for the 5% Pd-2.5% Cu than the 5% Pd, essentially due to the much lower decarbonylation activity on the alloy, as pointed out above.

The selectivity shift and lower activity when adding Cu to the Pd catalyst can be explained as a geometric effect. The presence of Cu reduces the ensembles required for the decarbonylation reaction that requires an η^2 –adsorbed aldehyde and the subsequent H abstraction forming η^1 acyl and η^2 ketene species. However, Cu is well-known for its ability to interact with the oxygen of the carbonyl to form the alkoxide species needed for the hydrogenation to alcohol and alcohol formation is not dramatically affected. The higher relative amount of alcohol (alkoxide) partially overcomes the loss of η^2 and the etherification yield remains substantial, giving rise to the increase in ratio of ether/pentane. Etherification from and alkoxide and an η^2 aldehyde is shown in Fig. 5.7.

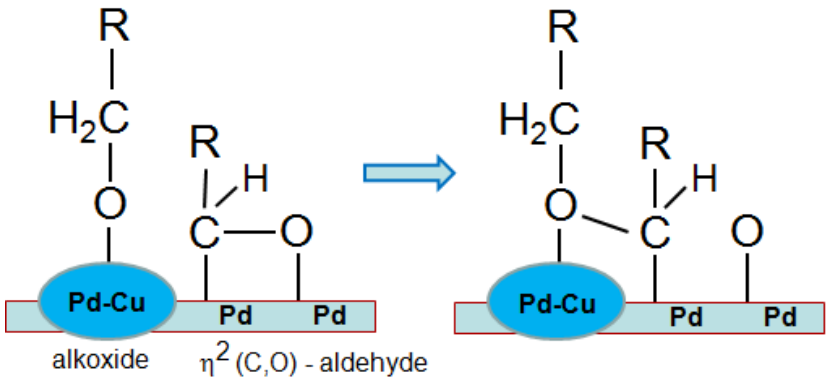

Fig. 5. 7. Adsorption of aldehyde and alcohol intermediates on bimetallic Pd-Cu alloy surface.

5.3.8 Model fitting

Pseudo first-order models were fitted to the data for the 5% Pd/SiO_2 and 5% Pd-2.5% Cu/SiO_2. These simple models therefore assume that competitive adsorption of products on the surface is not significant. For each catalyst, all product yield and conversion data were simultaneously fitted for a plug flow reactor model. The k values are kinetic parameters representing the hydrogenation, etherification and decarbonylation reactions as follows:

2-methyl-pentanal (η^1) + H_2 $\Leftrightarrow$ 2-methyl-pentanol (1) k_1 ,$K_{eq} = 44$

2-methyl-pentanal (η^2) + 2-methyl-pentanol (alkoxide) $\rightarrow$ ether (2) k_2

2-methyl-pentanal (η^2) $\rightarrow$ n-pentane + CO (3) k_3

Table 5. 2. Kinetic parameters of 2-methyl-pentanal on 5% Pd/SiO_2 and 5% Pd -2.5% Cu/SiO_2

k's		k_1	k_2	k_3	Total least square error
Catalyst					
	Pd	0.1	40.08	0.05	27.5
	Pd-Cu	0.09	11.43	0.01	43.9

The fitted rate constant k's are reported in Table 5.2. For the hydrogenation reaction, the rates are very similar for both. The rate of etherification on Pd alone is about 4

times higher than that of Pd-Cu. The rate of decarbonylation of Pd is 5 times higher than that of Pd-Cu. The addition of Cu does not significantly affect the hydrogenation activity, but only reduces the rates of etherification and decarbonylation, consistent with the earlier work by Ponec [13].

5.4. Conclusions

The reactions of 2-methyl-pentanal have been studied on SiO_2 supported Pd and bimetallic Pd-Cu catalysts. TPR results indicate that Pd and Cu substantially form an alloy. The 5% Pd – 0.25% Cu/SiO_2 has lower activity but very similar selectivities with 5% Pd/SiO_2. The 5 % Pd – 2.5% Cu also exhibits lower activity, however, the selectivities are quite different compared to the 5% Pd. That is, the ether selectivity is much higher while n-pentane selectivity is much lower for the same conversion. The kinetic model shows that the rates of hydrogenation remain about the same for both 5% Pd and 5 % Pd – 2.5% Cu, but the rates for decarbonylation and etherification decrease on the bimetallic catalyst; however, the rate of etherification does not drop as much as that of decarbonylation. The effect of the loss of η^2 sites impacts both decarbonylation and etherification. However, etherification is a secondary reaction requiring an alkoxide and an η^2 aldehyde in proximity, and the loss of η^2 sites is offset by the continued hydrogenation activity and alkoxide formation on the alloy.

References

[1] T. Danuthai, S. Jongpatiwut, T. Rirksomboon, S. Osuwan, D.E. Resasco, *Appl. Catal. A-Gen*, 361 (2009) 99.

[2] E.L. Kunkes, R.R. Soares, D.A. Simonetti, J.A. Dumesic, *Appl Catal B-Environ*, 90 (2009) 693.

[3] H. Bernas, K. Eranen, I. Simakova, A. Leino, K. Kordas, J. Myllyoja, P. Maki-Arvela, T. Salmi, D.Y. Murzin, *Fuel*, (2009).

[4] D. Prochazkova, P. Zamostny, M. Bejblova, L. Cerveny, J. Cejka, *Appl. Catal. A-Gen*, 332 (2007) 56.

[5] E. Furimsky, *Appl. Catal. A-Gen*, 199 (2000) 147.

[6] C.A. Fisk, T. Morgan, Y.Y. Ji, M. Crocker, C. Crofcheck, S.A. Lewis, *Appl. Catal. A-Gen*, 358 (2009) 150.

[7] T.T. Pham, S.P. Crossley, T. Sooknoi, L.L. Lobban, D.E. Resasco, R.G. Mallinson, *Appl. Catal. A*, (2010).

[8] G.A. Olah, Vol. 5520710, US, 1996.

[9] E.W. Flick, Industrial Solvents Handbook, 1998.

[10] R.J.J. Nel, A. de Klerk, *Ind Eng Chem Res*, 48 (2009) 5230.

[11] J.L. Davis, M.A. Barteau, *Surf. Sci.*, 235 (1990) 235.

[12] M. Mavrikakis, M.A. Barteau, *J Mol Catal a-Chem*, 131 (1998) 135.

[13] A. Vanderburg, J. Doornbos, N.J. Kos, W.J. Ultee, V. Ponec, *J. Catal.*, 54 (1978) 243.

[14] T.T. Pham, L.L. Lobban, D.E. Resasco, R.G. Mallinson, *J. Catal.*, 266 (2009) 9.

[15] G. Lietz, M. Nimz, J. Volter, *Appl. Catal.* , 45 (1988) 71.

[16] A. Benedetti, G. Fagherazzi, F. Pinna, G. Rampazzo, M. Selva, G. Strukul, *Catal. Lett.*, 10 (1991) 215.

[17] H. Lieske, G. Lietz, W. Hanke, J. Volter, *Z. Anorg. Allg. Chem.*, 527 (1985) 135.

[18] A. Palazov, C.C. Chang, R.J. Kokes, *J. Catal.*, 36 (1975) 338.

[19] A. Arteaga, F.M. Hoffmann, A.M. Bradshaw, *Surf. Sci.*, 119 (1982) 79.

[20] L.L. Sheu, Z. Karpinski, W.M.H. Sachtler, *J Phys Chem-Us*, 93 (1989) 4890.

[21] F. Skoda, M.P. Astier, G.M. Pajonk, M. Primet, *Catal. Lett.*, 29 (1994) 159.

[22] S.S. Ashour, J.E. Bailie, C.H. Rochester, J. Thomson, G.J. Hutchings, *J Mol Catal a-Chem*, 123 (1997) 65.

[23] G.J. Millar, C.H. Rochester, K.C. Waugh, *J. Chem. Soc. Faraday Trans*, 87 (1991) 1467.

CHAPTER 6: CONCLUSIONS AND OUTLOOK

6.1. CONCLUSIONS

The hydrogenation of 2-methyl-2-pentenal has been studied on supported metals Pt, Pd and Cu. 0.5 % Pd, and 0.5% Pt showed strong hydrogenation of the C=C bond to form the saturated aldehyde. At very low conversion, 5 wt.% Cu/SiO_2 showed strong initial hydrogenation activity of C=O to form primarily 2-methyl-2-pentenol. On Pt and Pd catalysts, decarbonylation leads to n-pentane via C-C cleavage, becoming significant at higher W/F or at higher temperature. On Cu, 2-methyl-pentane via C-O hydrogenolysis was observed on Cu as a minor product at 200 ^{o}C, but became the dominant product on Cu as the temperature was increased to 400 ^{o}C.

From the practical point of view, it may be desirable to produce the 2-methyl-pentanol using the Cu catalyst at lower temperatures, since these alcohols are stable and have fairly good octane numbers. At higher temperatures, Cu is a good catalyst for total removal of oxygen without loss of carbon.

The etherification reaction has been studied for 2-methyl-pentanal (MPAL) and 2-methyl-pentanol (MPOL) on supported Pd catalysts. While alcohols adsorb as alkoxide species on the surface, aldehydes adsorb as η^2 (C,O). For high rates of ether formation, it is necessary to have both alkoxide and η^2- adsorbed species on the surface and a stoichiometric mixture of 1:1 of aldehyde and alcohol has been found to be the optimum.

Larger metal particles, that have been sintered and annealed by high reduction temperatures, show lower conversion but higher ether selectivity due to enhancement of the ensembles required for etherification.

The reactions of 2-methyl-pentanal have been studied on bimetallic Pd-Cu catalysts. TPR results indicate that Pd and Cu form an alloy. The 5% Pd – 0.25% Cu/SiO_2 has lower activity but very similar selectivities at the same conversions with 5% Pd/SiO_2. The 5 % Pd – 2.5% Cu also shows lower activity, however, the selectivies are quite different to the 5% Pd, that is, the ether selectivity is much higher while n-pentane selectivity is much lower for the same conversion. The fitting model shows that the rates of hydrogenation remain about the same for both 5% Pd and 5 % Pd – 2.5% Cu, and the rates for decarbonylation and etherification decrease on the bimetallic; however, the rate of etherification does not drop as much as that of decarbonylation. The loss of η^2 on etherification, a secondary reaction requiring an alkoxide and an η^2

aldehyde in proximity, is offset by the hydrogenation activity while the loss on decarbonylation cannot be overcome with the addition of Cu.

6.2. OUTLOOK

The experimental results obtained in this work were analyzed to study the pathways and selectivities of products for the aldehydes and alcohols on different supported metals: Pt, Pd, Cu and Pd-Cu. Some basic knowledge and understandings are gained by varying reaction conditions, or modifying the catalysts by changing the loadings, reduction temperatures, or alloying. These experiments can be expanded to different metals across group VIII, such as Ni, Co, Fe, Ru, Rh and group IB Ag, Au, not only for the aldehyde and alcohol feed but also for other oxygenates.

With developing and obtaining a database from literatures and experimental works for different types of oxygenates, and different metals, a roburst model can be built using QSAR for structure-property relationship as presented by Dr. Crossley in his work "Molecular Engineering Strategies for the production of fuels from convenetional and renewable resources", correlation of conversion and selectivies can be constructed against the same catalysts or family of feed, for example, aldehydes, to study the effect of chain length, or effect of alkyl substitution.

Beside the help of QSAR in predicting and correlating quantitatively the performance of various feeds on a catalyst, theoretical calculation methods using Density Functional Theory (DFT) can be applied for hydrodeoxygenation reactions on metals and results can be used to varify experimental data. For example, DFT can be used to calculate the bond length and adsorption energies for propanal on Pt, Pd, Cu and expanded to Ni, Rh, and Ru. Not only these parameters can be obtained, but also the types of transition states or intermediates can be explored to see η^2 or η^1 adsorption species and their relative ratios when changing reaction conditions or changing different metals.

In this contribution, the hydrogenation and hydrodeoxygenation of the mixed feed of aldehyde and alcohol have been studied. However, the real feed of bio-oil contains thousands of compounds beside just aldehydes and alcohols. But these compounds can be categorized by groups such as: ketones, carboxylics, phenolics, furanics and levoglucosan. Experimentally, one can use a real feed of bio-oil to study deoxygenation; however, this approach is simply a "black box" method and what obtained can be analyzed before and after such as oxygen content, density, viscosity and heating values. In order to understand the chemistry to control product selectivities, the use of model compounds greatly helps provide information for the contribution and intereactions of functional groups toward a catalyst. For example, a

mixture of simple aldehyde and acid can be studied on a metal vs. a mixture of alcohol and acid. Then, the combination can be expanded to three components and maybe four or higher. The model mixtures should be kept as simple yet representative for a real feed of bio-oil.

BIBLIOGRAPHY

[1] http://www.eia.doe.gov/oiaf/aeo/pdf/overview.pdf.

[2] http://feedstockreview.ornl.gov/pdf/billion_ton_vision.pdf.

[3] D. Mohan, C.U. Pittman, P.H. Steele, *Energ Fuel*, 20 (2006) 848.

[4] G.W. Huber, J.A. Dumesic, *Catal. Today.*, 111 (2006) 119.

[5] G.W. Huber, S. Iborra, A. Corma, *Chem. Rev.*, 106 (2006) 4044.

[6] J.B.S. Bredenberg, M. Huuska, J. Raty, M. Korpio, *J. Catal.*, 77 (1982) 242.

[7] S.P. Crossley, Vol. PhD, University of Oklahoma, 2009.

[8] A.M. Hill, D.A. Feinberg, Fuel Products from Microalgae, National Renewable Energy Laboratory: Golden, CO., 1984.

[9] D.L. Klass, Biomass for Renewable Energy, Fuels and Chemicals, Academic Press: San Diego, 1998.

[10] T.Q. Hoang, Vol. PhD Desertation, University of Oklahoma, 2010.

[11] Q.V. Amen, Vol. M.S. Desertation, University of Oklahoma, 2009.

[12] R.D. Cortright, R.R. Davda, J.A. Dumesic, *Nature*, 418 (2002) 964.

[13] R.R. Davda, J.A. Dumesic, *Angew. Chem. Int. Ed. Engl.*, 42 (2003) 4068.

[14] R.R. Davda, J.A. Dumesic, *Chem Commun (Camb)*, (2004) 36.

[15] G.W. Huber, R.D. Cortright, J.A. Dumesic, *Angew Chem Int Ed Engl*, 43 (2004) 1549.

[16] G.W. Huber, J.W. Shabaker, J.A. Dumesic, *Science*, 300 (2003) 2075.

[17] J. Greeley, M. Mavrikakis, *JACS*, 124 (2002) 7193.

[18] R.H. Heck, N.Y. Chen, *Ind Eng Chem Res*, 32 (1993) 1003.

[19] M. Snare, I. Kubickova, P. Maki-Arvela, K. Eranen, D.Y. Murzin, *Ind Eng Chem Res*, 45 (2006) 5708.

[20] P. Maki-Arvela, M. Snare, K. Eranen, J. Myllyoja, D.Y. Murzin, *Fuel*, 87 (2008) 3543.

[21] P. Maki-Arvela, I. Kubickova, M. Snare, K. Eranen, D.Y. Murzin, *Energ Fuel*, 21 (2007) 30.

[22] X.Q. Wang, R.Y. Saleh, U.S. Ozkan, *J. Catal.*, 231 (2005) 20.

[23] T.B.L.W. Marinelli, J.H. Vleeming, V. Ponec, D. Wang, D.G. Blackmond, D. Arntz, G. Jannes, K. Kunimori, C.H. Rochester, *Stud. Surf. Sci. Catal.*, 75 (1993) 1211.

[24] V. Ponec, *Appl. Catal. A-Gen*, 149 (1997) 27.

[25] T.B.L.W. Marinelli, S. Nabuurs, V. Ponec, *J. Catal.*, 151 (1995) 431.

[26] F. Delbecq, P. Sautet, *Surf. Sci.*, 295 (1993) 353.

[27] M. Mavrikakis, M.A. Barteau, *J Mol Catal a-Chem*, 131 (1998) 135.

[28] J.L. Davis, M.A. Barteau, *Surf. Sci.*, 235 (1990) 235.

[29] Y. Yang, A. Gilbert, C.B. Xu, *Appl. Catal. A-Gen*, 360 (2009) 242.

[30] R.K.M.R. Kallury, T.T. Tidwell, D.G.B. Boocock, D.H.L. Chow, *Can J Chem*, 62 (1984) 2540.

[31] C.A. Fisk, T. Morgan, Y.Y. Ji, M. Crocker, C. Crofcheck, S.A. Lewis, *Appl. Catal. A-Gen*, 358 (2009) 150.

[32] R. Pestman, A. van Duijne, J.A.Z. Pieterse, V. Ponec, *J. Mol. Catal. A: Chem.*, 103 (1995) 175.

[33] E.L. Kunkes, E.I. Gurbuz, J.A. Dumesic, *J. Catal.*, 266 (2009) 236.

[34] E.I. Gürbüz, E.L. Kunkes, J.A. Dumesic, *Applied Catalysis B: Environmental*, In Press, Corrected Proof.

[35] S. Crossley, J. Faria, M. Shen, D.E. Resasco, *Science*, 327 (2010) 68.

[36] T. Sooknoi, T. Danuthai, L.L. Lobban, R.G. Mallinson, D.E. Resasco, *J. Catal.*, 258 (2008) 199.

[37] N. Gyorffy, Z. Paal, *J Mol Catal a-Chem*, 295 (2008) 24.

[38] P.N. Rylander, Hydrogenation Methods, Academic Press, San Diego, CA, 1985.

[39] M. Snare, I. Kubickova, P. Maki-Arvela, D. Chichova, K. Eranen, D.Y. Murzin, *Fuel*, 87 (2008) 933.

[40] G.C. Bond, Catalysis by Metals, Academic Press, New York, 1962.

[41] P. Sautet, J.F. Paul, *Catal. Lett.*, 9 (1991) 245.

[42] F. Delbecq, P. Sautet, *Catal. Lett.*, 28 (1994) 89.

[43] F. Delbecq, P. Sautet, *Langmuir*, 9 (1993) 197.

[44] F. Delbecq, P. Sautet, *Surf. Sci.*, 295 (1993) 353.

[45] D.S. Brands, E.K. Poels, A. Bliek, *Appl. Catal. A-Gen*, 184 (1999) 279.

[46] J.v. Beijnum, Ph.D. Thesis, University of Ultrech, 1991.

[47] C.J.G. Vandergrift, A.F.H. Wielers, B.P.J. Joghi, J. Vanbeijnum, M. Deboer, M. Versluijshelder, J.W. Geus, *J. Catal.*, 131 (1991) 178.

[48] F.T. Vandescheur, B. Vanderlinden, M.C. Mittelmeijerhazeleger, J.G. Nazloomian, L.H. Staal, *Appl. Catal. A-Gen*, 111 (1994) 63.

[49] J. Jenck, J.E. Germain, *J. Catal.*, 65 (1980) 141.

[50] N.M. Bertero, C.R. Apesteguia, A.J. Marchi, *Appl. Catal. A-Gen*, 349 (2008) 100.

[51] G.V. Smith, F. Notheisz, Heterogeneous Catalysis in Organic Chemistry, Academic Press, 1999.

[52] P. Do, S. Crossley, M. Santikunaporn, D.E. Resasco, Catalysis 2007.

[53] J.M. Luco, E. Marchevsky, *Curr. Comput.-Aided Drug Des.*, 2 (2000) 31.

[54] R.P. Verma, *Mini Rev. Med. Chem.* , 6 (2006) 467.

[55] F. Pompeo, N.N. Nichio, O.A. Ferretti, D. Resasco, *Int. J. Hydrogen Energy*, 30 (2005) 1399.

[56] CRC, Handbook of Chemistry and Physics, 2007-2008.

[57] V. Ponec, *Appl. Catal. A-Gen*, 149 (1997) 27.

[58] F. Delbecq, P. Sautet, *J. Catal.*, 152 (1995) 217.

[59] P. Beccat, J.C. Bertolini, Y. Gauthier, J. Massardier, P. Ruiz, *J. Catal.*, 126 (1990) 451.

[60] T. Birchem, C.M. Pradier, Y. Berthier, G. Cordier, *J. Catal.*, 146 (1994) 503.

[61] R.L. Augustine, *Catal Rev*, 13 (1976) 285.

[62] E.L. Rodrigues, A. Marchi, C.R. Apesteguia, J.M.C. Bueno, *Appl. Catal. A-Gen*, 294 (2005) 197.

[63] P.G.N. Mertens, P. Vandezande, X.P. Ye, H. Poelman, I.F.J. Vankelecom, D.E. De Vos, *Appl. Catal. A-Gen*, 355 (2009) 176.

[64] M. Boronat, M. May, F. Illas, *Surf. Sci.*, 602 (2008) 3284.

[65] M. Consonni, D. Jokic, D.Y. Murzin, R. Touroude, *J. Catal.*, 188 (1999) 165.

[66] J.N. Chheda, J.A. Dumesic, *Catal. Today*, 123 (2007) 59.

[67] R.M. West, Z.Y. Liu, M. Peter, J.A. Dumesic, *ChemSusChem*, 1 (2008) 417.

[68] L. Karas, W.J. Piel, Ethers, Kirk-Othmer Encyclopedia of Chemical Technology, John Wiley & Sons, Inc, 2004.

[69] G.A. Olah, Vol. US Patent 5 520 710, 1996.

[70] E.W. Flick, Industrial Solvents Handbook, 1998.

[71] R.J.J. Nel, A. de Klerk, *Ind Eng Chem Res*, 48 (2009) 5230.

[72] A. Corma, M. Renz, *Angew Chem Int Edit*, 46 (2007) 298.

[73] R.H. Clark, W.E. Graham, A.G. Winter, *JACS*, 47 (1925) 2748.

[74] F.F. Roca, Demourgu.L, Y. Trambouze, *J. Catal.*, 14 (1969) 107.

[75] H. Feuer, J. Hooz, The chemistry of the ether linkage (Ed: S. Patai), Interscience, London, 1967.

[76] Kobylins.Tp, H. Pines, *J. Catal.*, 17 (1970) 384.

[77] A. Vanderburg, J. Doornbos, N.J. Kos, W.J. Ultee, V. Ponec, *J. Catal.*, 54 (1978) 243.

[78] G.M.R. van Druten, V. Ponec, *Appl. Catal. A-Gen*, 191 (2000) 153.

[79] G.M.R. van Druten, V. Ponec, *Appl. Catal. A-Gen*, 191 (2000) 163.

[80] R. Shekhar, M.A. Barteau, R.V. Plank, J.M. Vohs, *J. Phys. Chem. B*, 101 (1997) 7939.

[81] T.T. Pham, L.L. Lobban, D.E. Resasco, R.G. Mallinson, *J. Catal.*, 266 (2009) 9.

[82] A. Palazov, C.C. Chang, R.J. Kokes, *J. Catal.*, 36 (1975) 338.

[83] A. Arteaga, F.M. Hoffmann, A.M. Bradshaw, *Surf. Sci.*, 119 (1982) 79.

[84] L.L. Sheu, Z. Karpinksi, W.M.H. Sachtler, *J Phys Chem-Us*, 93 (1989) 4890.

[85] F. Skoda, M.P. Astier, G.M. Pajonk, M. Primet, *Catal. Lett.*, 29 (1994) 159.

[86] M. FernandezGarcia, J.A. Anderson, G.L. Haller, *J Phys Chem-Us*, 100 (1996) 16247.

[87] F.M. Hoffmann, *Surf. Sci. Report.*, 3 (1983) 107.

[88] N.R. Avery, *Surf. Sci.*, 125 (1983) 771.

[89] A.B. Anton, N.R. Avery, B.H. Toby, W.H. Weinberg, *JACS*, 108 (1986) 684.

[90] N.R. Avery, W.H. Weinberg, A.B. Anton, B.H. Toby, *Phys. Rev. Lett.*, 51 (1983) 682.

[91] J.L. Davis, M.A. Barteau, *Surf. Sci.*, 187 (1987) 387.

[92] J.L. Davis, M.A. Barteau, *Surf. Sci.*, 235 (1990) 235.

[93] S.M. Gates, J.N. Russell, J.T. Yates, *Surf. Sci.*, 171 (1986) 111.

[94] B.A. Sexton, K.D. Rendulic, A.E. Hughes, *Surf. Sci.*, 121 (1982) 181.

[95] S.R. Bare, J.A. Stroscio, W. Ho, *Surf. Sci.*, 150 (1985) 399.

[96] S.M. Gates, J.N. Russell, J.T. Yates, *Surf. Sci.*, 159 (1985) 233.

[97] B. Hammer, J.K. Norskov, *Advances in Catalysis, Vol 45*, 45 (2000) 71.

[98] M. Mavrikakis, B. Hammer, J.K. Norskov, *Phys. Rev. Lett.*, 81 (1998) 2819.

[99] C.E. Tripa, T.S. Zubkov, J.T. Yates, M. Mavrikakis, J.K. Norskov, *J. Chem. Phys.*, 111 (1999) 8651.

[100] T. Danuthai, S. Jongpatiwut, T. Rirksomboon, S. Osuwan, D.E. Resasco, *Catal. Lett.*, 132 (2009) 197.

[101] E.L. Kunkes, R.R. Soares, D.A. Simonetti, J.A. Dumesic, *Appl Catal B-Environ*, 90 (2009) 693.

[102] H. Bernas, K. Eranen, I. Simakova, A. Leino, K. Kordas, J. Myllyoja, P. Maki-Arvela, T. Salmi, D.Y. Murzin, *Fuel*, (2009).

[103] D. Prochazkova, P. Zamostny, M. Bejblova, L. Cerveny, J. Cejka, *Appl. Catal. A-Gen*, 332 (2007) 56.

[104] E. Furimsky, *Appl. Catal. A-Gen*, 199 (2000) 147.

[105] T.T. Pham, S.P. Crossley, T. Sooknoi, L.L. Lobban, D.E. Resasco, R.G. Mallinson, *Appl. Catal. A*, (2010).

[106] G. Lietz, M. Nimz, J. Volter, *Appl. Catal.* , 45 (1988) 71.

[107] A. Benedetti, G. Fagherazzi, F. Pinna, G. Rampazzo, M. Selva, G. Strukul, *Catal. Lett.*, 10 (1991) 215.

[108] H. Lieske, G. Lietz, W. Hanke, J. Volter, *Z. Anorg. Allg. Chem.*, 527 (1985) 135.

[109] S.S. Ashour, J.E. Bailie, C.H. Rochester, J. Thomson, G.J. Hutchings, *J Mol Catal a-Chem*, 123 (1997) 65.

[110] G.J. Millar, C.H. Rochester, K.C. Waugh, *J. Chem. Soc. Faraday Trans*, 87 (1991) 1467.

APPENDICES

Appendix A. Gas Chromatograph samples

GC samples and spreadsheet sample calculation are shown here for the activity of 5% Pd-2.5% Cu/SiO_2 varying with time on stream (TOS –min). Carbon balance based and deactivation rate are also calculated in the following spreadsheet sample calculation.

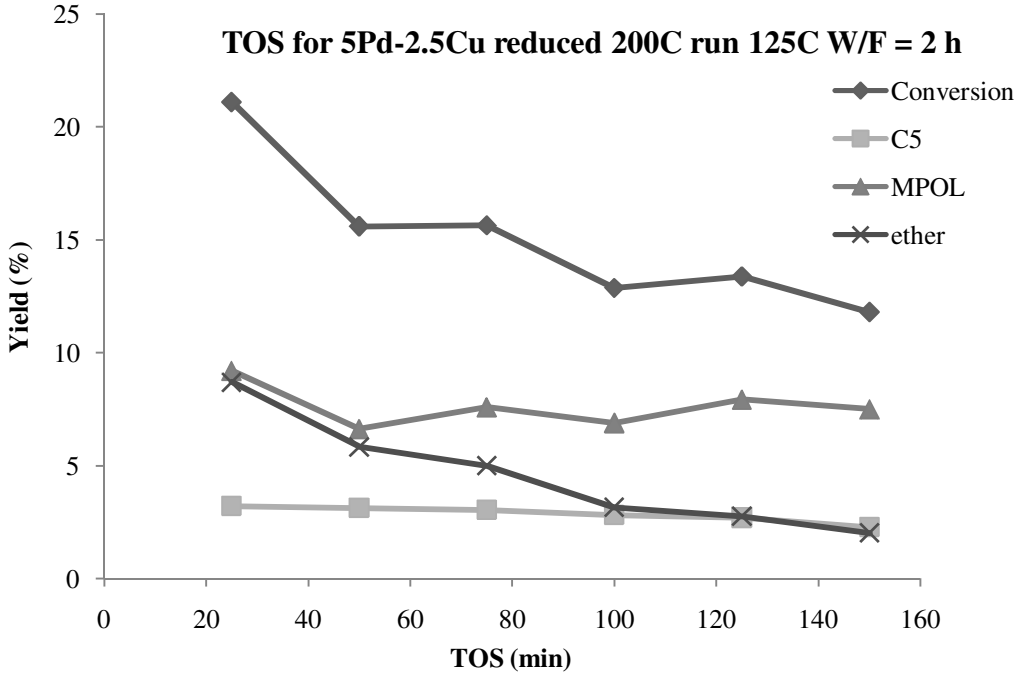

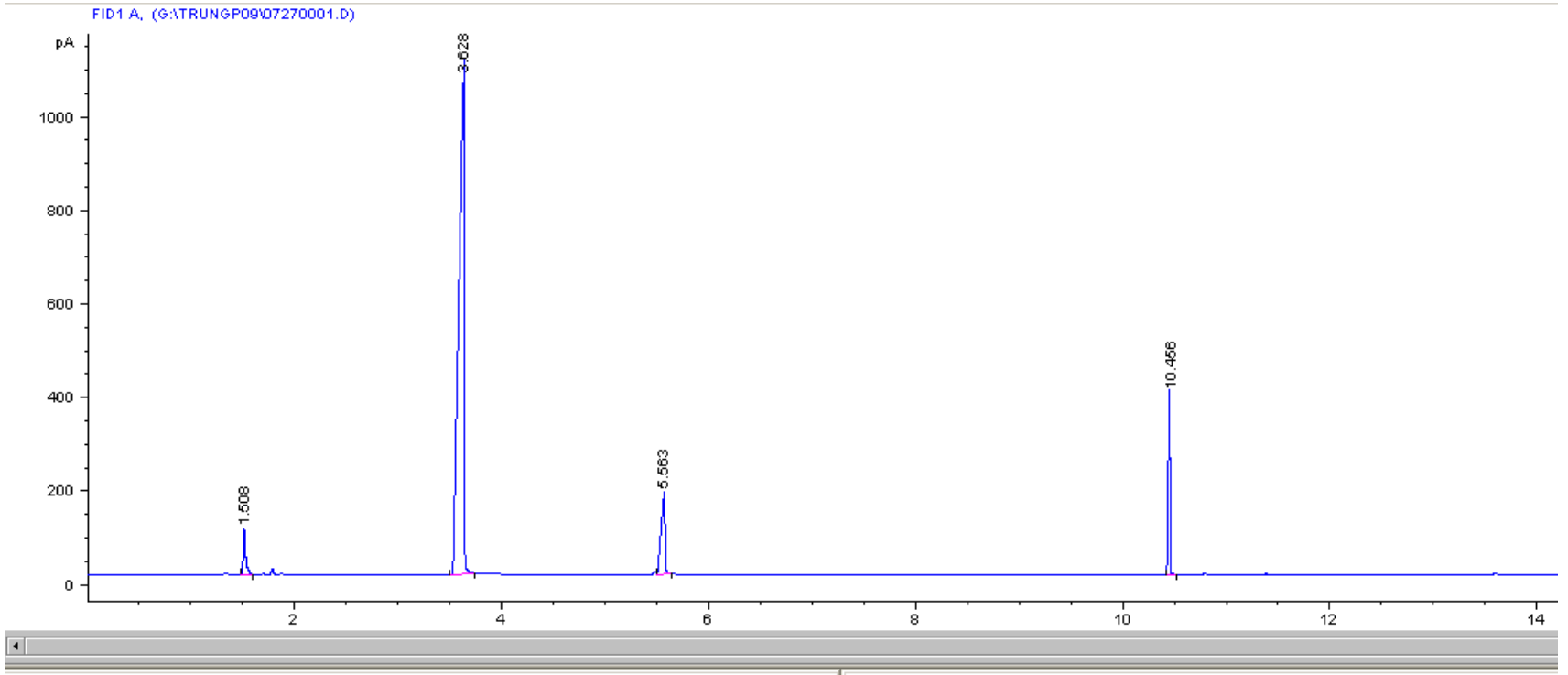

File Information	
GC-File	07270001.D
File Path	G:\TRUNGP09\
Date	7/27/09 4:29:31 PM
Sample	5%-2.5Cu Pd0.1g
Sample Info	feed C6AL in H2
	W/F series Cat 5Pd-2.5Cu red 250C run 125C 0.1
	0.05 ml/h
Barcode	
Operator	TP
Method	TP060908.M

#	Time	Area	Height	Width	Symmetry
1	1.508	163	95.8	0.0249	0.629
2	3.628	3996.9	1078.3	0.0532	5.683
3	5.563	466.4	172.2	0.0406	2.839
4	10.456	440.6	385.4	0.0183	1.323

Injection Date : 7/27/2009 4:29:31 PM
Sample Name : 5%-2.5Cu Pd0.1g Location : Vial
Acq. Operator : TP Inj : 1
Inj Volume : Manually
Acq. Method : C:\HPCHEM\1\METHODS\TP060908.M
Last changed : 3/9/2009 6:12:08 PM by TP
Analysis Method : C:\HPCHEM\1\METHODS\DEF_GC.M
Last changed : 2/1/2010 1:41:30 PM
(modified after loading)

==========

Area Percent Report

==========

Sorted By : Signal
Multiplier : 1
Dilution : 1

Signal 1:00 FID1 A

Peak #	RetTime [min]	Type	Width [min]	Area [pA*s]	Height [pA]	Area %
1	1.508	BB	0.0249	163.0396	95.78548	3.21771
2	3.628	PB	0.0532	3996.94	1078.272	78.8827
3	5.563	VB	0.0406	466.3705	172.1787	9.20419
4	10.456	BB	0.0183	440.5874	385.3972	8.69534
Totals :				5066.937	1731.63321	

==========

*** End of Report ***

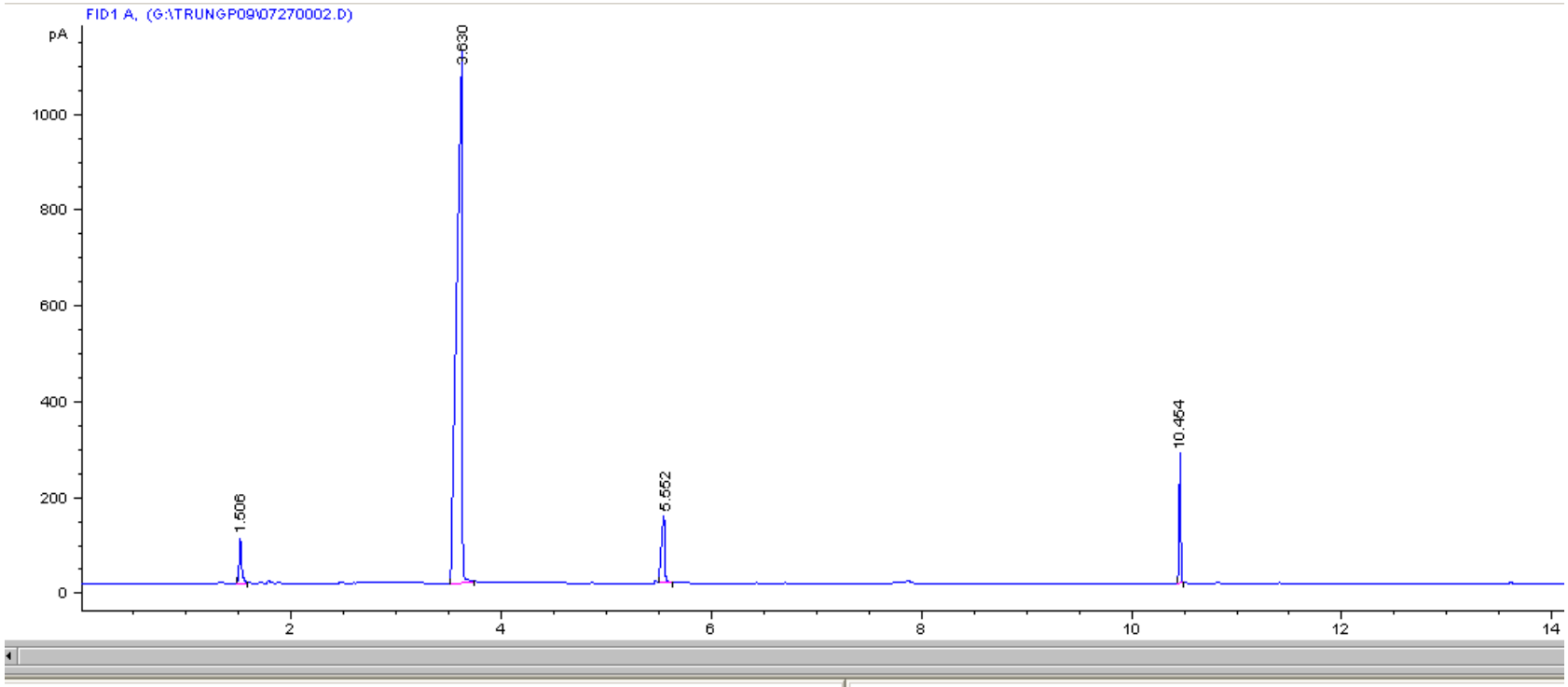

File Information	
GC-File	07270002.D
File Path	G:\TRUNGP09\
Date	7/27/09 4:53:34 PM
Sample	5%-2.5Cu Pd0.1g
Sample Info	feed C6AL in H2
	W/F series Cat 5Pd-2.5Cu red 250C run 125C 0.1
	0.05 ml/h
Barcode	
Operator	TP
Method	TP060908.M

#	Time	Area	Height	Width	Symmetry
1	1.506	151.5	93.4	0.0239	0.638
2	3.63	4077.5	1128.4	0.0452	6.751
3	5.552	320.5	139	0.0349	2.086
4	10.454	282.1	269	0.0162	1.198

```
================================================================
Injection Date       :  7/27/2009   4:53:34 PM
Sample    Name       :  5%-2.5Cu Pd0.1g  Location :  Vial
Acq.      Operator   :  TP          Inj      :  1
          Inj Volume :  Manually
Acq.      Method     :  C:\HPCHEM\1\METHODS\TP060908.M
Last      changed    :   3/9/2009   6:12:08 PM  by  TP
Analysis  Method     :  C:\HPCHEM\1\METHODS\DEF_GC.M
Last      changed    :   2/1/2010   4:28:02 PM
          (modified  after loading)
================================================================
          Area       Percent Report
================================================================

Sorted    By         :  Signal
Multiplier :          1
Dilution   :          1


Signal          1:00  FID1    A

Peak    RetTime  Type  Width    Area      Height    Area
        #        [min] [min]    [pA*s]    [pA]      %
----|-------|----|-------|----------|----------|--------|
     1    1.506  BB       0.0239  151.5402  93.37617   3.13645
     2     3.63  PB       0.0452  4077.454  1128.361  84.39175
     3    5.552  VB       0.0349  320.5296  139.0189   6.63405
     4   10.454  BB       0.0162  282.0553  268.9716   5.83774
Totals :                          4831.579  1629.727

================================================================
          ***    End      of      Report    ***
```

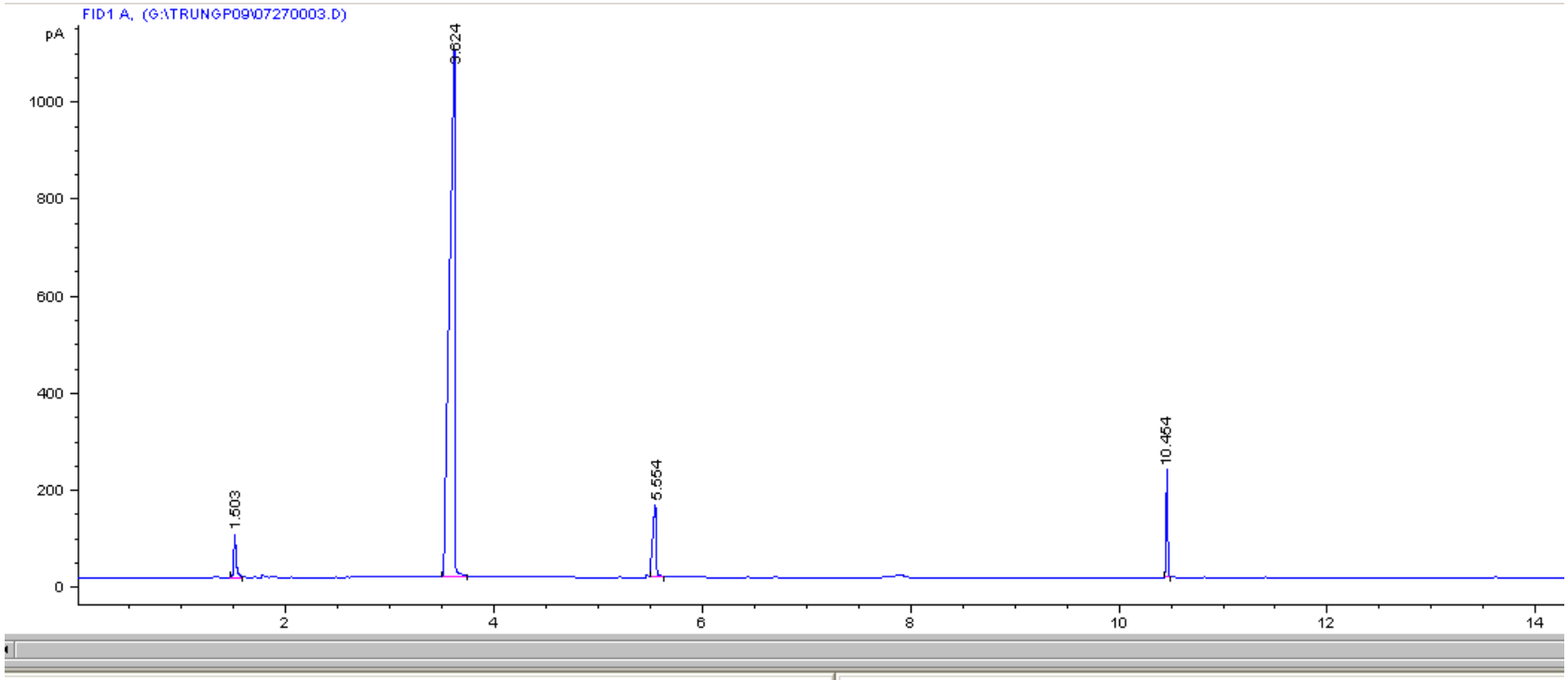

File Information	
GC-File	07270003.D
File Path	G:\TRUNGP09\
Date	7/27/09 5:18:13 PM
Sample	5%-2.5Cu Pd0.1g
Sample Info	feed C6AL in H2
	W/F series Cat 5Pd-2.5Cu red 250C run 125C 0.1
	0.05 ml/h
Barcode	
Operator	TP
Method	TP060908.M

#	Time	Area	Height	Width	Symmetry
1	1.503	139.9	88.3	0.0235	0.637
2	3.624	3877.3	1090.1	0.0465	5.775
3	5.554	349.1	149.3	0.0373	2.288
4	10.454	229.8	219.8	0.0162	1.135

Injection Date : 7/27/2009 5:18:13 PM
Sample Name : 5%-2.5Cu Pd0.1g Location : Vial
Acq. Operator : TP Inj : 1
Inj Volume : Manually
Acq. Method : C:\HPCHEM\1\METHODS\TP060908.M
Last changed : 3/9/2009 6:12:08 PM by TP
Analysis Method : C:\HPCHEM\1\METHODS\DEF_GC.M
Last changed : 2/1/2010 4:28:02 PM
(modified after loading)

==========

Area Percent Report

==========

Sorted By : Signal
Multiplier : 1
Dilution : 1

Signal 1:00 FID1 A

Peak #	RetTime [min]	Type	Width [min]	Area [pA*s]	Height [pA]	Area %
1	1.503	BB	0.0235	139.8908	88.32719	3.04371
2	3.624	PB	0.0465	3877.261	1090.122	84.36048
3	5.554	VB	0.0373	349.139	149.2687	7.59648
4	10.454	BB	0.0162	229.7723	219.8198	4.99933
Totals :				4596.063	1547.538	

==========

*** End of Report ***

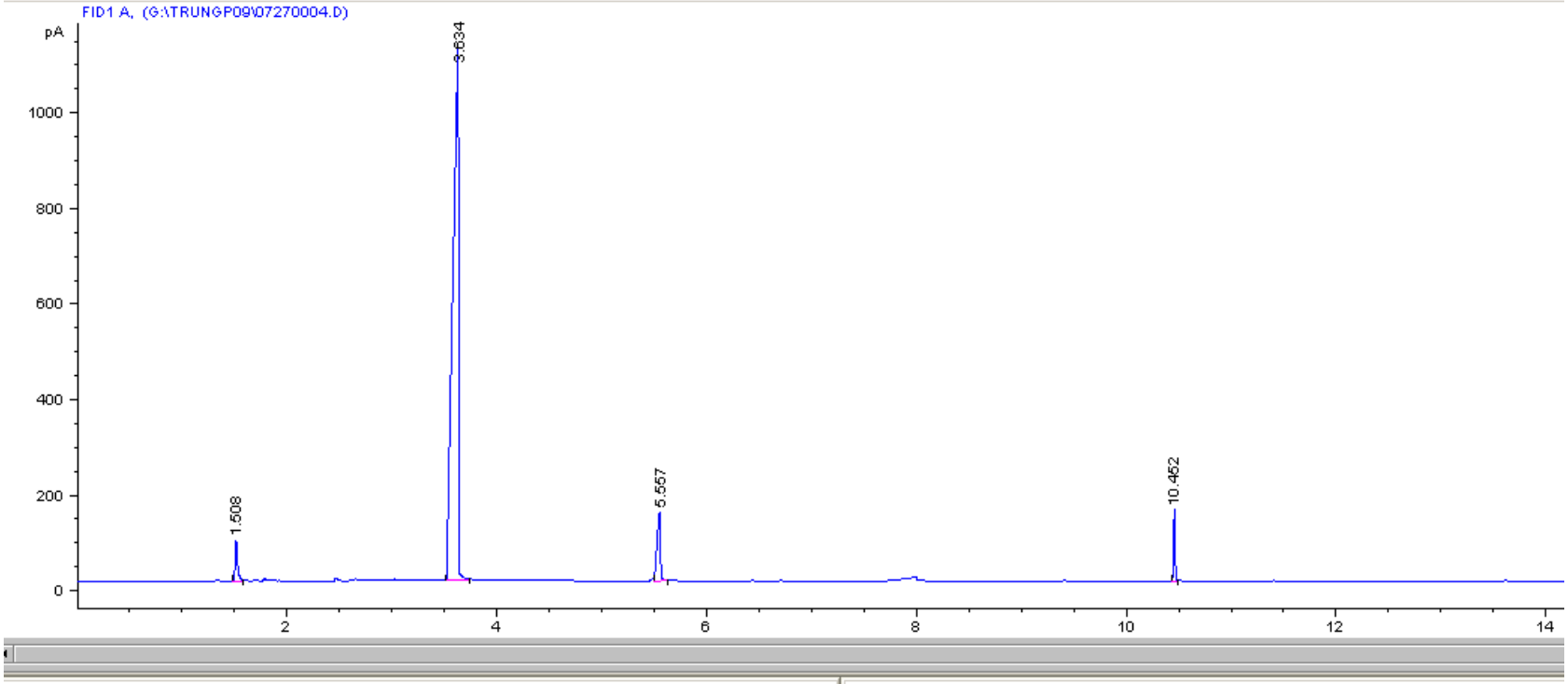

File Information	
GC-File	07270004.D
File Path	G:\TRUNGP09\
Date	7/27/09 5:41:57 PM
Sample	5%-2.5Cu Pd0.1g
Sample Info	feed C6AL in H2
	W/F series Cat 5Pd-2.5Cu red 250C run 125C 0.1
	0.05 ml/h
Barcode	
Operator	TP
Method	TP060908.M

#	Time	Area	Height	Width	Symmetry
1	1.508	132.8	82.2	0.0239	0.619
2	3.634	4102.8	1101	0.0515	5.823
3	5.557	324.8	141.4	0.0318	2.136
4	10.452	148.4	145.8	0.0159	1.038

Injection Date : 7/27/2009 5:41:57 PM
Sample Name : 5%-2.5Cu Pd0.1g Location : Vial
Acq. Operator : TP Inj : 1
Inj Volume : Manually
Acq. Method : C:\HPCHEM\1\METHODS\TP060908.M
Last changed : 3/9/2009 6:12:08 PM by TP
Analysis Method : C:\HPCHEM\1\METHODS\DEF_GC.M
Last changed : 2/1/2010 4:28:02 PM
(modified after loading)

==========

Area Percent Report

==========

Sorted By : Signal
Multiplier : 1
Dilution : 1

Signal 1:00 FID1 A

Peak #	RetTime [min]	Type	Width [min]	Area [pA*s]	Height [pA]	Area %
1	1.508	BB	0.0239	132.7551	82.15426	2.81935
2	3.634	PB	0.0515	4102.803	1101.004	87.13202
3	5.557	VB	0.0318	324.7533	141.4304	6.89685
4	10.452	BB	0.0159	148.4087	145.7979	3.15178
Totals :				4708.72	1470.386	

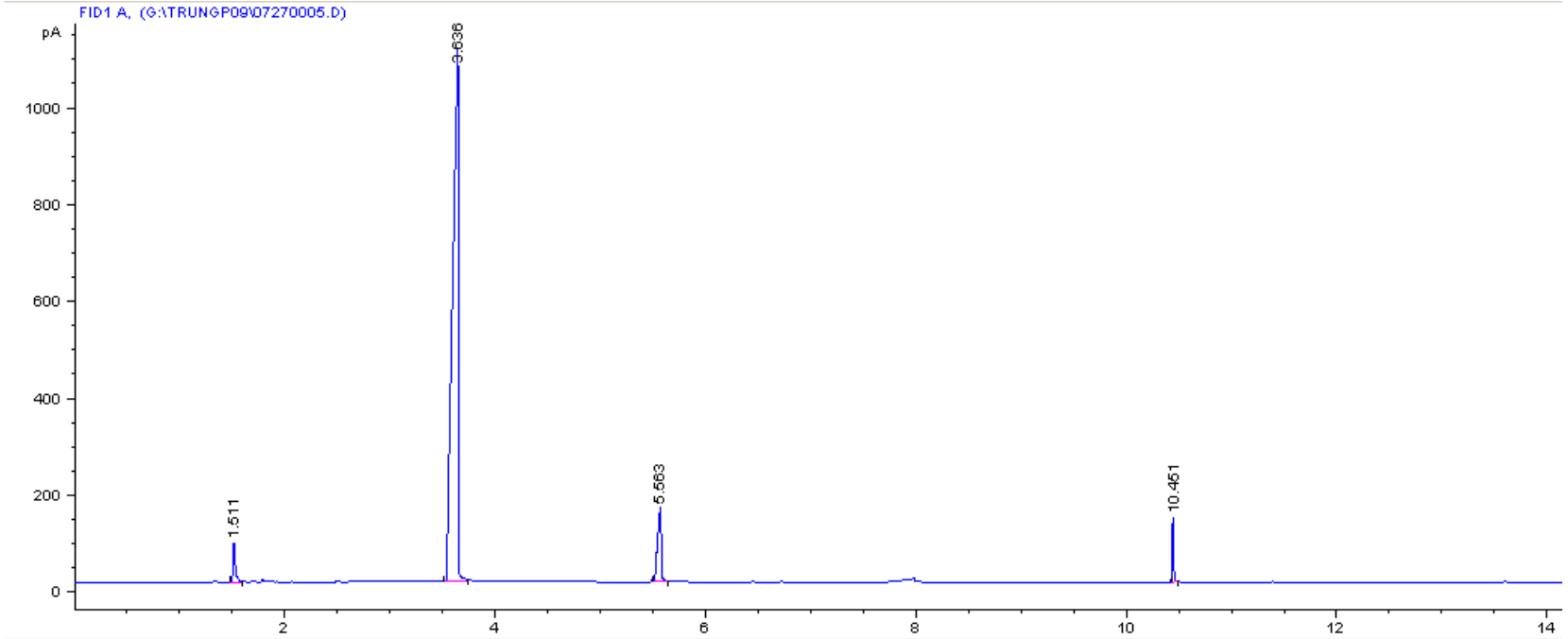

File Information	
GC-File	07270005.D
File Path	G:\TRUNGP09\
Date	7/27/09 6:05:38 PM
Sample	5%-2.5Cu Pd0.1g
Sample Info	feed C6AL in H2
	W/F series Cat 5Pd-2.5Cu red 250C run 125C 0.1
	0.05 ml/h
Barcode	
Operator	TP
Method	TP060908.M

#	Time	Area	Height	Width	Symmetry
1	1.511	126.4	78.4	0.0238	0.603
2	3.636	4063.2	1074.2	0.0481	6.234
3	5.563	372.1	151.2	0.0357	2.343
4	10.451	128.9	131.6	0.0154	1.038

Injection Date : 7/27/2009 6:05:38 PM
Sample Name : 5%-2.5Cu Pd0.1g Location : Vial
Acq. Operator : TP Inj : 1
Inj Volume : Manually
Acq. Method : C:\HPCHEM\1\METHODS\TP060908.M
Last changed : 3/9/2009 6:12:08 PM by TP
Analysis Method : C:\HPCHEM\1\METHODS\DEF_GC.M
Last changed : 2/1/2010 4:28:02 PM
(modified after loading)

==========

Area Percent Report

==========

Sorted By : Signal
Multiplier : 1
Dilution : 1

Signal 1:00 FID1 A

Peak #	RetTime [min]	Type	Width [min]	Area [pA*s]	Height [pA]	Area %
1	1.511	BB	0.0238	126.4185	78.39443	2.69517
2	3.636	PB	0.0481	4063.181	1074.233	86.62471
3	5.563	VB	0.0357	372.0963	151.195	7.93288
4	10.451	BB	0.0154	128.8608	131.6083	2.74724
Totals :				4690.557	1435.431	

==========

*** End of Report ***

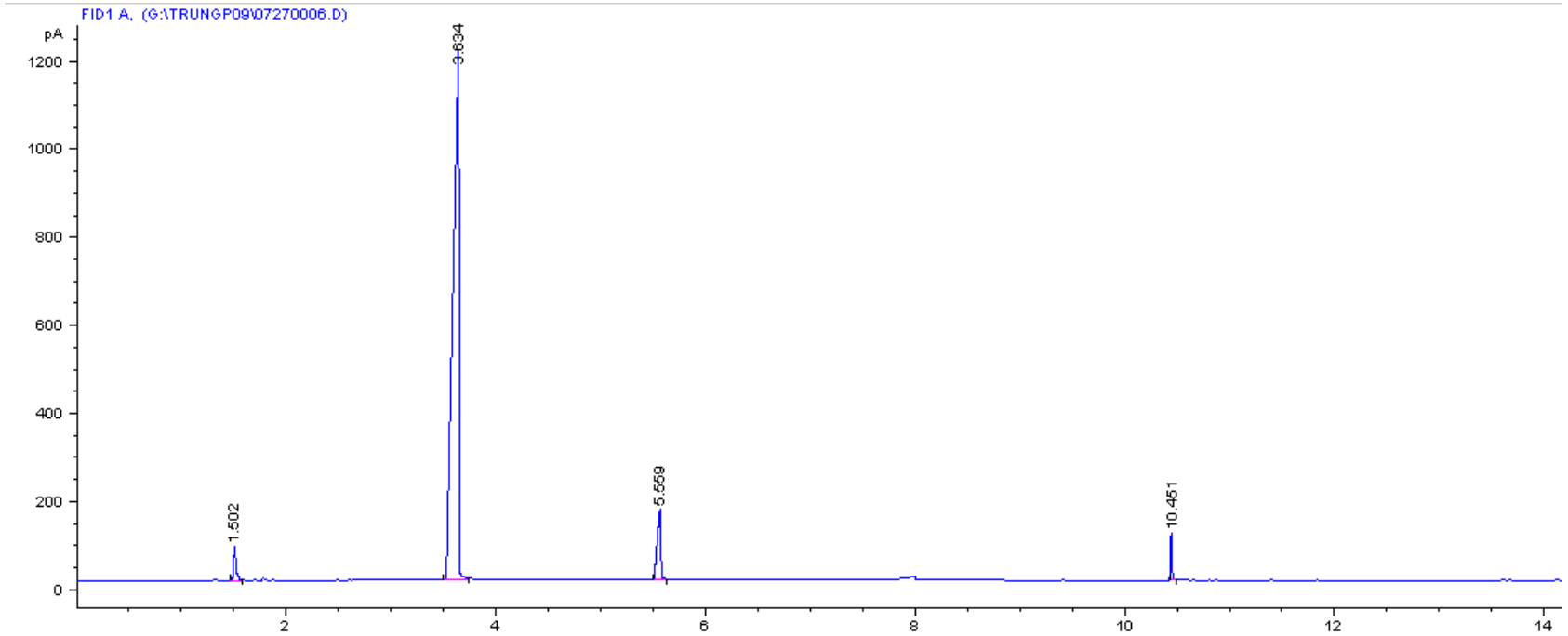

File Information	
GC-File	07270006.D
File Path	G:\TRUNGP09\
Date	7/27/09 6:29:19 PM
Sample	5%-2.5Cu Pd0.1g
Sample Info	feed C6AL in H2
	W/F series Cat 5Pd-2.5Cu red 250C run 125C 0.1
	0.05 ml/h
Barcode	
Operator	TP
Method	TP060908.M

#	Time	Area	Height	Width	Symmetry
1	1.502	119.8	74.8	0.0237	0.605
2	3.634	4628.2	1193.8	0.0512	6.374
3	5.559	393.4	156.5	0.0343	2.544
4	10.451	105.9	103.8	0.0159	0.993

Injection Date : 7/27/2009 6:29:19 PM
Sample Name : 5%-2.5Cu Pd0.1g Location : Vial
Acq. Operator : TP Inj : 1
Inj Volume : Manually
Acq. Method : C:\HPCHEM\1\METHODS\TP060908.M
Last changed : 3/9/2009 6:12:08 PM by TP
Analysis Method : C:\HPCHEM\1\METHODS\DEF_GC.M
Last changed : 2/1/2010 4:28:02 PM
(modified after loading)

==========

Area Percent Report

==========

Sorted By : Signal
Multiplier : 1
Dilution : 1

Signal 1:00 FID1 A

Peak #	RetTime [min]	Type	Width [min]	Area [pA*s]	Height [pA]	Area %
1	1.502	BB	0.0237	119.8334	74.84788	2.28373
2	3.634	PB	0.0512	4628.177	1193.773	88.20148
3	5.559	VB	0.0343	393.3762	156.4668	7.49677
4	10.451	BB	0.0159	105.8913	103.8209	2.01802
Totals :				5247.278	1528.908	

==========

*** End of Report ***

Appendix B. Spreadsheet sample calculations

Spreadsheet sample calculations are shown for the 5% Pd-2.5% Cu/SiO_2 reduced at 200°C run at 125°C at W/F = 2h with varying time on stream (TOS-min)

Peak 1 = C5

Peak 2 = 2-methyl-pentanal

Peak 3 = 2-methyl-pentanol

Peak 4 = dimethylpentyl ether

The area percentages of the peaks from the GC reports are input into Excel. Total area is also input in order to calculate carbon balance for the experiment.

Conversion of 2-methyl-pentanal = 100 – area % of 2-methyl-pentanal

Yield of C5 = area % of C5 peak

Yield of 2-methyl-pentanol = area % of 2-methyl-pentanol

Yield of ether = area % of ether

W/F =2

TOS	25	50	75	100	125	150
Conversion	21.12	15.61	15.64	12.87	13.38	11.80
C5	3.22	3.14	3.04	2.82	2.70	2.28
MPOL	9.20	6.63	7.60	6.90	7.93	7.50
ether	8.70	5.84	5.00	3.15	2.75	2.02
Total area	5067	4832	4596	4709	4691	5247
C balance	92.58					

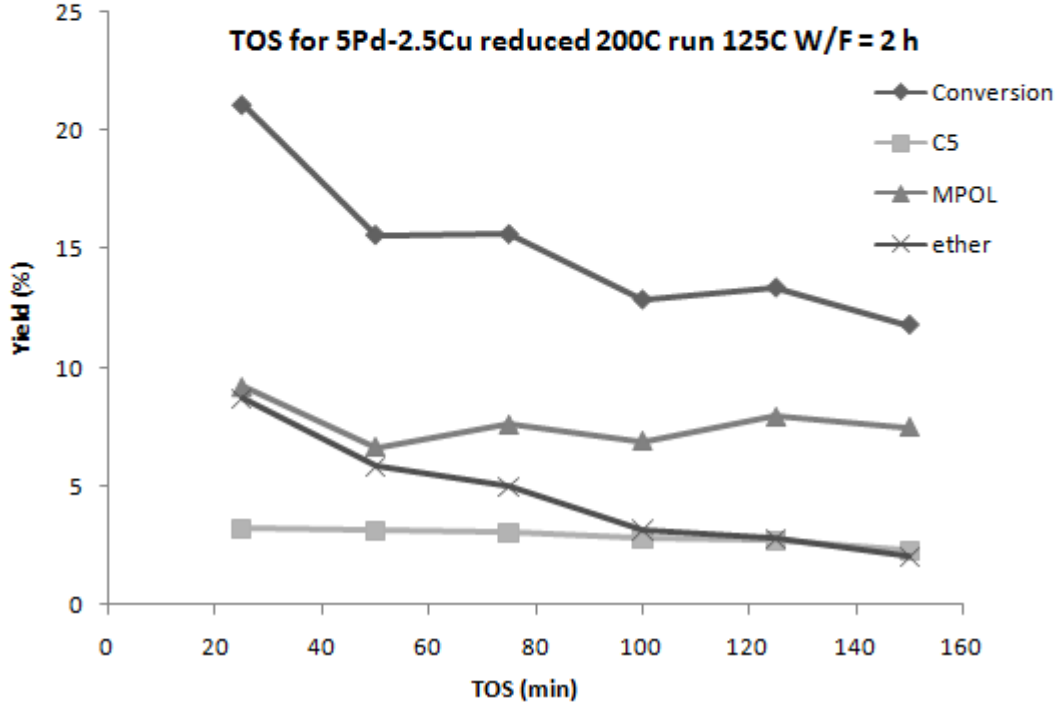

Carbon balance = (total area at 125min) / (total area at 25 min) = 92.5%

Calculation of deactivation rate:

Activity of the catalyst can be expressed as: $a = b/(1+kt)$

where $b = 25$ *for* TOS = 0 min (by intrapolation)

Error squared values = (conversion – a)^2 at 25, 50, 75 …150 min were calculated.

Excel Solver was used to solve for k with an objective of minimizing total of squared error.

a = 25/(1+kt)						
k	0.0084					
t	25	50	75	100	125	150
a	20.67	17.62	15.35	13.60	12.21	11.08
Conversion	21.12	15.61	15.64	12.87	13.38	11.80
Error squared	0.20	4.04	0.08	0.54	1.35	0.52
Total least square	6.74					

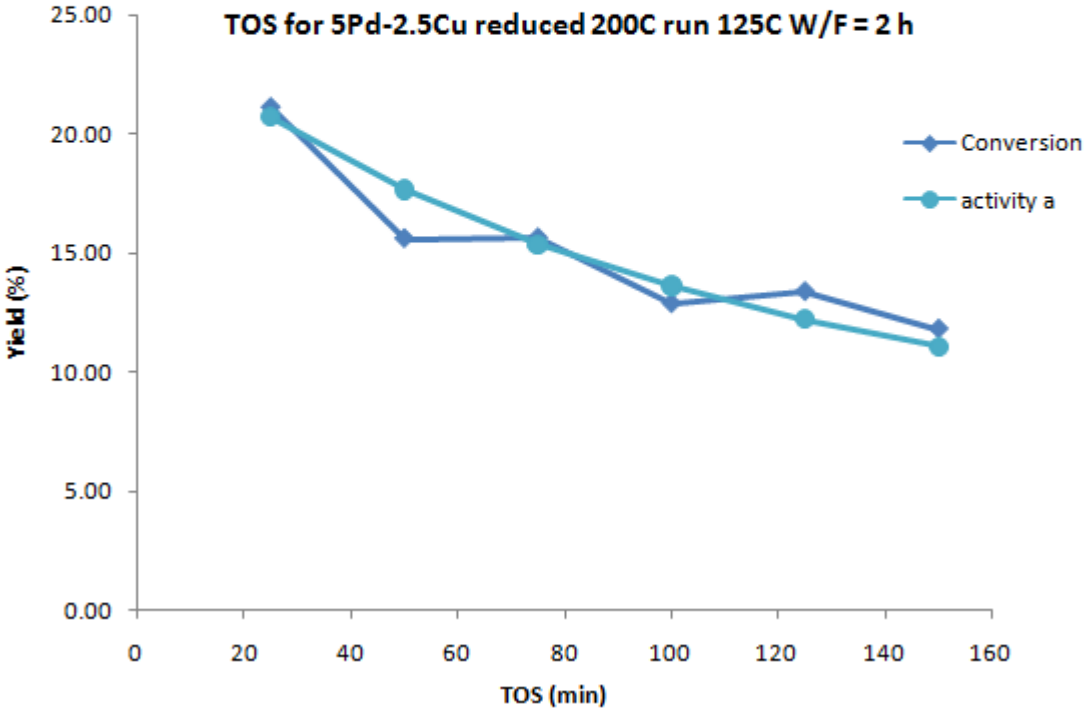

Appendix C. Kinetic model fitting

Kinetic modeling for 5% Pd /SiO_2 using differential reactor method.

Differential reactor method was used by choosing small differential time interval dt = 0.003 h and calculating the partial pressures of each species based on their previous values at previous time. These partial pressures were then normalized to molar composition and fitted with experimental data by least square error method. That is, error square at each data point was calculated; Solver was used to simultaneously solve for rate constants k_1, k_2, k_3 with an objective to minimize the total squared error.

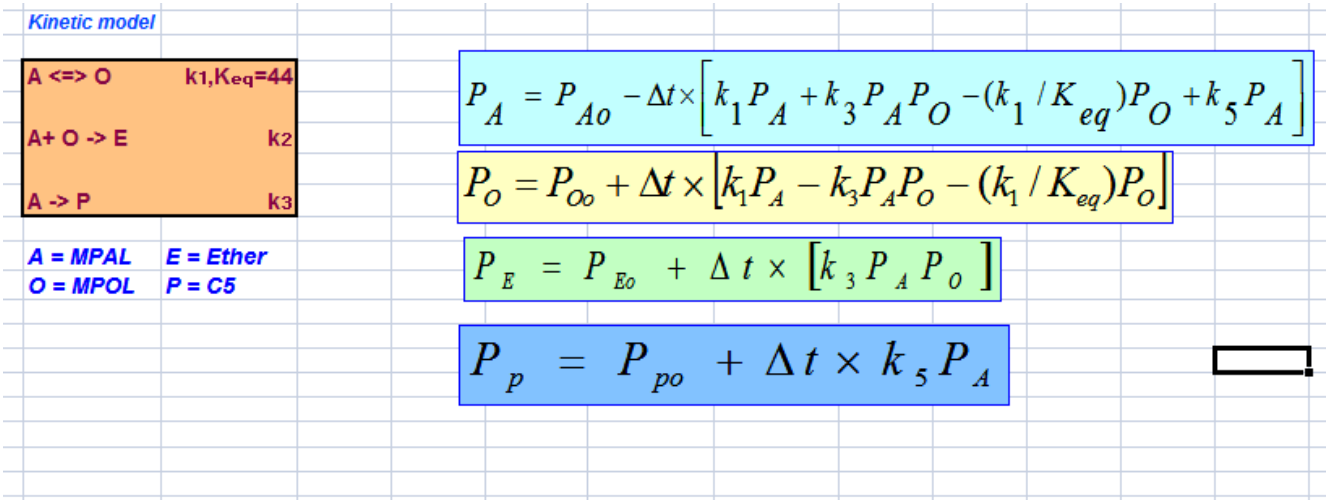

k1	0.1003
k2	40.0803
k3	0.05073
dt	0.003
Totall least square erro	27.3994

W/F	5	4	3	2	1
MPAL	39.72	48.13	60.00	73.00	86.11
C5	18.31	17.00	15.00	11.00	6.50
MPOL	5.40	3.27	2.80	2.48	2.21
ether	36.57	31.06	22.67	13.00	5.00

t	PA	C5	PO	PE	Pt
0	0.08333	0	0	0	0.08333

t	PA	C5	PO	PE	Pt
0	100	0	0	0	100
0.048	99.2773	0.24272	0.44561	0.03432	100
0.051	99.2323	0.25784	0.47108	0.03875	100

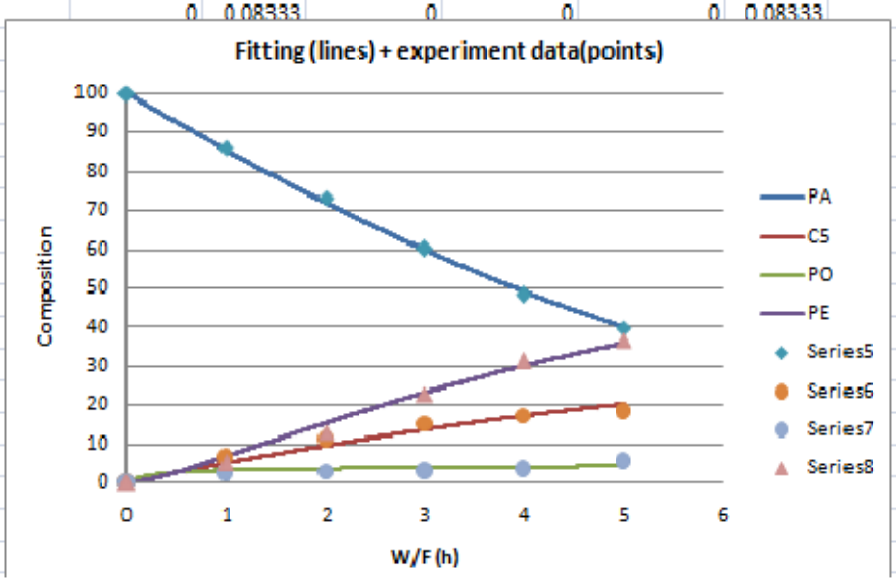

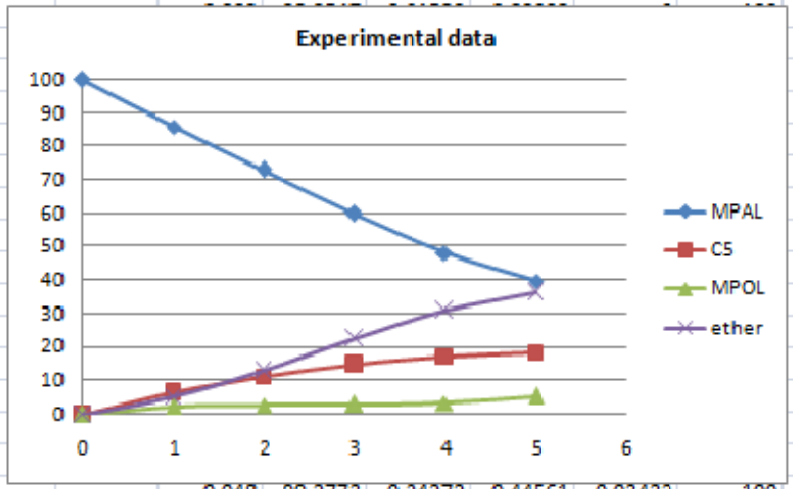

Kinetic modeling for 5% Pd – 2.5% Cu/SiO_2

The same differential reactor method was applied. The rate equations remained the same for this catalyst. The fitting procedure was the same but carried out different data set on the 5% Pd – 2.5% Cu/SiO_2.

Kinetic model

A <=> O	k1,Keq=44
A+ O -> E	k2
A -> P	k3

A = MPAL E = Ether
O = MPOL P = C5

$$P_A = P_{Ao} - \Delta t \times \left[k_1 P_A + k_3 P_A P_O - (k_1 / K_{eq}) P_O + k_5 P_A \right]$$

$$P_O = P_{Oo} + \Delta t \times \left[k_1 P_A - k_3 P_A P_O - (k_1 / K_{eq}) P_O \right]$$

$$P_E = P_{Eo} + \Delta t \times \left[k_3 P_A P_O \right]$$

$$P_p = P_{po} + \Delta t \times k_5 P_A$$

k1	0.100302
k2	40.08028
k3	0.050727
dt	0.003
Total least square error	27.39942

W/F	5	4	3	2	1
MPAL	39.72	48.13	60.00	73.00	86.11
C5	18.31	17.00	15.00	11.00	6.50
MPOL	5.40	3.27	2.80	2.48	2.21
ether	36.57	31.06	22.67	13.00	5.00

t	PA	C5	PO	PE	Pt
0	0.083333	0	0	0	0.083333

t	PA	C5	PO	PE	Pt
0	100	0	0	0	100
0.048	99.27734	0.242722	0.445614	0.03432	100
0.051	99.23233	0.257841	0.471076	0.038753	100